International Doctorate Program in Molecular Oncology and Endocrinology
Doctorate School in Molecular Medicine

XXII cycle - 2006–2009
Coordinator: Prof. Giancarlo Vecchio

Different effects of single and fractionated light delivery regimes in photodynamic therapy with hypericin on HT-29 cells *in vitro*

Lucia Grada Kuliková

University of Naples Federico II
Dipartimento di Biologia e Patologia Cellulare e Molecolare
"L. Califano"

Administrative Location

Dipartimento di Biologia e Patologia Cellulare e Molecolare “L. Califano”
Università degli Studi di Napoli Federico II

Partner Institutions

Italian Institutions
Università degli Studi di Napoli “Federico II”, Naples, Italy
Istituto di Endocrinologia ed Oncologia Sperimentale “G. Salvatore”, CNR, Naples, Italy
Seconda Università di Napoli, Naples, Italy
Università degli Studi di Napoli “Parthenope”, Naples, Italy
Università del Sannio, Benevento, Italy
Università di Genova, Genoa, Italy
Università di Padova, Padua, Italy
Università degli Studi “Magna Graecia”, Catanzaro, Italy
Università degli Studi di Firenze, Florence, Italy
Università degli Studi di Bologna, Bologna, Italy
Università degli Studi del Molise, Campobasso, Italy
Università degli Studi di Torino, Turin, Italy
Università di Udine, Udine, Italy

Foreign Institutions
Université Libre de Bruxelles, Brussels, Belgium
Universidade Federal de Sao Paulo, Brazil
University of Turku, Turku, Finland
Université Paris Sud XI, Paris, France
University of Madras, Chennai, India
Pavol Jozef Šafárik University in Košice, Slovakia
Universidad Autonoma de Madrid, Centro de Investigaciones Oncologicas (CNIO), Spain
Johns Hopkins School of Medicine, Baltimore, MD, USA
Johns Hopkins Krieger School of Arts and Sciences, Baltimore, MD, USA
National Institutes of Health, Bethesda, MD, USA
Ohio State University, Columbus, OH, USA
Albert Einstein College of Medicine of Yeshiwa University, N.Y., USA

Supporting Institutions
Ministero dell’Università e della Ricerca
Associazione Leonardo di Capua, Naples, Italy
Dipartimento di Biologia e Patologia Cellulare e Molecolare “L. Califano”, Università degli Studi di Napoli “Federico II”, Naples, Italy
Istituto Superiore di Oncologia (ISO), Genoa, Italy
Università Italo-Francese, Torino, Naples, Italy
Università degli Studi di Udine, Udine, Italy
Agenzia Spaziale Italiana
Istituto di Endocrinologia ed Oncologia Sperimentale “G. Salvatore”, CNR, Naples, Italy

Italian Faculty

Giancarlo Vecchio, MD, Co-ordinator
Salvatore Maria Aloj, MD
Francesco Saverio Ambesi Impiombato, MD
Francesco Beguinot, MD
Maria Teresa Berlingieri, MD
Angelo Raffaele Bianco, MD
Bernadette Biondi, MD
Francesca Carlomagno, MD
Gabriella Castoria, MD
Angela Celetti, MD
Mario Chiariello, MD
Lorenzo Chiariotti, MD
Vincenzo Ciminale, MD
Annamaria Cirafici, PhD
Annamaria Colao, MD
Alma Contegiacomo, MD
Sabino De Placido, MD
Gabriella De Vita, MD
Monica Fedele, PhD
Pietro Formisano, MD
Alfredo Fusco, MD
Michele Grieco, MD
Massimo Imbriaco, MD
Paolo Laccetti, PhD
Antonio Leonardi, MD
Paolo Emidio Macchia, MD
Barbara Majello, PhD
Rosa Marina Melillo, MD
Claudia Miele, PhD
Francesco Oriente, MD
Roberto Pacelli, MD
Giuseppe Palumbo, PhD
Silvio Parodi, MD
Nicola Perrotti, MD
Giuseppe Portella, MD
Giorgio Punzo, MD
Antonio Rosato, MD
Guido Rossi, MD
Giuliana SalvatoreMD,
Massimo Santoro, MD
Giampaolo Tortora, MD
Donatella Tramontano, PhD
Giancarlo Troncone, MD
Giuseppe Viglietto, MD
Roberta Visconti, MD
Mario Vitale, MD

Foreign Faculty

Université Libre de Bruxelles, Belgium
Gilbert Vassart, MD
Jacques E. Dumont, MD

Universidade Federal de Sao Paulo, Brazil
Janete Maria Cerutti, PhD
Rui Monteiro de Barros Maciel, MD PhD

University of Turku, Turku, Finland
Mikko Laukkanen, PhD

Université Paris Sud XI, Paris, France
Martin Schlumberger, MD
Jean Michel Bidart, MD

University of Madras, Chennai, India
Arasambattu K. Munirajan, PhD

Pavol Jozef Šafárik University in Košice, Slovakia
Eva Čellárová, PhD
Peter Fedoročko, PhD

Universidad Autonoma de Madrid - Instituto de Investigaciones Biomedicas, Spain
Juan Bernal, MD, PhD
Pilar Santisteban, PhD

Centro de Investigaciones Oncologicas, Spain
Mariano Barbacid, MD

Johns Hopkins School of Medicine, USA
Vincenzo Casolaro, MD
Pierre A. Coulombe, PhD
James G. Herman MD
Robert P. Schleimer, PhD

Johns Hopkins Krieger School of Arts and Sciences, USA
Eaton E. Lattman, MD

National Institutes of Health, Bethesda, MD, USA
Michael M. Gottesman, MD
J. Silvio Gutkind, PhD
Genoveffa Franchini, MD
Stephen J. Marx, MD
Ira Pastan, MD
Phillip Gorden, MD

Ohio State University, Columbus, OH, USA
Carlo M. Croce, MD
Ginny L. Bumgardner, MD PhD

Albert Einstein College of Medicine of Yeshiwa University, N.Y., USA
Luciano D'Adamio, MD
Nancy Carrasco, MD

Different effects of single and fractionated light delivery regimes in photodynamic therapy with hypericin on HT-29 cells *in vitro*

“Science never solves a problem
withou creating ten more”

George Bernard SHAW

TABLE OF CONTENTS

LIST OF PUBLICATIONS **9**
ABSTRACT **10**
1 INTRODUCTION **11**
1.1 Photodynamic therapy 11
1.1.1 Hypericin as a potential photosensitizer 12
1.1.2 Mechanisms in photodynamic therapy 13
1.2 Hormesis – adaptive cell response - resistance 14
1.2.1 Resistance to different stimuli 15
1.2.2 Resistance to photodynamic therapy 18
1.3 Molecules playing role in resistance to cancer therapies 20
1.3.1 Heat shock proteins 20
1.3.2 Nuclear transcription factor-kappaB 23
1.3.3 Mitogen activated protein kinases 24
2 AIMS OF THE STUDY **27**
3 MATERIAL AND METHODS **28**
3.1 Cell culture 28
3.2 Hypericin activation 28
3.3 Experimental design 28
3.4 Quantification of cell viability and cell number 28
3.5 MTT assay 29
3.6 Cell cycle analysis 29
3.7 Colony-forming assay 30
3.8 Detection of phosphatidylserine externalization and cell membrane permeability 30
3.9 Production of ROS 30
3.10 Hypericin content analysis 30
3.11 Luciferase activity assay 30
3.12 Western blot analysis 31
3.13 Statistical analysis 31
4 RESULTS AND DISCUSSION **32**
4.1 Fractionated photodynamic treatment with hypericin doesn't improve the outcome as compared with to single irradiation scheme 32
4.2 Fractionated photodynamic treatment with a longer dark pause does not alter the original cell cycle regulation 36
4.3 Longer dark pause between two unequal light doses repressed cell death in HT-29 cell after hypericin-mediated PDT 37
4.4 Longer dark pause between two unequal light doses enhanced clonogenic potential of HT-29 cells after PDT with hypericin 39
4.5 Duration of a dark pause affects PDT-mediated ROS level induced by second light dose 40
4.6 Pre-sensitization did not affect physiological elimination of hypericin, however light administration regime affects hypericin elimination after lethal dose 42
4.7 Sub-lethal photodynamic treatment induced NF-κB activity 43
4.8 Even sub-lethal light dose increased whole protein expression that altered the timing of a second photodynamic treatment 45

4.9 Inhibition of p38 MAPK did not enhanced effect of hypericin-mediated PDT 48
5 CONCLUSIONS 49
6 ACKNOWLEDGEMENTS 50
7 REFERENCES 52
8 ORIGINAL PAPERS 66

LIST OF PUBLICATIONS

This dissertation is based upon following publications:

Sačková V, **Kuliková L**, Mikeš J, Kleban J, Fedoročko P. Hypericin-mediated photocytotoxic effect on HT-29 adenocarcinoma cells is reduced by light fractionation with longer dark pause between two unequal light doses. Photochem Photobiol 2005; 81:1411-1416

Kuliková L, Mikeš J, Hýžďalová M, Palumbo G, Fedoročko P. Possible implication of NF-κB in photo-resistance of HT-29 adenocarcinoma cells to fractionated light delivery with a longer dark pause between two unequal light doses. Photochem Photobiol *manuscript submitted*

Mikeš J, Kovaľ J, Jendželovský R, Sačková V, Uhrinová I, Kello M, **Kuliková L**, Fedoročko P. The role of p53 in efficiency of photodynamic therapy with hypericin and subsequent long-term survival of colon cancer cells. Photochem Photobiol Sci 2009; 8(11):1558-1567.

ABSTRACT

Photodynamic therapy (PDT) is an alternative cancer cure which involves the selective uptake and retention of a photosensitizer in a cancer tissue, followed by irradiation with light of a specific wavelength to kill tumour cells via the production of reactive oxygen species (ROS). Fractionation of the light administration is one of the protocol modifications in PDT based on the hypothesis of tissue reoxygenation during the one or more dark intervals between illuminations with a subsequent greater production of singlet oxygen and thus greater PDT effect. However we demonstrate in the present study that two-fold illumination scheme with equal light doses (3 or 6 $J.cm^{-2}$) separated by a dark interval 1 or 6 h do not enhanced, even reduced hypericin-mediated photocytotoxic effect in HT-29 adenocarcinoma cells *in vitro* by illumination with unequal light doses (1 + 11 $J.cm^{-2}$) separated with a longer dark pause (6 h). Fractionation with a longer dark pause increased cell number and cell survival in HT-29 cells when compared with such treatment but with a 1 h dark pause or with a single light delivery (12 $J.cm^{-2}$). Even proportion of cells in G1 and G2 phase of cell cycle were near to control. Longer dark pause also repressed cell death and enhanced clonogenic potential of HT-29 cells. Since longer dark interval after the irradiation by first sub-lethal light dose (1 $J.cm^{-2}$) makes cells resistant to the effect of the lethal light dose (11 $J.cm^{-2}$), we studied the events proceeded during a dark pause after sub-lethal dose (1 $J.cm^{-2}$) up to the second illumination. We show that pre-sensitization did not affect physiological elimination of hypericin however administration regime affected hypericin elimination after lethal dose. Inhibition of p38 MAPK did not improve photocytotoxic effect of light fractionation. Cell pre-sensitization induced ROS production, increased activity of redox-regulated nuclear transcription factor NF-κB and expression of proteins connected with a cell survival (NF-κB p50 and p65 subunits, IκB-α, Mcl-1, HSP70, GRP94, Clusterin-α). Although the role of heat shock proteins was generally established in response upon photo-induced stress, we uncovered that HSPs are not necessarily the "key" molecules in photo-resistance. Our findings indicate that timing of the second light dose before or after NF-κB activation could be crucial for the fate of cancer cell. We estimate successful application of hypericin in a high-dose multi-fraction PDT with dark intervals reduced bellow 1 h that might yield improved outcome.

1 INTRODUCTION

Relatively new and promising anticancer modality is photodynamic therapy using two individually nontoxic components – photosensitizer and light. The research of new natural photosensitizers such as hypericin as well as a modification in the delivery of photo-radiation is a promising additional approach in this therapeutic method. Recently, modification in the light delivery regime has been introduced on the standard photodynamic protocol (single-dose photosensitizer, single-dose light) to maximize the therapeutic effect of PDT, for example fractionated light regime. We have observed, that fractionated light regime with a longer dark period resulted in a decrease of hypericin cytotoxicity in HT-29 adenocarcinoma cancer cells. Longer dark interval after the irradiation of cells by first light dose makes cells resistant to the effect of the second illumination. The serious problem in photodynamic anticancer therapy is photo-resistance or photo-tolerance. However, molecular mechanism of photo-resistance is not unraveled till now. New information about this phenomenon should be useful in managing of cancer cells metabolism and improving of therapeutic effect. Inhibition of rescue metabolic pathways activated in photodynamic insulted cancer cells should be promising treatment tool in cancer therapy. Recent studies indicate that stimulation of the expression of the heat shock proteins upon photo-induced stress may be involved in this process. However, there is a variety of cancer cells responses to treatment resulted in a cell death or rescue pathways. Apart from the study of cell death, there is also important the research of the resistance development to cancer therapies. Therefore, this study is focused on the molecules and molecular pathways involved in a cancer cell survival probably playing role in a photo-resistance to fractionated light delivery regime. We investigated the impact of a sub-lethal light dose (1 $J.cm^{-2}$) and length of a following dark pause (1 or 6 h) on the development of resistance to the effect of the second illumination (11 $J.cm^{-2}$). We investigated the relationship between a dark interval and PDT response on HT-29 adenocarcinoma cancer cell line with respect to cellular and sub-cellular events after fractionated photodynamic therapy.

1.1 Photodynamic therapy

Photodynamic therapy (PDT) is a binary therapy in which two individually nontoxic components are combined to mediate cell and tissue death. The first component is the localization of a photosensitizing molecule in the target tissue, and the second component is the activation of the photosensitizer (PS) by light. In the light activation process, the photosensitizer acts as an energy transducer and transfers energy to molecular oxygen, resulting in the generation of a series of highly reactive oxygen species (ROS), particularly singlet oxygen. These ROS have been shown to cause oxidative damage to a number of molecules including lipids, proteins, and glycoproteins, and as a consequence damage to cellular membranes, organelles, and protein complexes (Dougherty et al. 1998). An efficacy of PDT is affected by many factors such as cell type, type of photosensitizer and its intracellular localization, light dose and its fluency rate, drug to light interval and photodynamic protocol (Blant et al. 1996, Henderson et al. 2004, Noodt et al. 1999, Ris et al. 1993, Sackova et al. 2005, Wyld et al. 2001). Photodynamic therapy has come a long way since beginning up to the present. The research of new natural photosensitizers as well as synthesis of photosensitizers with desired characteristics contributed to increased efficiency of this therapy. The ideal photosensitizer should fulfil several requirements. One of them is low level of a dark toxicity as well as low incidence of allergic reactions of patients. The photosensitizer should absorb light in the red or far-red wavelengths to achieve the

higher efficiency of the tumour treatment as a consequence of deeper penetration of the light in treated tissue. The photosensitizer should be easy available, it means that its extraction or synthesis should be inexpensive. The stability, water solubility and rapid pharmacokinetic elimination of PS from the patients are other important characteristics of these drugs (Fritsch et al. 1998, Kalka et al. 2000).

The therapeutic effect of photodynamic therapy is mediated by reactive oxygen species that can damage cellular components leading to cell death. Photochemical reaction creates reactive oxygen species and singlet oxygen with the lifetime not longer than 4 μs in aqueous solution (Redmond and Kochevar 2006). Since singlet oxygen movement is limited, the target of cell damage is expected at sub-cellular sites of PS localization. Therefore, predominant localization of PS in cell membranes leads to lipid oxidation and to formation of protein crosslinks (Shen et al. 1996, Spikes et al. 1999).

1.1.1 Hypericin as a potential photosensitizer

A natural substance with potent photosensitizing properties is hypericin, a naphthodianthrone derivative with a chemical structure 1, 3, 4, 6, 8, 13-hexahydroxy-10, 11-dimethylphenanthro[1, 10, 9, 8-opqra]perylene-7, 14-dione (Fig. 1a) isolated in 1939 as a secondary metabolite from *Hypericum perforatum L.* (St John`s wort) displaying a potential as a photosensitizer for PDT (Brockmann et al. 1939) (Fig. 1b). Apart from hypericin, the other metabolites of St John`s wort are investigated for their medical use. For example hyperforin is an acylphloroglucinol derivative with antibacterial activity (Gurevich et al. 1971) and antitumoral properties (Hostanska et al. 2003, Schempp et al. 2002). Hyperforin is also known as a dual inhibitor of 5-LOX and COX-1 suggesting therapeutic potential in inflammatory and allergic diseases connected to eicosanoids (Albert et al. 2002). A promising approach in the treatment of cancer diseases seems to be a combination of hypericin and hyperforin (Hostanska et al. 2003).

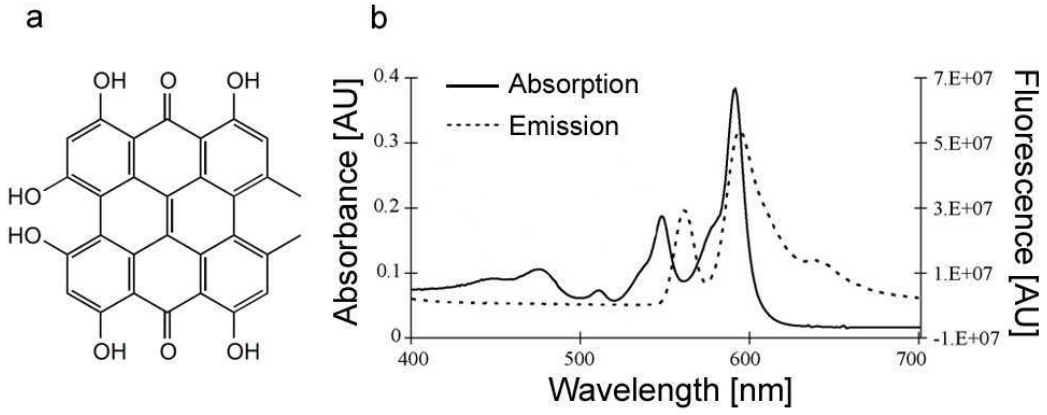

Figure 1. Hypericin. Chemical structure of hypericin (a), spectra of hypericin (b) (Mw=504.46) dissolved in ethanol (2.5 μg/ml) (excitation at 280 nm). Adapted from (Zeisser-Labouebe et al. 2006).

A potential application of hypericin in a photodynamic therapy in clinical oncology is an interesting research area for researchers as well as its using as a diagnostic tool in photodynamic diagnosis (PDD) of neoplastic lesions (Sim et al. 2005). Apart from anticancer properties, hypericin displays an antidepressant activity (Perovic and Muller 1995) and antiviral activity against a variety of viruses, in brief outline including influenza virus, herpes virus, leukemia virus, herpes simplex virus

type 1 in mice (Lavie et al. 1989, Tang et al. 1990) and anti-HIV activity (Holden 1991). Hypericin seems to be an effective drug in an anticancer therapy due to its advantageous properties. Hypericin inhibits key steps of angiogenesis (Martinez-Poveda et al. 2005), has not genotoxic activity (Miadokova et al. 2009) and its antimetastatic activity in the dark was also described (Blank et al. 2004). It was reported that hypericin increased activity and expression of drug efflux transporters in HT-29 cells (Jendzelovsky et al. 2009). The other biological effects of HYP are an inhibition of epidermal growth factor receptor tyrosine kinase activity (de Witte et al. 1993), specific inhibition of protein kinase C (Takahashi et al. 1989) and inhibition of succinoxidase (Thomas et al. 1992). Photodynamic properties of HYP are mediated through peroxidation of membrane lipids. Photo-activated HYP increases superoxide dismutase activity, decreases cellular glutathione levels, impairs mitochondrial function (Hadjur et al. 1996, Chaloupka et al. 1999, Miccoli et al. 1998, Thomas et al 1992, Utsumi et al. 1995, Vantieghem et al. 2001) and contributes to a drop of pH (Fehr et al. 1995). The HY is a source of high triplet quantum yield and superoxide anions (Ehrenberg et al. 1998, Thomas et al 1992, Thomas and Pardini 1992), therefore singlet oxygen (Type II mechanism) as well as reactive oxygen radicals (Type I mechanism) plays a major role in the photo-activity of hypericin in cells (Park et al. 1998). Hypericin seems to be very effective photosensitizer which has hydrophilic/lipophilic properties (Crnolatac et al. 2005) and binds to low density lipoproteins (LDL) at the boundary between the lipidic and protein part of the particle (Kascakova et al. 2005). Due to its hydrophilic/lipophilic properties the preferential localization of hypericin is in lipid membranes in cytoplasmic membranes. This compound accumulates in membranes of endoplasmic reticulum and Golgi complex, but not in mitochondria (Ho et al. 2009, Thomas and Pardini 1992) however mitochondrial membranes are central trgets of hypericin photodynamic action (Agostinis et al. 2002). Accumulation of HY was shown also in a nuclear plasma membranes (Miskovsky et al. 1995, Sattler et al. 1997) and lysosomes (Buytaert et al. 2006a). Hypericin uptake was shown to be higher in cells with elevated number of LDL receptors, however it seems that cellular uptake of hypericin is determined by diffusion and solubility and does neither require active transport nor specific receptors (Thomas and Pardini 1992). It seems that cellular localization of HY is a cell type dependent and its cellular targets are membranes (Hadjur et al. 1996, Chaloupka et al. 1999, Thomas and Pardini 1992).

1.1.2 Mechanisms in photodynamic therapy

The consequences of PDT on a cellular level vary according to activation of specific pathways, including apoptotic, autophagic, necrotic as well as pro-survival pathways. Apoptosis is programmed mechanism of cell death suitable for cancer therapies including PDT. Apoptosis contrary to necrosis is a type of cell death manifested by shrinking and blebbing of membrane, chromatin condensation and genomic DNA fragmentation. Cells forms membrane-enclosed vesicles called apoptotic bodies that are ingested by neighboring cells and phagocytes without involvement of immune system and without inflammatory reactions (Fiers et al. 1999, Kerr et al. 1972). Apoptosis may be activated by extrinsic pathway upon binding ligands the surface death receptors as TNF receptor 1, TRAIL receptor, or Fas receptor. Apoptotic program executes effector procaspase-3/7 cleaved by activated caspase-8/10 (Bellnier et al. 2003, Granville et al. 2001). A dominant role in PDT-induced apoptosis has intrinsic pathway mediated through mitochondria. PDT-mediated stress may cause loss of the mitochondrial transmembrane potential ($\Delta\Psi m$) and the release of cytochrome c (Cyc) from the intermembrane space into the intracellular space (Granville et al. 1998).

Cytoplasmic Cyc associates with the apoptotic protease activating factor 1 (Apaf-1) and forms the heptameric apoptosome that integrates procaspase-9, leading to its cleavage and resultant activation. Caspase-9 hydrolyzes and activates caspases-3/7, reaching the same terminal path as the extrinsic pathway (Granville et al. 1997, Varnes et al. 1999). Apart from cytoplasmic Cyc other mitochondrial protein may enhance apoptotic response. One of them is Smac/DIABLO (Second mitochondria-derived activator of caspase/direct inhibitor of apoptosis-binding protein with low pI) is such a protein and its release depends on cell type and photosensitizing protocol (Usuda et al. 2002). Smac/DIABLO interferes with a family of proteins called inhibitor of apoptosis (IAP) on procaspase-9, thus making it available for activation in the apoptosome. Apoptosis-inducing factor (AIF) is a mitochondrial protein that gets released during the initiation of apoptosis and translocates to the cell nucleus. There it degrades DNA independently of caspases (Furre et al. 2005). Other controlled cell death process occurred in PDT is autophagocytosis or autophagy (Buytaert et al 2006a, Buytaert et al. 2006b, Xue et al. 2007). The cell components, including whole organelles are sequestered in membrane-bound vesicles that fuse with lysosomes for degradation and reutilization of their components damaged by ROS (Klionsky 2005). In contrary to apoptosis, necrosis is a cell death characterized by cellular swelling, organelles alterations, rupture of plasma membrane, and finally cell lysis and leakage of the cellular components (Luo and Kessel 1997). Although cell death is expected and required response to PDT, in some cases, PDT induces signaling pathways associated with cell survival. Photodynamic treatment affects tumour cells directly as well as tumour vasculature and immune system. The PDT damages vasculature of tumors and can leads to tumour hypoxia (Agarwal et al. 1991), platelet aggregation, vessel constriction and vessel leakage (Evans et al. 1990, Schempp et al. 2001). These vascular events after PDT contribute to improved effect of the tumour treatment. Cytotoxic reactive oxygen species (ROS) induce vascular occlusion and may cause local inflammatory response mediated by complement activation cytokines (Korbelik et al. 2004, Korbelik 2006).

1.2 Hormesis – adaptive cell response - resistance

It is well known that cancer therapy is often complicated and could be attended by treatment failure. The response to cancer therapy can be significantly determined by stress response that depends on the stress conditions. Stress may activate increased production of reactive oxygen species (ROS) in the cells. When they are stimulated with ROS, cell signalling cascades are activated. It appears that the cellular redox potential is an important determinant of cell function and interruption of redox balance may it adversely affect. ROS damage cells by interactions with critical macromolecules including DNA, proteins, and lipids leading to cell death, mutation, and other toxicities (Martin and Barrett 2002). Apart from the involvement of ROS in apoptosis, ROS can also enhance mitogenesis in a number of cell types, including normal cells, initiated cells, and cancer cells. It is known that low levels of ROS may stimulate cell division and promote tumor growth, presumably through regulation of proliferative genes (Davies 1999, Dreher and Junod 1996). However, sub-toxic ROS production may affect cellular responses via alterations in cell signaling. It is well accepted that relatively low levels of ROS promote cellular proliferation rather that cause cell degeneration or death (Finkel 2000). This cellular response is related with the phenomenon called hormesis. Previously hormesis has been generally defined in terms of potential beneficial effects (Chapman 2002) and was used to describe the stimulatory effects on growth following single exposures to low doses of genotoxic agents which are toxic at high doses (Joiner et al. 1996). Nowadays, hormesis should be considered as an adaptive response

characterized by biphasic dose responses of generally similar quantitative features with respect to amplitude and range of the stimulatory response that are either directly induced or the result of compensatory biological processes following an initial disruption in homeostasis. Hormetic responses are characterized as biphasic dose-response relationships exhibiting low-dose stimulation and high-dose inhibition (Calabrese and Baldwin 2002). The ability of the cells, tissues or organism to better resist stress damage by prior to a lesser amount of stress is known as adaptive response. Oliviery et al. (1984) have demonstrated that cells exposed to small doses become less susceptible to the genotoxic effect of a subsequent high dose it referred as adaptive cell response. We can tell that cells seem to be resistant to the influence of a high dose.

There exist many definitions of resistance: the sum total of body mechanisms that interpose barriers to the invasion or multiplication of infectious agents, or to damage by their toxic products. Inherent resistance is an ability to resist disease independent of immunity or specifically developed tissue responses; it commonly resides in anatomic or physiologic characteristics of the host and may be genetic or acquired, permanent or temporary (http://www.doh.wa.gov/notify/other/glossary.htm).

Another definition referred resistance as the ability of an organism to exclude or overcome, completely or in some degree, the effect of a pathogen or other damaging factor. Resistance is sometimes referred as a tolerance - the ability of an organism to sustain the effects of a disease without dying or suffering serious injury (http://ppathw3.cals.cornell.edu/glossary/Defs_R.htm). Different stress conditions can cause resistance in biological systems. There are some examples of stresses such as heat shock, radiation, drugs, chemicals and photodynamic action.

1.2.1 Resistance to different stimuli

Thermo-tolerance

The response to heat shock provides probably the most spectacular example of the cellular capacity to react in an active manner to toxic stress. An exposure to mild heat shock induces the development of thermo-tolerance, a state of extreme resistance to severe heat shock (Gerner and Schneider 1975). The thermo-tolerance develops within a few hours after exposure to heat shock and lasts for 2–3 days. Its development is accompanied by the transcriptional activation and accumulation of a group of highly conserved proteins called heat shock proteins (HSPs) (Landry et al. 1982, Li and Werb 1982, Subjeck et al. 1982). Until recently, the protective role of HSPs was confined to their chaperone function, it means, their capacity to bind heat-denatured proteins and prevent their irreversible aggregation (Lindquist 1986). However, recent findings reveal that HSPs can regulate both the signaling and the execution of major cell death pathways (Beere and Green 2001, Jaattela 1999). Consequently, HSPs play a primordial role in the resistance to a variety of toxic agents and situations that do not necessarily involve protein denaturation (Beere et al. 2000, Gabai et al. 2000, Mosser et al. 1997, Nylandsted et al. 2000, Pandey et al. 2000). This evolutionary conserved response is triggered at least in part by heat-induced accumulation of denatured proteins (Ananthan et al. 1986). At normal temperatures, HSP70, HSP40, and HSP90 are expressed at low basal level and maintain the heat shock transcriptional factor (HSF) in a repressed state. Relief of repression occurs via the titration of the HSPs by the stress-induced unfolding and denaturation of native proteins (Lindquist and Craig 1988, Morimoto 1993, Mosser et al. 1990, Zou et al. 1998). This results in the activation of HSF, the activation of hsp genes, and the accumulation of HSPs, which contributes in enhancing cell survival against subsequent protein-denaturing heat shock and in turning off HSF. HSPs

accumulation occurs in terms of hours. Another evolutionary conserved heat shock response develops in minutes and leads to the activation of the major signaling transduction pathways involving mitogen-activated protein kinases (MAPKs). The members of MAPK are extracellular lignal-regulated kinase (ERK), stress-activated protein kinase 1 (SAPK1)–c-Jun N-terminal kinase (JNK) (called here JNK), and SAPK2/p38 (called here p38) (Dorion et al. 1999, Guay et al. 1997). These signalling cascades play a central role in the regulation and determination of cell fate, such as growth, differentiation, or apoptosis in numerous physiological as well as stress conditions. The mechanisms of activation and the roles of these pathways during heat shock have been the subject of recent investigations.

Activation of p38 and JNK early during heat shock is a mechanism of heat-induced cell death and that the desensitization process may be a mechanism of thermo-tolerance. Support for this idea has been obtained in the case of JNK, where blocking its activation was shown to be sufficient to protect cells against various stressors including heat shock (Gabai et al. 2000, Mosser et al. 2000, Park et al. 2001). Recent studies further proposed that regulation of JNK activity is a mechanism of HSP70-mediated protection. Overexpression of HSP70 can inhibit JNK activation by various stimuli, including heat shock, sorbitol, TNF, UV light, IL-1, and H_2O_2 (Gabai et al. 1997, Mosser et al. 1997). Mechanism of JNK inhibition involves the direct binding of HSP70 to JNK (Park et al. 2001) or an HSP70-mediated protection of a JNK phosphatase from heat denaturation (Meriin et al. 1999). The inhibition of JNK activity could therefore be a factor of acquired thermo-tolerance. In contrast, the activation of the p38 pathway leads to the phosphorylation of one of the HSPs, HSP27 (Huot et al. 1995, Chretien and Landry 1988, Landry et al. 1991), an event that is generally assumed to be protective. The phosphorylation of HSP27 is catalyzed by MAPKAP kinase-2, a serine-protein kinase itself activated by phosphorylation by p38 (Huot et al 1995, Rouse et al. 1994). Upon phosphorylation, major changes are induced in the supramolecular organization of HSP27, changes that are thought to activate a homeostatic function of the protein (Lambert et al. 1999). One of the phosphorylation-modulated functions of HSP27 is the regulation of actin dynamics. HSP27 phosphorylation is involved in the stabilization of the actin filament during stress (particularly oxidative stress) and also in mediating rapid change in actin filament dynamics in response to stimuli that activate the p38 pathway (Guay et al 1997, Landry and Huot 1999, Lavoie et al. 1995, Schafer et al. 1999). HSP27 phosphorylation occurs not only after heat shock but also after stimulation by various types of agonists, including tyrosine kinase, serpentine, or cytokine receptor activators. Although it is essential in several physiological events requiring modulation of actin polymerization, this activity of HSP27 can also mediate inappropriate actin polymerization activity and lead to extensive cell blebbing and apoptosis. This was shown to occur when an incorrect balance is generated between the activity of p38 and ERK, as for example, during treatment with toxic agents such as cisplatin (Deschesnes et al. 2001, Huot et al. 1998). Toxic effects resulting from excessive or badly timed actin polymerization activities may also occur upon stress, when the concentration of HSP27 is very high (Deschesnes et al. 2001). It is thus possible that p38 desensitization is protective during thermo-tolerance, preventing an overload in the homeostatic response and stringently circumscribing the induced stimulatory effects in a given time frame. This restriction in the duration of activation of the signaling pathway may be important to ensure that an adequate response is generated (Dorion et al. 1999).

Chemo-resistance

The failure of cancer cells, viruses, or bacteria to respond to a drug used to kill or weaken them is termed as drug resistance. The cells, viruses, or bacteria may be resistant to the drug at the beginning of treatment, or may become resistant after being exposed to the drug (http://www.nci.nih.gov/dictionary/?CdrID=416100). Resistance to chemotherapeutic drugs is a principal problem in the treatment of cancer. Because of the serious problem of clinical drug resistance, much effort has been expended to advance understanding of the mechanisms of drug resistance in cancer cells. The molecular mechanisms of drug resistance, however, are not fully understood (Tsuruo et al. 2003). Resistance to a broad spectrum of chemotherapeutic agents in cancer cell lines and human tumors has been called multidrug-resistance (MDR) (Tsuruo 1988). In chemo-resistance and chemo-sensitivity of tumor cells play important roles membrane transporters mediating this phenomenon. ATP binding cassette (ABC) transporters, such as ABCB1/MDR1, ABCC1/MRP1 and ABCG2/BCRP, are frequently associated with decreased cellular accumulation of anticancer drugs and multidrug resistance of tumors. Solute carrier transporters, such as folate, nucleoside, and amino acid transporters, commonly increase chemo-sensitivity by mediating the cellular uptake of hydrophilic drugs. Ion channels and pumps variably affect sensitivity to anticancer therapy by modulating viability of tumor cells (Huang and Sadee 2006). In particular, ABC transporters, such as the multiple drug resistance transporter MDR1 (multidrug resistance 1, ABCB1 or P-glycoprotein), mediate energy-dependent drug efflux and play a main role in chemo-resistance (Gottesman et al. 2002). Multiple types of membrane transporters contribute to chemo-sensitivity and chemo-resistance of tumor cells. Water-soluble drugs, such as cisplatin, nucleoside analogues and antifolates, cannot cross the plasma membrane unless they 'piggy-back' onto membrane transporters, or enter through hydrophilic channels in the membrane. Resistance may result from decreased activity of the uptake transporters, or alternatively, enhanced efflux. For hydrophobic drugs, such as the natural product vinblastine, doxorubicin, and paclitaxel, entry occurs largely by diffusion across the membrane, although this process can be critically enhanced by transport proteins. Cellular resistance to these drugs commonly results from increased drug efflux mediated by energy-dependent transporters. Indirect mechanisms may also modulate chemo-sensitivity. For example, transporters and channels can affect chemo-sensitivity by providing nutrients to cancer cells or modulating the electrochemical gradient across membranes, thereby, modifying apoptosis pathways or the efficiency of drug diffusion along electrochemical gradients into cells. Transporters can be classified into passive and active transporters. The latter are further classified as primary- (ABC transporters) or secondary-active transporters according to the mechanism of energy coupling (Huang and Sadee 2006).

Radiation resistance

The adaptive response is a phenomenon in which the resistance to high-dose ionizing radiation is acquired by prior exposure to low-dose radiation. Olivieri et al. (1984) first identified this type of adaptive response using human lymphocytes *in vitro*, and others later confirmed it in many studies showing, for example, resistance to the induction of mutations (Ueno et al. 1996), chromosomal aberrations (Wolff 1996) and apoptosis (Sasaki et al. 2002). Evidence of an adaptive response during embryogenesis has also been reported in chicken embryos (Tempel and Schleifer 1995) and in limb buds (Wang et al. 1998). Its molecular mechanisms are largely unknown. The optimum dose of prior low-dose radiation required for observation of the radiation adaptive response is below 10 cGy in mammalian cells (Sasaki 1995). However, in studies

carried out *in vivo*, the priming whole-body doses 1.0 Gy (Mitchel et al. 1999), 30 cGy (Wang et al. 1998), 15–60 cGy (Takahashi et al. 2003) to which mice were exposed were higher than those given in the *in vitro* studies. The radiation adaptive response was observed in cultured mouse cells in the 1-h interval between the priming and challenge radiation exposures, reaching its peak level at 4–9 h after the priming dose (Sasaki 1995). Radiation-sensitivity is quite high during organogenesis (Russell and Russell 1954). In the adaptive response during embryogenesis of mice, 2 cGy g rays may be a large enough primary conditioning dose to suppress radiation-induced teratogenesis, and that the period of gestation when fetuses are exposed to radiation might be important (Okazaki et al. 2005).

1.2.2 Resistance to photodynamic therapy

Relatively new approach in photodynamic therapy is modification in the delivery of photo-radiation (Gibson et al. 1990). Recently, new modifications in light delivery regime have been introduced on the standard photodynamic protocol (single-dose photosensitizer, single-dose light) to maximize the therapeutic effect of PDT. For example by reducing the fluency rate to improve oxygenation (Henderson et al. 2004, Hua et al. 1995, Pogue and Hasan 1997, Robinson et al. 1998, Sitnik et al. 1998, Thong et al. 2006), enabling re-oxygenation in treated tissue (Curnow et al. 1999, Takahashi and Ohnishi 2009) or by fractionated drug administration (Cavarga et al. 2005, Dolmans et al. 2002, Webber et al. 2005). It has been hypothesized that splitting the light dose into fractions by interrupting illumination for a certain time allows the treatment site to be re-oxygenated, which results in increased generation of singlet oxygen and thus a greater PDT effect (Hua et al. 1995, Pogue et al. 2001, Robinson et al. 2000). Fractionated light regime uses light disrupted at a particular point for a period of darkness to increase the efficacy of photodynamic therapy {Ascencio et al. 2008, Babilas et al. 2003, Curnow et al. 2000, Curnow et al. 1999, de Bruijn et al. 2007, de Bruijn et al. 2006, de Bruijn et al. 1999, Gibson et al. 1990, Huygens et al. 2005, Iinuma et al. 1999, Messmann et al. 1995, Paba et al. 2001, Pogue et al. 2008, Sackova et al. 2005, Togashi et al. 2006, Varriale et al. 2002, Xiao et al. 2007). In contrast to *in vivo* studies, in which enhanced or no effect of fractionated irradiation was shown, the so far known *in vitro* works report either on photo-resistance/photo-tolerance (Paba et al. 2001, Varriale et al. 2002) or on decreased production of reactive oxygen species and cytotoxicity via regeneration of glutathione (Oberdanner et al. 2005). In the last decade, an application of light fractionation in PDT achieved increased attention of researchers and led to the comparison of continuous and fractionated light regimes (Ascencio et al. 2008, Curnow et al. 2000, de Bruijn et al. 1999, Sackova et al 2005, Xiao et al. 2007). Indeed, improved efficiency of fractionated light delivery was demonstrated on various models *in vivo* (Ascencio et al 2008, Curnow et al 2000, de Bruijn et al 1999, Pogue et al. 2008, Takahashi and Ohnishi 2009, Xiao et al 2007). However, the outcome of fractionated light regime is still limited by some parameters such as distribution of photosensitizers in tissue (de Bruijn et al. 2007), dark intervals between light doses (de Bruijn et al. 1999, de Bruijn et al. 2006, Sackova et al. 2005, Togashi et al. 2006, Uehara et al. 1999) or oxygen depletion (Huygens et al. 2005). It was shown that fractionated light regime with a longer dark period resulted in a decrease of hypericin cytotoxicity. Longer dark interval after the irradiation of cells by first light dose makes cells resistant to the effect of the second illumination. These findings confirm that the light application scheme together with other photodynamic protocol components is crucial for the photocytotoxicity of hypericin (Sackova et al. 2005). The photo-activation of hypericin with low doses of light-induced apparent photo-resistance in

human histiocytic lymphoma U937 cells (Paba et al. 2001) and HT-29 cells (Sackova et al. 2005). Pre-sensitized U937 cells with hypericin appear to be fully resistant to light doses that normally determine massive cellular apoptosis in experimental photodynamic therapy. Pre-sensitization renders cells insensitive to higher light doses. Photo-resistance was manifested by changes in levels of expression of pro- and antiapoptotic proteins, PARP fragmentation and cell viability (Paba et al. 2001).

Also, low-energy pre-sensitization caused enhanced photo-tolerance of hypericin-loaded HEC1-B cells (Varriale et al. 2002). Fractionated illumination did not enhance the efficacy of PDT using methyl 5-aminolevulinate but it did in case of ALA application (de Bruijn et al. 2007). Singh and his co-workers (2001) examined mechanism(s) of action for PDT via the generation of PDT-resistant cell lines. In this study they used three human cell lines, namely, human colon adenocarcinoma (HT-29), human bladder carcinoma and human neuroblastoma. The three photosensitizers used were Photofrin, Nile Blue A and aluminum phthalocyanine tetrasulfonate. The protocol for inducing resistance consisted of repeated *in vitro* photodynamic treatments with a photosensitizer to the 1–10%-survival level followed by regrowth of single surviving colonies. Varying degrees of resistance were observed. They determined that the mechanisms and pathways of cellular death are sensitizer specific. For the HT-29 cell line they were able to create resistant variants for all three photosensitizers. It is not apparent from either the initial clonogenic survival curves or any properties intrinsic to this cell line why resistance was possible here and not in the other two cell lines. The cells HT-29 was significantly more resistant to Nile Blue A–mediated PDT but displayed intermediate sensitivity to the other sensitizers. As such, they were unable to identify any characteristics of the three cell lines that were predictive of their ability to generate resistant variants upon repeated PDT action (Singh et al. 2001).

In PDT, the photo-tolerance, as any type of unexpected resistance should be regarded as a potential adverse process. The present data do not unravel the molecular mechanism underlying the appearance of photo-resistance. However, the observed stimulation of the expression of the HSP70 protein upon photo-induced stress, may suggest its involvement in this process (Paba et al. 2001). There is strong evidence that HSP induction coincides with acquisition of tolerance to stress which otherwise may kill the cell. For example, heat-shocked cells are more resistant to environmental stress and death (Jaattela et al. 1992, Lindquist and Craig 1988). Similarly, apoptosis induced by various stresses is inhibited in heat-shocked cells suggesting that HSPs play a role in resistance mechanisms (Mosser and Martin 1992). Finally, it was demonstrated that mild pre-sensitization endows cells with an unexpected high degree of photo-tolerance, enhances HSP70 synthesis, sequentially promotes the expression of specific apoptosis-related proteins and causes cell cycle arrest (Varriale et al. 2002). Photofrin-mediated PDT can also induce expression of mitochondrial heat shock protein HSP60 in colon cancer cell line HT-29 and its PDT-induced resistant variant HT-29-P14 as well as the radiation-induced fibrosarcoma cells RIF-1 and its PDT-resistant variant, RIF-8A (Hanlon et al. 2001). Photodynamic therapy-mediated hypoxia may induce also expression of hypoxia-inducible factor-1α (HIF-1α) and plays the role in resistance to apoptosis in ALA-mediated PDT (Ji et al. 2006). However in normoxic condition is induction of HIF-1α is mediated by the prostaglandin pathway (Mitra et al. 2006).

The role of extracellular signal-regulated kinases (ERKs) in the cell survival after PDT is less clear. However sustained ERK1/2 activation protects cells from Photofrin-mediated phototoxicity and duration of ERK1/2 activation is regulated by mitogen-activated protein kinase phosphatase MKP-1. Blocking of the sustained ERK

activity with inhibitor of mitogen-activated protein/ERK kinase significantly decreased cell survival of PDT-resistant LFS087 cells (Tong et al. 2002).

In photodynamic therapy, with the phthalocyanine photosensitizer Pc 4 [HOSiPcOSi(CH3)2(CH2)3N(CH3)2] was an oxidative stress associated with induced activation of sphingomyelinase, ceramide generation and subsequent induction of apoptosis in various cell types. Although ceramide was elevated in normal lymphoblast after PDT, accumulation of ceramide in Niemann–Pick human lymphoblasts (NPD) was significantly suppressed. Resistance of NPD cells seems to be associated with the loss of acid sphingomyelinase function (Separovic et al. 1999). This result agrees with the similar defects observed in NPD cells in response to ionizing radiation (Santana et al. 1996).

Resistance to cancer therapies is a serious problem. Each of information which contributes to better understanding of events underlying resistance development can improve therapeutic outcome. Therefore it is important to pay attention to phenomenon of resistance.

1.3 Molecules playing role in resistance to cancer therapies

1.3.1 Heat shock proteins

All living organisms respond at a cellular level to unfavourable conditions such as heat shock, or other stressful situations of many different origins. Reactions of stressed cells are characterized by an expression of a small number of specific genes (heat shock genes). Consequently, the products of this genes – heat shock proteins or stress proteins – are also present under normal conditions but in lesser amounts. Cellular stress can engage two fundamental responses: apoptosis, a cell death mechanism that eliminates irreparably damaged cells, and stress response. In stress response the heat shock proteins (HSPs) function to sustain survival by limiting cellular damage and accelerating recovery. Evidence indicates that the coordinated interaction between these two functionally opposing pathways, apoptosis and the stress response, may determine cellular susceptibility to damaging stresses. The HSPs are a large family of highly conserved proteins broadly categorized according to their size. Some are constitutively expressed and associated with specific intracellular organelles, and others are rapidly induced in response to cellular stress. HSPs function collectively to protect cells from the potentially fatal consequences of adverse environmental, physical, or chemical stresses by their ability to prevent protein aggregation and to promote the refolding of denatured proteins (Parsell and Lindquist 1993). The protective function of the HSPs may be extended to include an antiapoptotic role for several members of the HSP family, including HSP70, HSP90 and HSP27 (Beere and Green 2001).

HSP70

HSP70 and its cochaperones, especially the Bcl-2–associated athanogene family proteins, are well-recognized antiapoptotic factors. The mechanisms by which they exert their effects, however, are just beginning to be understood in detail. It was shown that HSP70 *in vitro* (Beere et al. 2000) and in whole cells (Saleh et al. 2000) blocks the assembly of a multiprotein complex termed the apoptosome. This complex is essential for activating the cascade of cysteine-aspartyl proteases known as caspases that are responsible for executing the apoptotic program. Enforced overexpression of HSP70 in stably transfected cells provides protection from stress induced apoptosis at the levels of both cytochrome c release and initiator caspase activation. Furthermore, it has been shown that the actual chaperoning function of HSP70 is required for this protection

(Mosser et al 2000). Conversely, antisense-mediated inhibition of HSP70 expression has been shown to cause massive death in multiple breast cancer cell lines, whereas nontumorigenic breast epithelial cells are not affected (Nylandsted et al. 2000). The first study to demonstrate a correlation between the antiapoptotic effects of HSP70 and an inhibition of caspase activity provided no specific mechanism except to suggest that the point of HSP70 intervention was upstream of caspase-3 activation (Mosser et al. 1997). Subsequently, it has been demonstrated that HSP70 is able to directly inhibit caspase processing by interacting with Apaf-1 to prevent the recruitment of procaspase-9 to the apoptosome (Beere et al. 2000, Saleh et al. 2000). HSP90 and HSP27 are also reportedly able to inhibit the formation of a functionally competent apoptosome, HSP90 by directly associating with Apaf-1 to prevent its oligomerization (Pandey et al 2000), and HSP27 by binding and sequestering cytosolic cytochrome c away from its target Apaf-1 (Bruey et al. 2000). Although it is unlikely that the disruption of apoptosome assembly is the only point of intervention by the HSPs, it represents a likely target for HSPs with the potential for a significant effect on cell survival (Beere and Green 2001).

HSP90

In vertebrates, two distinct genes encode constitutive and inducible isoforms of the protein (HSP90h and HSP90a, respectively), but functional differences between these isoforms are poorly understood. Homologues of HSP90 are also found in the endoplasmic reticulum (GRP94) and mitochondrion (TRAP1). Recently, HSP90 variant (HSP90N) has been identified (Grammatikakis et al. 2002) that seems to be primarily membrane associated as a result of its unique hydrophobic NH2-terminal domain. Limited information exists on its precise cellular functions. HSP90 resides primarily in the cytoplasm, where it exists predominantly as a homodimer. Each homodimer is made up of monomers consisting of three main functional domains that display important functional interactions. The NH2-terminal domain contains an adenine nucleotide binding pocket of the GHKL superfamily (Dutta and Inouye 2000). Structural alterations driven by the hydrolysis of ATP to ADP in this pocket are thought to play an essential role in the chaperoning activity of the protein. This pocket is also the binding site of the structurally unrelated natural products geldanamycin and radicicol as well as the growing number of semisynthetic derivatives and synthetic compounds. These drugs bind with higher affinity than nucleotides do, and they lock the domain in its ADP-bound conformation. These drugs thus alter many if not all of the normal functions of the chaperone (Roe et al. 1999).

Endoplasmic reticulum and Golgi apparatus are folding sites of newly synthesized proteins. This chaperone is pivotal for stability and function of a large group of client proteins including ser/thr quinces, tyrosine quinces, mutated p53, cyclin D-associated Cdk4 (Helmbrecht et al. 2000) and Cdk6, and wild-type Plk (Simizu and Osada 2000). Replication mechanisms in cells that lose HSP90-protective function are severely compromised, disabling cell progression through the cell cycle (Piper 2001). Indeed, HSP90 modulators such as geldanamycin or radicicol, which interact with the ATP binding pocket of HSP90, exhibit potent anticancer effects (Neckers 2002).

In photodynamic therapy used photosensitizer hypericin is localized to endoplasmic reticulum and Golgi apparatus (Uzdensky et al. 2001) which are folding sites of newly synthesized proteins as mentioned before. Hypericin can cause reduction in intracellular pH by proton transfer to surrounding molecules (Sureau et al., 1996) leading to pH-dependent structural changes in proteins (Tcherkasskaya and Uversky 2001). The broad range of activities may, thus, result from hypericin targeting chaperone networks. Hypericin inactivates the chaperone activity via ubiquitinylation.

This effect appears to be exclusive to HSP90 and not to affect HSP70 chaperones (Blank et al. 2003). HSP90 and its cochaperones are also reported to modulate tumor cell apoptosis. Much of this activity seems to be mediated through effects on AKT (Basso et al. 2002), tumor necrosis factor receptors (Vanden Berghe et al. 2003), and nuclear factor-κB function (Chen et al. 2002). However, HSP90 may also play a more global role in facilitating neoplastic transformation than just inhibiting apoptosis. Among the heat shock proteins, HSP90 is unique because it is not required for the biogenesis of most polypeptides (Nathan et al. 1997). This finding has led to the suggestion that HSP90 inhibitors may prove of unique therapeutic benefit (Bagatell and Whitesell 2004).

GRP94 is a glucose-regulated protein of 94 kDa, also known as gp96 or endoplasmin, the ER paralog of HSP90 and is found only in higher eukaryotes. GRP94 is essential for proper assembly and maturation of numerous client proteins (Melnick et al. 1992, Nigam et al. 1994, Randow and Seed 2001). Wassenberg at al. (2000) described bis-ANS and heat shock induction of GRP94 multimerisation. A tertiary conformational change is accompanied by a marked elevation of chaperone and peptide binding activity. In this conformation, GRP94 can undergo, in a concentration-dependent manner, homotypic oligomerization. Exposure to heat shock caused a relatively rapid formation of tetramers, hexamers and octamers of GRP94 with high molecular weights (Wassenberg et al. 2000).

HSP27

Elevated levels of HSP27 are observed in many tumor types and are often correlated with a drug-resistant phenotype. When overexpressed *in vitro*, HSP27 confers enhanced cellular survival in response to a variety of proapoptotic stimuli. Exposure of cells to stresses such as heat shock, IL-1, TNF-α, and chemotherapeutic agents induces the transcription-dependent accumulation and rapid phosphorylation of HSP27 (Rouse et al. 1994). This p38-dependent, MAPK-activated protein kinase-2-mediated phosphorylation of HSP27 is essential for its survival-promoting effects (Lavoie et al. 1995). The protective capacity of HSP27 is likely due to its unique ability to modulate the dynamics of microfilament reorganization so as to maintain stability of the cytoskeleton under conditions of cellular stress (Guay et al 1997, Huot et al. 1996). Aldrian et al. (2002) demonstrated that HSP27 overexpression decreased invasion of melanoma cells (Aldrian et al. 2002). In contrast, others have shown that HSP27 increases cell migration in both breast and smooth muscle cells (Hansen et al. 2001, Hedges et al. 1999).

Clusterin

Clusterin/apolipoprotein J is an enigmatic protein which has chaperone-like activity similar to that of small heat shock proteins and may play role in cytoprotection (Humphreys et al. 1999). In human cells are two isoforms of clusterin generated by an alternative splicing. The main product of the clusterin gene is a ~60 kDa pre-secretory form (pre-sCLU), which is targeted to the endoplasmic reticulum by an initial leader peptide and could be glycosylated and cleaved into ~40 kDa α- and β-subunits which held together by disulphide bonds. The mature form ~80 kDa of sCLU is secreted to extracellular space (Burkey et al. 1991, Wong et al. 1993). Intracellular pre-nuclear isoform (pre-nCLU) is 50-55 kDa is localized in the cytoplasm and not exerts apoptotic effect whereas activated pre-nCLU (n-CLU) translocates to nucleus and contributes to cell death (Leskov et al. 2003). At low doses of irradiation, secretory clusterin (sCLU) production provides a cytoprotective molecular chaperone defence mechanism in

clearing cell debris from traumatised tissue. At higher doses, the pre-nCLU becomes activated. Activated nuclear clusterin (nCLU), a prodeath mature 55 kDa protein that causes apoptosis, is formed (Araki et al. 2005). Increased ROS and lipid peroxidation levels, while not affecting cell viability, elicit a significant and concomitant increase in levels of clusterin mRNA and protein (Strocchi et al. 2006). It was described that decreased expression of clusterin is involved in rheumatoid arthritis and high levels of extracellular CLU and low expression of intracellular CLU may enhance NF-κB activation and survival of the synoviocytes (Devauchelle et al. 2006). Disruption of the clusterin gene promotes NF-κB activation (Devauchelle et al. 2006, Santilli et al. 2003). Attenuation of NF-κB activation after heat shock is both dose- and time-dependent (Schell et al. 2005).

1.3.2 Nuclear transcription factor-kappaB

Apoptosis is negatively regulated by the activities of "survival factors" such as insulin-like growth factor-1 (IGF-1), nerve growth factor (NGF), and platelet-derived growth factor (PDGF). These factors mediate their survival-promoting effects at least partly by activation of the phosphatidylinositol 3-kinase (PI3K) to serine-threonine proteine kinase B or Akt (PKB/Akt) signaling cascade (Datta et al. 1999). Activation of PKB/Akt occurs at the plasma membrane and has been shown in several studies to be followed by its translocation to both the cytosol and nucleus (Borgatti et al. 2000, Filippa et al. 2000). Many of the substrates of PKB/Akt are proteins that function in the nucleus. PKB/Akt may promote cell survival by directly phosphorylating transcription factors that control the expression of pro- and anti-apoptotic genes. PKB/Akt appears to both negatively regulate factors that promote the expression of death genes and positively regulate factors that induce survival genes (Nicholson and Anderson 2002). Akt-mediated phosphorylation of the proapoptotic Bcl-2 family protein Bad at Ser136 induces its dissociation from Bcl-XL (to which Bad is constitutively bound), to promote the sequestration of BAD by 14-3-3 proteins in the cytosol. Thus prevents BAD from interacting with Bcl-2 or Bcl-XL at the mitochondrial membrane (Zha et al. 1996). Akt-mediated phosphorylation and functional inactivation of caspase-9 may also contribute to the antiapoptotic activity of Akt (Cardone et al. 1998). The scope of Akt survival-promoting activity broadens further with its ability to regulate the activity of transcription factors such as forkhead (FKHRL1) (Brunet et al. 1999) and nuclear factor κB (NF-κB) (Romashkova and Makarov 1999). PKB/Akt has been shown to interact with and activate IKKa. Data suggest that PKB/Akt phosphorylates IKKa directly but more importantly PKB/Akt is believed to be essential for IKK-mediated destruction of I-κB and activation of NF-κB (Romashkova and Makarov 1999).

CREB is transcription factor which bind to certain sequences called cAMP responses elements (CREs) in DNA and thereby increase or decrease the transcription of certain genes. CREB is also a direct target for phosphorylation by PKB/Akt (Du and Montminy 1998) and this phosphorylation occurs on site that increases binding of CREB to accessory proteins necessary for induction of genes containing CREs in their promoter regions. CREB has also been shown to mediate PKB/Akt-induced expression of anti-apoptotic gene mcl-1 (Wang et al. 1999).

Transcription factor NF-κB is undoubtly one of the major regulators of the inflammatory response initiated in the context of numerous pathologic and nonpathologic events. NF-κB is playing a key role in tumor demise by eliciting the onset of the immune defense against the tumor. Yet, NF-κB also modulates the expression of anti-apoptotic genes which may, in turn, favour tumor cell survival in response to pro-apoptotic therapeutics (Matroule et al. 2006). Akt can increase NF-κB

activity by accelerating the degradation of inhibitor of κB (IκB), which associates with and retains NF-κB in the cytosol (Kane et al. 1999). NF-κB is then available to regulate the expression of genes, which include the antiapoptotic Bcl-2 family member A1 (Zong et al. 1999) and the caspase inhibitors c-IAP1 (You et al. 1997) and c-IAP2 (Chu et al. 1997). NF-κB is likely involved in tumor recurrence phenomena by upregulating COX-2 and MMPs that are primary actors in tumor cells proliferation and angiogenesis (Lee et al. 2006). NF-κB is also sensitive to the cellular oxidative status. Since then, the key role of ROS as second messengers in NF-κB activation has been investigated in the context of multiple stimuli (TNF-α, IL-1β, UVs, calcium ionophore, LPS) (Schoonbroodt and Piette 2000). NF-κB is involved in the regulation of cell proliferation, apoptosis, and survival by a wide range of cytokines and growth factors and also it is critical in tumourigenesis (Baldwin 2001). Its survival-promoting activity is mediated through its ability to induce prosurvival genes such as c-IAP-1 and c-IAP-2. NF-κB is regulated through its association with an inhibitory cofactor I-κB, which sequesters NF-κB in the cytoplasm. Phosphorylation of I-κB by upstream kinases, known as IKKs, promotes its degradation allowing NF-κB to translocate to the nucleus and induce target genes (Romashkova and Makarov 1999). Low level of ROS may function as second messengers activating pathways that protect cells against apoptotic stimuli (Chandra et al. 2000). Reactive oxygen intermediates (ROI) serve as messengers mediating directly or indirectly the release of the inhibitory subunit IκB from transcription factor NF-κB (Schreck et al. 1991). NF-κB is often considered to be a ROS-responsive transcription factor (Chandra et al 2000, Janssen-Heininger et al. 2000) also shown to be implicated in a cancer cell responses to photodynamic therapy (Legrand-Poels et al. 1995). Phosphorylation and degradation of IκB is an important step for NF-κB releasing from complex with IκB, translocation from cytoplasm to nucleus and binding to DNA. Human colonic epithelial cells HT-29 have altered regulation of IκB-α degradation and activation of NF-κB activity can occur independently of IκB degradation (Jobin et al. 1997, Wang et al. 2000).

1.3.3 Mitogen activated protein kinases

The MAPKs are group of serine/threonine protein kinases that are activated in response to a variety of extracellular stimuli and mediate signal transduction from the cell surface to the nucleus. Together with several others signaling pathways, they can alter fosforylation status of numerous proteins, including transcription factors, cytoskeletal proteins, kinases and other enzymes, and influence gene expression, metabolism, cell morphology, cell division and cell survival. There are four major groups of MAPKs in mammalian cells – the ERKs, p38 MAPKs, JNKs and ERK5 or BMK cascades (Wada and Penninger 2004). Mitogen-activated protein kinases (MAPKs) are activated in a cascade of phosphorylation reactions in which individual MAP kinases are phosphorylated. In general, each group of MAP kinases is activated by a specific MAPK kinase (Fanger et al. 1997). Upstream signaling molecules involve kinases, adaptors, and receptors or sensors, which connect the pathway to specific stimuli (Chang and Karin 2001, Widmann et al. 1999).

The p38 (also known as CSBP, mHOG1, RK, and SAPK2) is the member of the MAPK-related pathway in mammalian cells (Han et al. 1994, Lee et al. 1994) and consists of the four known p38 isoforms (α, β, γ and δ) (Kyriakis and Avruch 1990). In mammalian cells, the p38 isoforms are strongly activated by environmental stresses, inflammatory cytokines and VEGF but not appreciably by mitogenic stimuli. Most stimuli that activate p38 also activate JNK (Lee et al. 1994). The p38 pathway consists of membrane receptors or sensors that are connected through adapter proteins to GTP-

ases that are upstream of MAPK kinase, (MKK), and the MAPK itself (Brancho et al. 2003). The p38 also regulates the immune response by stabilizing specific cellular mRNAs involved in this process (Ono and Han 2000). While the exact mechanisms involved in p38 immune functions are starting to emerge, activated p38 has been shown to phosphorylate several cellular targets, including cytosolic phospholipase A2, the microtubule-associated protein Tau, and the transcription factors ATF1 and ATF2, MEF2A, Sap-1, Elk-1, NF-B, Ets-1, and p53 (Kyriakis and Avruch 1990). It was previously shown that p38 MAP kinase is necessary for the regulation of TGFβ-mediated increases in cell adhesion and invasion (Hayes et al. 2003) and also, inhibition of p38 MAP kinase blocks HSP27 phosphorylation, and decreases invasion in smooth muscle cells (Hedges et al. 1999). Hypericin mediated PDT of human cancer cells leads to up-regulation of the inducible cyclooxygenase-2 enzyme and the subsequent release of PGE2. COX-2 protein levels are up-regulated in cancer cells by hypericin-mediated PDT in a time- and dose-dependent fashion. This COX-2 expression is remarkably dependent on the PDT stress. Inhibition of p38a MAPK resulted in suppression of the PDT-induced COX-2 expression, PGE2 and VEGF release, and tumor-induced endothelial cell migration. The p38 MAPK α and β mediate COX-2 up-regulation at the protein and messenger levels. The half-life of the COX-2 messenger was drastically shortened by p38 MAPK inhibition in transcriptionally arrested cells, suggesting that p38 MAPK mainly acts by stabilizing the COX-2 transcript, however transcriptional regulation by nuclear factor NF-κB was not involved in COX-2 up-regulation by PDT. Although p38 MAPK activation by PDT is required to up-regulate COX-2, this enzyme is not likely the direct downstream mediator of the p38 MAPK anti-apoptotic response. This indicates that p38 MAPK is a common target of hypericin-based PDT and a general mediator of COX-2 up-regulation in photo-damaged cancer cells (Hendrickx et al. 2003).

Many stresses that engage apoptosis simultaneously induce the activation of c-Jun NH2-terminal kinase (JNK). However, the precise role of JNK signaling in apoptosis remains controversial. Although several studies favor a proapoptotic role for JNK signaling, equally valid are a number of observations indicating an enhancement of cellular survival by the JNK pathway (Davis 2000, Chen and Tan 2000). Many of the stresses that cause the elevation of JNK activity also increase the expression of HSPs. Several studies have shown that HSP70 can inhibit JNK activation induced by a number of stresses, including heat shock (Gabai et al. 1997, Mosser et al 1997), ethanol (Gabai et al. 1997), proteasome inhibitors (Meriin et al 1999), and ultraviolet (UV) irradiation (Park et al. 2001). The precise mechanism for HSP70-mediated suppression of JNK activity is unclear. Two different models have been proposed to explain how HSP70 inhibits JNK activation. Based on the observation that elevated JNK activity following stimuli (such as heat shock, ethanol, arsenite, and oxidative stress) is a consequence of inhibition of JNK dephosphorylation. Meriin et al. (1999) suggested that HSP70 modulates JNK activity by inhibiting this stress-induced suppression of dephosphorylation. Alternatively, HSP70 may function to inhibit UV-induced JNK activation by directly interacting with JNK to suppress its association with, and phosphorylation by, SEK1. This effect requires the COOH-terminal peptide-binding domain of HSP70 (Park et al. 2001), which is entirely consistent with earlier observations that HSP70-mediated suppression of JNK activation is independent of its ATPase domain (Mosser et al 1997, Volloch et al. 1999). Importantly, both of these models and their supporting data indicate that HSP70 can suppress JNK activation independently of its capacity as a chaperone protein. This is in contrast to HSP70-mediated suppression of heat shock-induced apoptosis and cytochrome c release, which

require both the peptide-binding and ATPase domains (Mosser et al 1997, Volloch et al 1999). The conflicting pro- and antiapoptotic roles of JNK signaling are suggested to reflect the duration of JNK activation such that a transient elevation of JNK activity selectively engages a survival pathway (Chen and Tan 2000). Perhaps a careful examination of the kinetics of JNK signaling and HSP70 expression would reveal a relationship consistent with the idea that simultaneous induction of HSP70 and JNK tempers the magnitude and duration of JNK activation and, in doing so, favors the engagement of cellular survival (Beere and Green 2001).

2 AIMS OF THE STUDY

Photodynamic therapy is an attractive, emerging therapeutic procedure suitable for the treatment of a variety of tumor and non-malignant disorders. The efforts to improve therapeutic outcome of PDT led to modification of standard photodynamic protocol by light fractionation.

The first aim of the study was to compare continuous and fractionated light regime in which a total light dose was delivered in two equal or unequal light fractions separated by a dark interval 1 or 6 h. The purpose was to identify photodynamic protocol suitable to enhance (or for enhancing) hypericin-mediated photocytotoxic effects on HT-29 adenocarcinoma cells. Since MTT assay preliminary experiments revealed no or minor photocytotoxic effects in response to various fractionated light delivery regimes as compared to standard protocol, we were promoted to investigate the reasons of the observed failure of fractionated administration of PDT.

The second aim of the study was addressed to unravel the reasons of this decrease of photo-cytotoxicity caused by a fractionated light delivery regime when a sub-lethal light dose (1 $J.cm^{-2}$) was followed by a lethal light dose (11 $J.cm^{-2}$) 1h or 6 h later. In such regard, we have described the various effects caused by continuous and fractionated illumination schedules in some details. We analyzed cell viability modifications, cell cycle alterations, cell death induction (by dual staining Annexin V/PI) and colony-forming activity. All together, these data resulted particularly useful in identifying cellular and sub-cellular events determined by different light delivery regimes.

As we observed significant alterations in all cellular parameters studied depending upon the extension of the dark phase between two unequal exposures to light, the third aim of our study was clarifying the events that take place during the dark pause. For this reason we analyzed the production of reactive oxygen species, the fluctuations of hypericin content, the activation of redox-regulated nuclear transcription factor NF-κB (by luciferase activity assay), the changes in the expression of proteins connected with a cell survival, namely NF-κB p50 and p65 subunits, IκB-α, Mcl-1, HSP70, GRP94, Clusterin-α (by Western Blotting) and role of p38 MAPK inhibition in cell survival. In whole these information have given some insight into molecules processes and mechanisms which are involved in the development of resistance to PDT.

3 MATERIAL AND METHODS

3.1 Cell culture

Human adenocarcinoma cell line HT-29 was purchased from American Tissue Culture Collection (ATCC, Rockville, MD, USA). Cells were cultured in RPMI-1640 medium (Gibco, Grand Island, NY, USA) supplemented with 10% heat-inactivated fetal calf serum (FCS; PAA Laboratories GmbH, Linz, Austria) and antibiotics (penicillin 100 U/ml, streptomycin 100 μg/ml and amphotericin 25 μg/ml; Invitrogen Corp., Carlsbad, CA, USA). Cells were maintained at 37 °C in a humidified 5% CO_2 atmosphere and constantly kept under dark conditions.

3.2 Hypericin activation

The cells were irradiated in hypericin-free medium by placing cultivation dishes (TPP, Trasadingen, Switzerland) on a plastic diffuser sheet above a set of eleven L18W/30 lamps (Osram, Berlin, Germany) with maximum emission between 530 and 620 nm (the absorption peak of hypericin is ~ 600 nm) (Fig. 2). Uniform fluency rate at the surface of the diffuser was 3.15 $mW.cm^{-2}$ and the temperature did not exceed 37 ˚C. Light dose was calculated as multiplication of fluency rate by time.

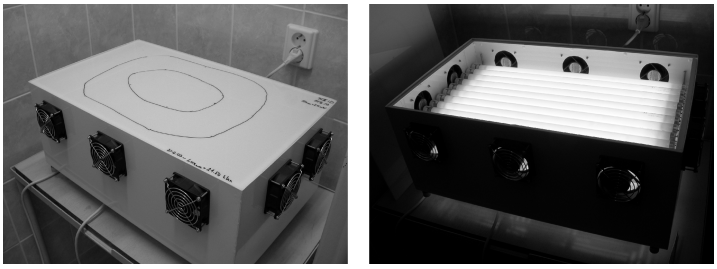

Figure 2. Irradiation device. Eleven L18W/30 lamps with maximum emissium in the range of 530-620 nm are located under plastic diffuser sheet (Photo: L. Grada Kuliková).

3.3 Experimental design

HT-29 cells ($2\times10^4/cm^2$) were seeded and cultivated 24 h in a complete medium with 10% FCS. Hypericin ((4,5,7,4´,5´,7´-hexahydroxy-2,2´-dimethylnaphtodiantron, HPLC grade), AppliChem GmbH, Darmstadt, Germany) at final concentration 60 nM was added and then incubated 16 h with cells in dark conditions. Prior to light application, the medium was replaced with a fresh one, free of hypericin (Fig. 2A). The hypericin was photoactivated with a sub-lethal or lethal single light dose (1 or 12 $J.cm^{-2}$) or fractionated light doses (1 + 11 $J.cm^{-2}$) with a dark interval 1 or 6 h. The cells photoactivated with a sub-lethal light dose were analyzed 1 or 6 h after PDT. The effects of single or fractionated light regime deliveries were analyzed up to 24 h after PDT (Fig. 2B) and cell viability, cell number and cell cycle were analyzed 24 or 48 h after PDT.

3.4 Quantification of cell viability and cell number

Cells were treated according to the standard protocol (Fig. 3A) and at defined incubation times after hypericin photoactivation (24 or 48 h) eosin vital dye (0.15 %) exclusion assay was used to determine both cell viability and cell number (microscopically). The viability was expressed as the percentage of live cells out of the

total number of cells. Cell number was assessed by counting live cells in a Bürker chamber.

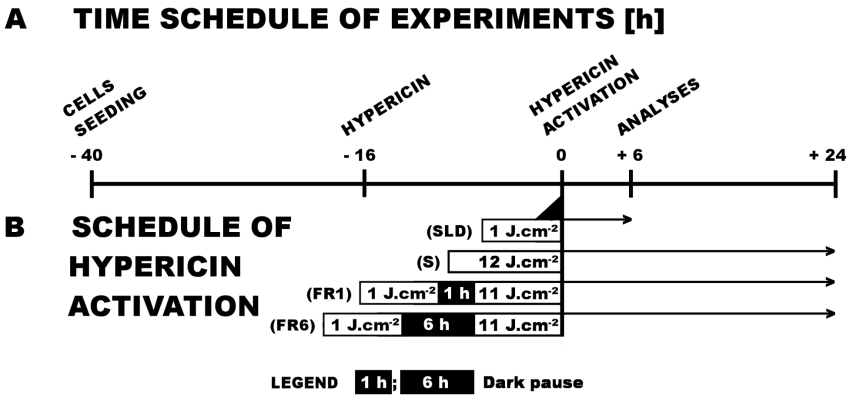

Figure 3. Experimental design. (A) Time schedule of experiments - HT-29 cells were seeded (point -40 h in time schedule of experiments) and cultivated 24 h in a complete medium and then hypericin was supplemented (point -16 h). Medium with hypericin was removed from cells 16 h later and replaced for hypericin free medium with subsequent activation of intracellular hypericin (point 0 h). Analyses were performed up to 6 h or up to 24 h after PDT (point +6 h or +24 h). (B) Schedule of hypericin activation - hypericin loaded HT-29 cells were illuminated with a single light dose (sub-lethal 1 J.cm^{-2} or lethal 12 J.cm^{-2} light dose) or two unequal light dose (1+11 J.cm^{-2}) separated with 1 h or 6 h dark pause. (S) single light delivery 12 J.cm^{-2}, fractionated light dose 1+11 J.cm^{-2} with a 1 h (FR1) or 6 h (FR6) dark pause between the two light doses.

3.5 MTT assay

Cells were seeded into 96 wells plates in amount 2×10^4 cells per well and then were treated according to standard protocol (Fig. 3A). Analyses were performed: a) 24 h after photodynamic treatment with a range of single light doses 0, 1, 2, 4, 8 or 12 J.cm^{-2} (Fig. 4); b) 24 and 48 h after photodynamic treatment with single (S) or fractionated light delivery regimes (FR1, FR6) (Fig. 6); c) inhibitor of GRP94 and HSP90 proteins geldanamycin (AXXORA, Nottingham, UK) was added 1 h prior to hypericin treatment (Fig. 18); d) inhibitor of p38 MAPK, SB202190 (Sigma-Aldrich Corporation, St. Louis, MO, USA), was added 2 h prior photoactiovation of hypericin (Fig. 19) and then in both cases MTT assay was performed 24 h after photodynamic treatment with a single or fractionated light delivery. MTT (3-(4,5-dimethylthiazol-2-yl)-2,5-diphenyl tetrazolium bromide (Sigma-Aldrich) assay was performed to evaluate the survival of cultured cells as previously reported (Mosmann 1983). The amount of dye extracted was quantified by absorbance measurements at 584 nm using FLUOstar Optima (BMG Labtechnologies GmbH, Offenburg, Germany) and expressed as a percentage of the dye extracted from untreated control.

3.6 Cell cycle analysis

For the DNA content determination, cells treated according to the standard protocol (Fig. 3A) were harvested 24 or 48 h after PDT and washed with phosphate-buffered saline (PBS) and fixed with 70% ice cold ethanol at -20 ºC. Fixed cells were centrifuged, washed with PBS and stained with staining solution (5 mg/mL propidium iodide, 10 mg/mL RNase A and 10% Triton X-100 in PBS). Then samples were kept in dark conditions for 30 min and measured on a flow cytometer (FACS Calibur, Becton

Dickinson, San Diego, CA, USA). For each sample, 15 000 cells were evaluated and the sample flow rate during analysis did not exceed 200–300 cells per second. The data obtained were analyzed using the Cell Quest Pro software (Becton Dickinson).

3.7 Colony-forming assay

Cells were treated according to the standard protocol (Fig. 3A), then harvested 24 h after single or fractionated light delivery and counted microscopically using a Bürker chamber. Equal cell numbers (500 cells per 60 mm Petri dish (TPP)) were seeded and cultivated under standard conditions for 7 days. Colonies were stained using coloured solution (40 mg methyl blue diluted in 50 ml 78% ethanol).

3.8 Detection of phosphatidylserine externalization and cell membrane permeability

For a phosphatidylserine externalization and cell viability analysis, an annexin V-FITC and propidium iodide (PI) double-staining kit (Bender MedSystems, Vienna, Austria) was used according to the manufacturer's instructions. The cells were treated according to the standard protocol (Fig. 3), then adherent and floating cells were harvested together 0.5, 3 and 24 h after PDT and stained with annexin V-FITC in binding buffer for 10 min, washed, stained with PI for 5 min and analyzed using the FACSCalibur flow cytometer. Results were analyzed with CellQuest Pro software. The cell populations were differentiated as living (annexin V^-/PI^-), apoptotic (annexin V^+/PI^-), secondary necrotic (annexin V^+/PI^+) or necrotic (annexin V^-/PI^+) cells. The results are presented as a mean ± SD of three independent experiments.

3.9 Production of ROS

The cells were treated according to the standard protocol (Fig. 3), then harvested 0.25, 0.5, 1, 6 h after a sub-lethal light dose or 0.5, 3, 24 h after single or fractionated light delivery, washed twice in phosphate-balanced salt solution (PBS), and resuspended in Hank's balanced salt solution (HBSS). Dihydrorhodamine-123 (DHR-123, Fluka, Buchs, Switzerland) was added at a final concentration of 0.2 μM, samples were then incubated for 15 min at 37 °C in 5% CO_2 atmosphere and subsequently kept on ice during analysis. Fluorescence was analyzed using a FACSCalibur flow cytometer in the FL-1channel. Forward and side scatters were used to gate the viable populations of cells. CellQuestPro software (Becton Dickinson) was used to quantify the intensity of DHR-123 fluorescence in the cells expressed as the ratio of DHR-123 fluorescence in the treated cells compared to fluorescence of untreated control cells.

3.10 Hypericin content analysis

The cells were treated according to the standard protocol (Fig. 3), then harvested 0.25, 0.5, 1, 6 h after a sub-lethal light dose or 0.5, 3, 24 h after single or fractionated light delivery, washed twice in PBS, and resuspended in HBSS. Fluorescence of hypericin was analyzed using the FACSCalibur flow cytometer in the FL-2 channel (1 x 10^4 cells per sample). CellQuestPro software was again used to quantify the intensity of hypericin fluorescence in the cells, expressed as the ratio of hypericin fluorescence in treated cells compared to the fluorescence of untreated control cells.

3.11 Luciferase activity assay

Luciferase reporter construct and stable cell transfection were executed as described previously (Hyzd'alova et al. 2008). Stable transfected HT-29 cells were treated according to the standard protocol (Fig. 3). Cells were rinsed with PBS 0, 0.5, 1,

3, 6 h after hypericin photo-activation with a sub-lethal light dose, and lysed with 400 μl of reagent (Luciferase Assay System; Promega Corp., Madison, WI, USA). Protein concentrations of the cell extracts were determined using detergent-compatible protein assay (BioRad Laboratories Inc., Hercules, CA, USA). One sample at a time was diluted in equal amount of proteins and 50 μl of extract was mixed with 50 μl of luciferase substrate and luminescence was measured immediately using the FLUOstar Optima. The luminescent signal of each sample was measured for the same period.

3.12 Western blot analysis

The cells were treated according to the standard protocol (Fig. 3), then harvested 1 and 6 h after low light dose, 24 h after single or fractionated light delivery (Fig. 16) or 24 h after light doses 0, 1, 2, 4, 8, or 12 $J.cm^{-2}$. The cells were then washed twice in cold PBS and lysed in lysis buffer (100 mM Tris-HCl, pH 7.4, 1% SDS, 10% glycerol and protease inhibitor cocktail P2714 (Sigma-Aldrich Corporation, St. Louis, MO) for 10 min on ice. The cell lysates were sonicated and centrifuged. Protein concentration was determined using detergent-compatible protein assay (BioRad Laboratories Inc.). Samples were diluted in equal amounts (30 - 50 μg proteins) with 0.01 % bromphenol blue and 1% 2-mercaptoethanol, then separated with SDS-polyacrylamide gel and transferred onto nitrocellulose membrane (Advantec, Tokyo, Japan) or PVDF membrane (Millipore, Bedford, MA, USA) in a transfer buffer containing 192 mM glycine, 25 mM Tris and 10 % methanol. The membrane was blocked in 5 % non-fat milk (or 5 % BSA) in TBS (20 mM Tris-HCl, pH=7.6; 150 mM NaCl; 0.05 % TWEEN 20, pH=7.4) for 1 h at first and then the membrane blots were incubated 2 h at RT or overnight at 4 °C (depending on the particular antibody) with primary antibody: anti-NF-κB p65 (sc-372), anti-NF-κB p50 and p105 (sc-8414), anti-IκB-α (sc-203), anti-GRP94 (sc-1794), anti-clusterin (sc-6420), all from Santa Cruz Biotechnology, anti-Mcl-1 (#4572 Cell Signalling), anti-HSP70 (MA3-006, Affinity BioReagents). After 30 min washing in wash buffer, membranes were incubated with appropriate horseradish-conjugated secondary antibody for 1 h at RT (AntiMouse IgG-HRP, NA931 (1:3000), AntiGoat IgG-HRP (1:20 000), AntiRabbit IgG-HRP (1:20 000) (Amersham Biosciences, Buckinghamshire, UK). Detection of antibody reactivity was performed using a chemiluminescence detection kit ECL+ (Amersham Biosciences) and visualized on X-ray films (Foma Slovakia, Skycov, Slovakia). Equal sample loading was verified by immunodetection of β-actin (A5441, Sigma-Aldrich).

3.13 Statistical analysis

Data were processed with GraphPadPrism (GraphPad Software Inc., San Diego, CA) and statistically analyzed using one-way ANOVA with Tukey's multiple comparison test and are expressed as mean ± standard deviation (S. D.). Significance was evaluated at three levels; $p < 0.05$, $p < 0.01$ and $p < 0.001$.

4 RESULTS AND DISCUSSION

The efficiency of PDT may be improved by modification of standard photodynamic protocol through light dose fractionating to several illuminations with dark pauses between light fractions (Ascencio et al. 2008, Babilas et al. 2003, de Bruijn et al. 1999, Pogue et al. 2008, Takahashi and Ohnishi 2009, Xiao et al. 2007). As it was mentioned before light fractionation is based on the premise of reoxygenation at the treated side during a dark pause and therefore higher ROS production improves the outcome of PDT (Curnow et al. 1999, Takahashi and Ohnishi 2009). Even though, such treatment doesn't avoid troubles. Light fractionation may lead to resistance development under specific circumstances (Paba et al. 2001, Sackova et al. 2005, Varriale et. al 2002). The molecular mechanisms underlying resistance development to PDT with hypericin are not completely understood. We therefore would like to contribute to better understanding of these events at a cellular and sub-cellular level.

4.1 Fractionated photodynamic treatment with hypericin doesn't improve the outcome as compared with to single irradiation scheme.

On the bases of our screening experiments provided by MTT assay were selected light doses as well as hypericin concentrations for further analysis. The most interesting results are depicted in Figure 4. Although MTT assay is considered to be a rapid colorimetric assay for cellular growth and survival suitable as an application to proliferation and cytotoxicity assay (Mosmann 1983). However we and others observed apparently increased proliferation over the control specifically in the case of analysis performed shortly after PDT (1 h); this increase has been interpreted as the consequence of enhanced mitochondrial metabolic activity rather than in cell proliferation or survival (Figure 4). A high light-dose mediated oxidative stress probably stimulated mitochondria oxidative metabolism that resulted in increased reduction of MTT to formazan by mitochondrial succinate dehydrogenase. MTT assay provides reliable information about cytotoxic effects of light doses over an extended timespan. The results revealed that a fluence rate of 1 J.cm^{-2} had no effect on cell survival. In this

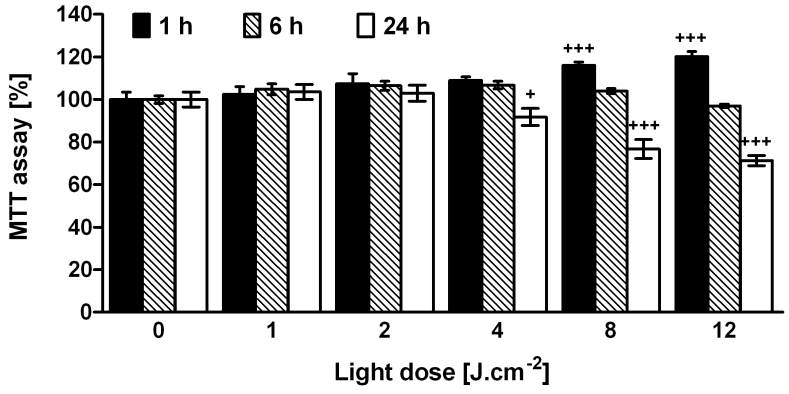

Figure 4. MTT assay of HT-29 cells 1, 6 and 24 h after hypericin (60 nM) mediated photodynamic treatment with single light doses 1, 2, 4, 8 and 12 J.cm^{-2}. Results are expressed as percentage of/over the control. The results are the mean ± SD of three independent experiments presented as percentage of untreated control. Statistical significance is expressed as follows: light dose versus untreated control in a given time of analysis (+) on the significance level $p<0.05$ (+); $p<0.001$ (+ + +). (C) control cells.

work, this dose is thereafter considered as the "sub-lethal" dose, while, in opposition the fluence rate of 12 J.cm^{-2} is considered the fully lethal dose. Light doses between 2 and 4 J.cm^{-2} are borderline and are considered as the threshold of an explicit photodynamic cytotoxic effect.

When this research was initiated, our expectations were foreseeing an improvement of PDT upon fractionated irradiation. On the contrary, our preliminary results revealed non-significant or minor cytotoxic effects of various light irradiation schemes as compared to standard photodynamic protocol. The results (Table 1) indicate not only different cytotoxic effects of photodynamic treatment at the various light irradiation schemes but also the relevance of a dark-interval duration within a light fractionation. According to Robinson et al. (2003) a two-fold illumination with a 2 h dark interval using two equal doses (50 J.cm^{-2}) delivered after topical ALA application on hairless mouse skin resulted in an increase in PDT response over that observed following a single illumination with 100 J.cm^{-2}.

Table 1. Cytotoxicity of hypericin after various light-irradiation schemes

Light dose (J.cm^{-2})	Dark pause (h)	Cytotoxicity (MTT assay evaluated 24 h after PDT)
3 + 3 *vs* 6	1	NS*
	6	NS
6 + 6 *vs* 12	1	NS
	6	NS
1 + 11 *vs* 12	1	NS
	6	$P < 0.001$
1 *vs* 0 (control)	1	NS**
	6	NS***

* NS – not significant
** 1 h after PDT
*** 6 h after PDT

However in our case, two equal light doses (3 + 3 J.cm^{-2}) or (6 + 6 J.cm^{-2}) separated with 1 or 6 h dark interval did not improve PDT response. They have also reported that if the first fraction was reduced to 5 J.cm^{-2} and if 95 J.cm^{-2} was delivered in the second fraction, the PDT response was significantly greater then when the two fractions are equal (Robinson et al 2003). However, when a light fractionation scheme 1 + 11 J.cm^{-2} was applied, we could not confirm such findings in our system. Moreover we observed even a decreased cytotoxic effect. Our present findings therefore agree more strictly with previous *in vitro* studies with hypericin on HEC1-B cells and U937 cells, which reported that pre-sensitized cells become fully resistant to light doses that normally determine massive cellular apoptosis in experimental photodynamic therapy (Paba et al. 2001, Varriale et al. 2002). Relative to our results presented in Table 1, we have selected light irradiation scheme for further study in which the selected total dose (12 J.cm^{-2}) was divided in two unequal doses, i.e. 1 J.cm^{-2} (sub-lethal) followed by 1 or 6 hours later by the dose of 11 J.cm^{-2} (close to the fully lethal). This scheme (1 + 11 J.cm^{-2}) applied to HT-29 adenocarcinoma cells model *in vitro*, has been chosen as reference scheme in our experimental model for the study of events that promote resistance development to PDT. Therefore we compared the effects of single and fractionated light delivery regimes and continued with the study concerning the effects

of a sub-lethal light dose as well as the importance of dark-interval duration within a light fractionation and their participation on the resistance outcome. Although *in vivo* and *in vitro* experimental models are not easy to compare because the different order of complexity that determines sometimes totally different responses to PDT, we consider the knowledge of intracellular mechanisms of photo-resistance as a standpoint for further study aimed to the improvement of its use in cancer therapy.

The comparison of the effects of hypericin treatment on tumour cell number (Fig. 5) and metabolic activity evaluated by MTT assay (Fig. 6) after a single light-dose (12 $J.cm^{-2}$) with those obtained after fractionated light delivery (1 + 11 $J.cm^{-2}$) revealed, except for viability, measurable differences when the irradiation was interrupted for 6

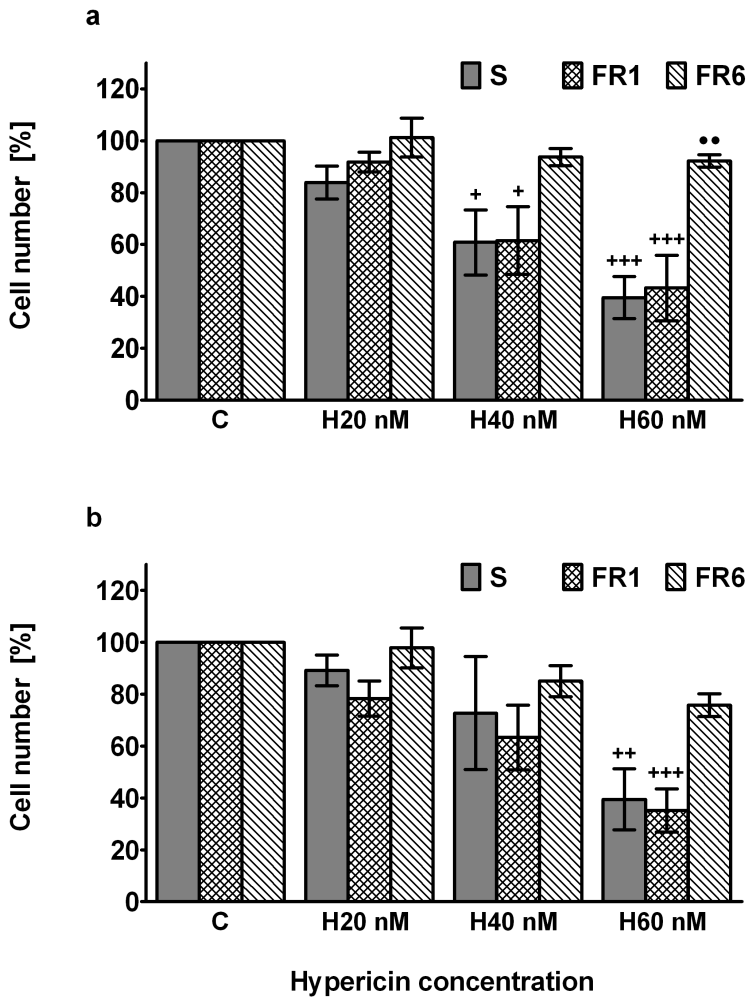

Figure 5. HT-29 cell numbers 24 h (a) and 48 h (b) after hypericin-mediated photodynamic treatment with both single (12 $J.cm^{-2}$) or fractionated (1 + 11 $J.cm^{-2}$) light delivery regime. Results are expressed as relative cell numbers related to untreated control groups. The results are the mean ± SD of three independent experiments. Statistical significance is expressed as follows: experimental groups versus control (+) and fractionated light delivery versus single light delivery (●) on the significance level $p<0.05$ (+ or ●); $p<0.01$ (++ or ●●); $p<0.001$ (+++ or ●●●). (C) control cells, (S) single light dose 12 $J.cm^{-2}$, fractionated light dose 1+11 $J.cm^{-2}$ with a 1 h (FR1) or 6 h (FR6) dark pause between the two light doses.

but not 1 hours. While fractionation with a shorter dark period induced the same cytotoxic effect in HT-29 tumor cells as a single-dose application, the effect of hypericin activated with light fractions separated by a dark interval of 6 h was reversed. Increased cell number (Fig. 5) and rise in metabolic activity evaluated by MTT assay indicate a sustained proliferation and mitochondrial function. This means that the behavior of cells was similar to that of the control. In contrast to earlier analysis (Fig. 6a), the only significant change was observed in the metabolic activity of cells receiving 60nM hypericin evaluated 48 h after light sensitization (Fig. 6b), which was significantly les as compared to that of the control.

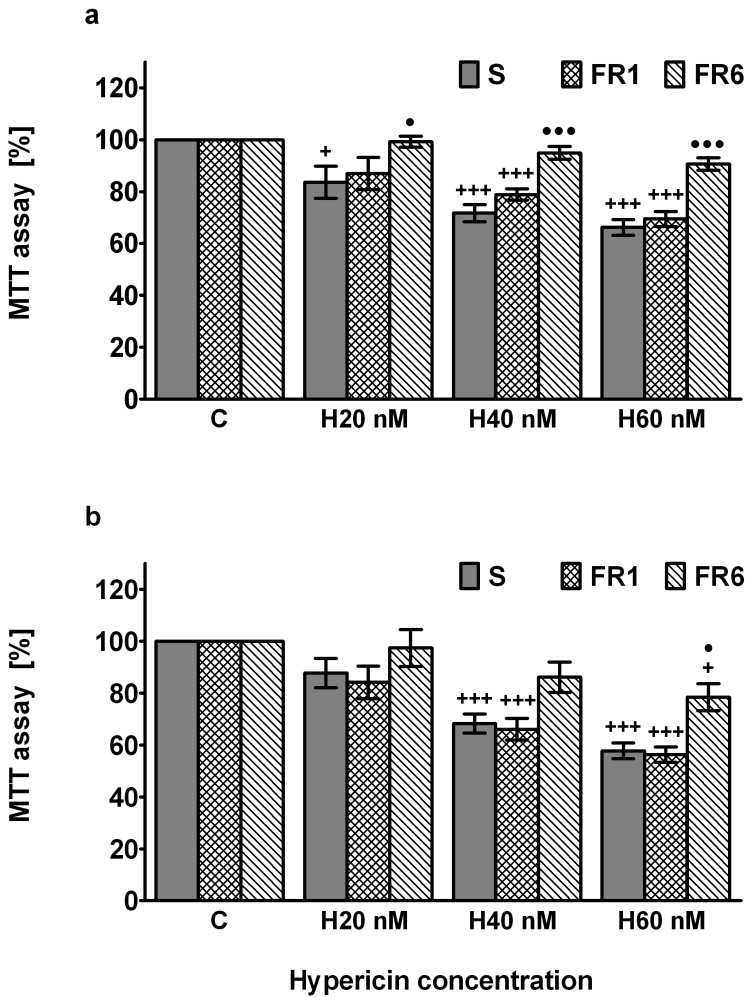

Figure 6. MTT assay of HT-29 cells 24 h (a) and 48 h (b) after hypericin-mediated photodynamic treatment with both single (12 J.cm^{-2}) or fractionated (1 + 11 J.cm^{-2}) light delivery regime. Results are expressed as percentage of control. The results are the mean ± SD of four independent experiments. Statistical significance is expressed as follows: experimental groups versus untreated control (+) and fractionated light delivery versus single light delivery (●) on the significance level $p<0.05$ (+ or ●); $p<0.001$ (+++ or ●●●). (C) control cells, (S) single light dose 12 J.cm^{-2}, fractionated light dose 1+11 J.cm^{-2} with a 1 h (FR1) or 6 h (FR6) dark pause between the two light doses.

4.2 Fractionated photodynamic treatment with a longer dark pause does not alter the original cell cycle regulation

The results mentioned formerly were in agreement with cell cycle analysis outcome. Fractionation with a longer dark pause (FR6) induced increased proportion of cells in the G1 phase of cell cycle (Fig. 7) and a significant decrease in the percentage of G2 phase cells (to the control level) (Fig. 8a, b). Our results therefore indicate sustained proliferation and preservation of original cell cycle regulation. On the other hand, the percentage of cells in the G2 phase of cell cycle increased when cells were treated with hypericin photoactivated by single (S) or fractionated irradiation with a shorter dark pause (FR1). These findings are in line with those reporting interconnection of hypericin-induced photocytotoxicity with G2/M arrest in HT-29 (Sackova et al. 2006). However, in contrast to our findings Varriale et al. (2002) reported that longer dark interval (20 h) between the first (2 J.cm^{-2}) and the second (5 J.cm^{-2}) exposure to light, resulted in accumulation of HEC1-B cells in G2/M phase. These differences in cell sensitivity and cell cycle regulation observed upon double irradiation cannot be easily understood. However, it is possible that different p53 status of HT-29 and HEC1-B cells may be implicated. Considering reduced p21 and p53 expression at longer dark pause in HEC1-B cells exposed to light twice (Varriale et al. 2002) as well as mutation in p53 of the colon adenocarcinoma cell line HT-29 (Barberi-Heyob et al. 2004, Zacal et al. 2005). Mutations of p53 generally results in the inactivation of its tumour-suppressor functions and is known to be linked to p53 overexpression, probably due to the production of a more stable form (Rodrigues et al. 1990) and its consequent accumulation may play a key role in the photo-sensitivity of HT-29 in PDT with hypericin (Mikes et al. 2007). There is also different ratio between first and second light dose in our experiment (1:11 vs. 2:5), which might be, together with different time schedule of light delivery, responsible for the differences.

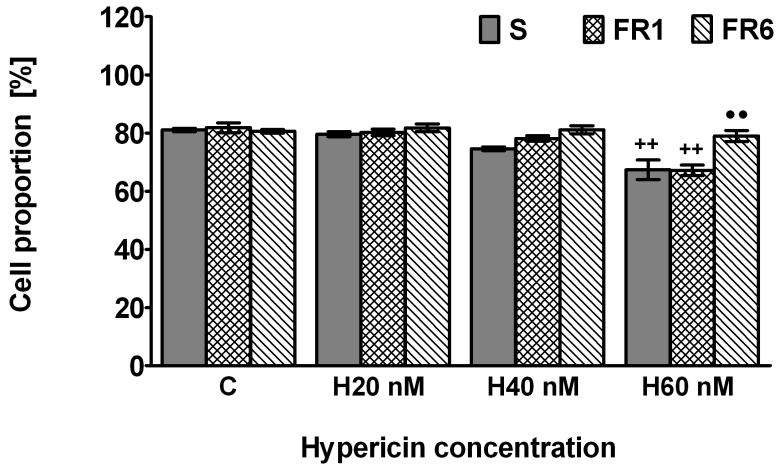

Figure 7. Proportion of HT-29 cells in G1 phase 48 h after hypericin-mediated photodynamic treatment with both single (12 J.cm^{-2}) and fractionated (1 + 11 J.cm^{-2}) light delivery regime. The results are the mean ± SD of two independent experiments. Statistical significance is expressed as follows: experimental groups versus untreated control (+) and fractionated light delivery versus single light delivery (●) on the significance level $p<0.01$ (++ or ●●). (C) control cells, (S) single light dose 12 J.cm^{-2}, fractionated light dose 1+11 J.cm^{-2} with a 1 h (FR1) or 6 h (FR6) dark pause between the two light doses.

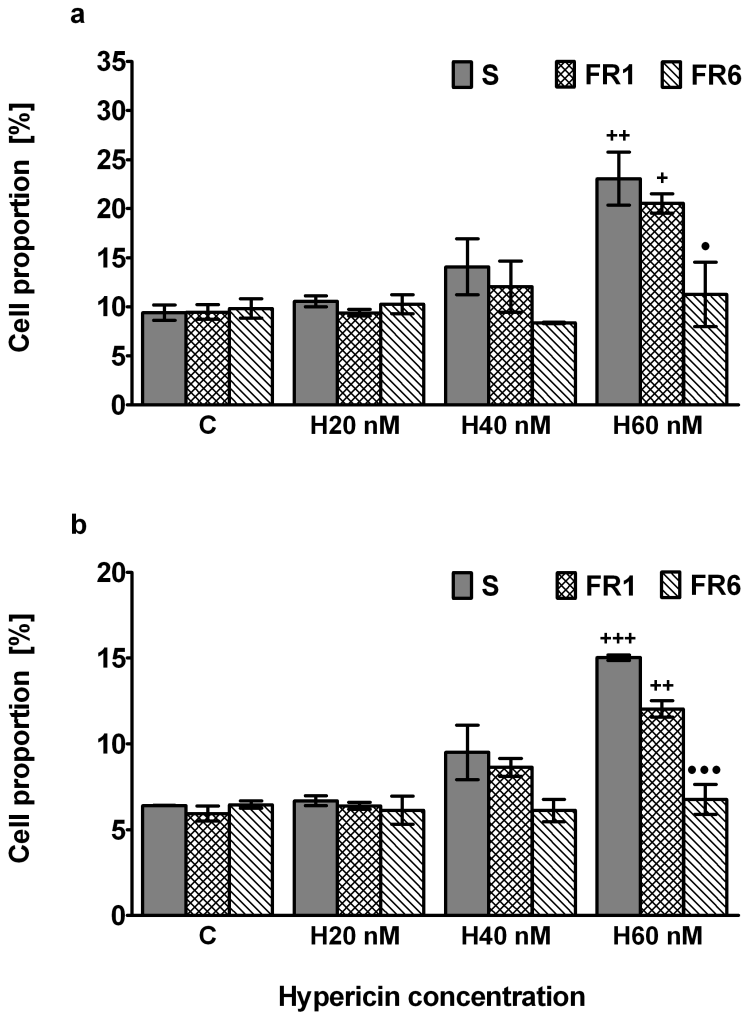

Figure 8. Proportion of HT-29 cells in G2 phase 24 h (a) and 48 h (b) after hypericin-mediated photodynamic treatment with both single (12 J.cm^{-2}) and fractionated (1 + 11 J.cm^{-2}) light delivery regime. The results are the mean ± SD of two independent experiments. Statistical significance is expressed as follows: experimental groups versus untreated control (+) and fractionated light delivery versus single light delivery (●) on the significance level $p<0.05$ (+ or ●); $p<0.01$ (++); $p<0.001$ (+++ or ●●●). (C) control cells, (S) single light dose 12 J.cm^{-2}, fractionated light dose 1+11 J.cm^{-2} with a 1 h (FR1) or 6 h (FR6) dark pause between the two light doses.

4.3 Longer dark pause between two unequal light doses repressed cell death in HT-29 cell after hypericin-mediated PDT

Only one concentration of hypericin (60 nM) was selected for further analysis aimed to better understanding of processes underlying reduced photocytotoxic effect of overextended fractionated regime. When the phosphatidylserine externalization and cell permeability analysis were performed, we obtained results in agreement with all the above findings. In summary, light fractionation with a longer dark pause between two unequal light doses (FR6) reduced hypericin-mediated photocytotoxic effect on HT-29 adenocarcinoma cells *in vitro* (Sackova et al. 2005). In contrary to earlier analysis (Fig.

9a), significantly higher survival of FR6 group was accompanied by regress in ratio of apoptotic and secondary necrotic cells that appeared 24 h after PDT (Fig. 9b). As it might be noticed, PDT effects of single and fractionated light delivery when the dark pause is short are very similar. So far all reported results on the changes in cellular parameters were concerned with the effects of three different light delivery regimes. We have demonstrated increased viability and cell metabolic activity. Such changes were accompanied to increased cell proportion in G1 and decrease in G2 cell cycle phase

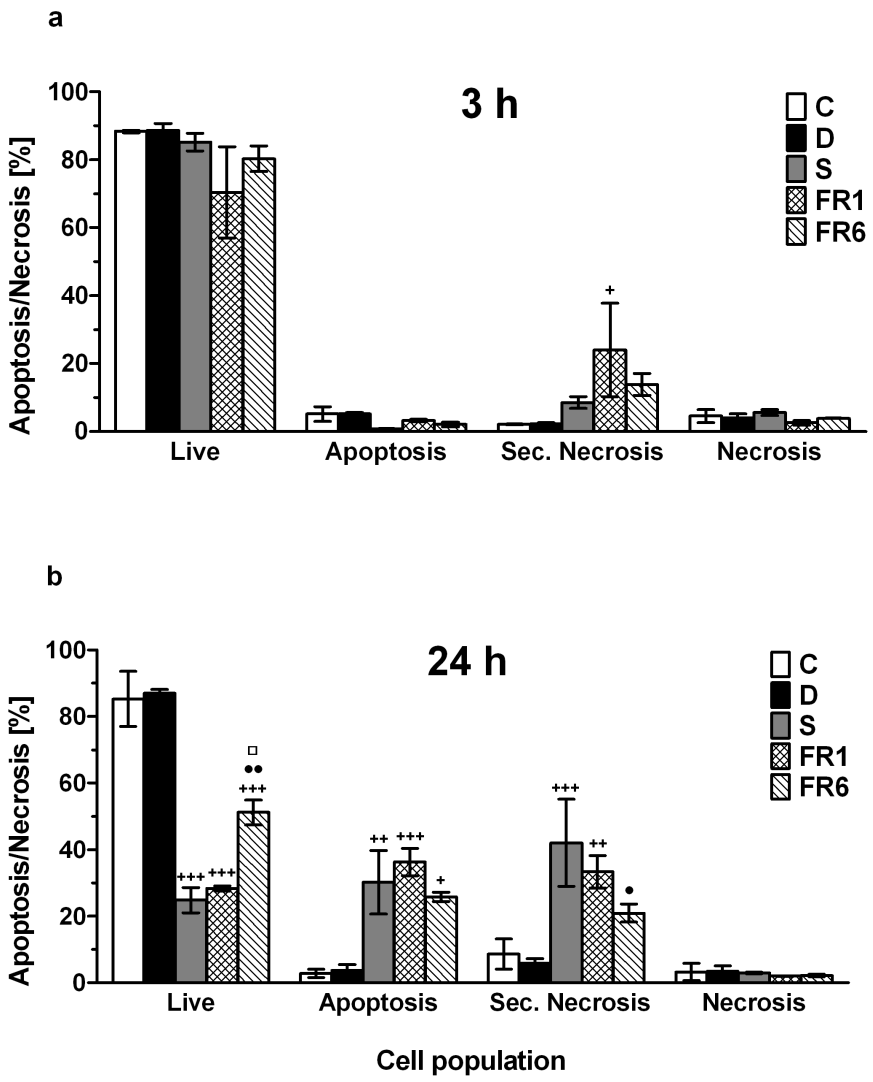

Figure 9. Detection of phosphatidilserine externalization and membrane permeability of HT-29 cells by dual annexin V/PI staining 3 h (a) and 24 h (b) after single (12 J. cm^{-2}) or fractionated (1 + 11 $J.cm^{-2}$) light dose. Cells were harvested and evaluated 3 or 24 h after PDT. The results are the mean ± SD of three independent experiments presented as a percentage to control. Statistical significance is expressed as follows: experimental groups versus untreated control (+); fractionated light delivery versus single light delivery (●); fractionated light delivery with a 6 h versus 1 h dark pause (□) on the significance level $p<0.05$ (+ or ● or □); $p<0.01$ (++ or ●●); $p<0.001$ (+++). (C) control cells, (D) hypericin under dark conditions, (S) single light dose 12 $J.cm^{-2}$, fractionated light dose 1+11 $J.cm^{-2}$ with a 1 h (FR1) or 6 h (FR6) dark pause between the two light doses.

while death in HT-29 cells, irradiated twice with a longer dark pause between two unequal light doses, was repressed. It appears that cell pre-sensitization and extension of the dark pause play an important role in the photo-resistance. While we have demonstrated significant reduction in PDT efficacy of fractionation along with prolonged dark pause, the adverse effect has been observed in the skin of the hairless mouse. In this case the dark interval cannot be reduced below 2 h without a significant reduction in Protoporphyrin IX-PDT efficacy (de Bruijn et al. 1999). These discrepancies still await explanation. On the other hand there are numerous reports in the literature of successful light fractionation regimes, varying the photosensitizer and with single or multiple breaks in illumination that can last from a few seconds to days (Anholt and Moan 1992, Hua et al. 1995, Mlkvy et al. 1996, Pe et al. 1994, van der Veen et al. 1994). However only very few researchers have explored the biological processes that are activated during the dark interval (Babilas et al. 2003, Huygens et al. 2005, Varriale et al. 2002) therefore we focused our attention to events occurring after sub-lethal light dose and before the second exposure to light.

4.4 Longer dark pause between two unequal light doses enhanced clonogenic potential of HT-29 cells after PDT with hypericin

We examined impact of a sub-lethal light dose and duration of a dark pause on HT-29 cells proliferation. In comparison with both controls, the effect all of three different photodynamic irradiation schedules resulted in reduced colony-forming activity. As is depicted in Figure 10, single (S) or fractionated light delivery (FR1) with 1 h dark pause, demonstrated very low colony-forming activity. Longer pause continuing for 6 h (FR6) proved much higher ability to create visible colonies, even when compared to FR1 group. As might be seen, hypericin under dark conditions (D) did not affect clonogenic potential of HT-29 cells. Sub-lethal light dose resulted not only in increased amount of viable cells, but resistance manifested also by increased clonogenic activity when prolonged dark pause was applied. These findings rose a query what events underlie resistance to protracted fractionated light delivery regime. Low intensity of stress in general may accelerate stress-inducible pathways and cell signaling that result in defence mechanisms in terms of survival. Since low-dose cell survival is described mainly in context of radiation- or heat-induced adaptive cell response (Shadley et al. 1987, Yoshida et al. 1993), we presume that even sub-lethal light dose in PDT may trigger similar biological events as well. When we look for the answers in the reports discussing adaptive response to ionizing radiation, we can find connections. For example similarly as in our case augmentation of colony-forming ability of myeloid leukemia cells was observed *in vitro* after low-dose irradiation and showed thermo-resistance 1 h after low-dose pre-irradiation and also showed radiation-reistance 4 h after irradiation. Induction of heat shock protein HSP70 was not detectable by Western blot therefore it seems that some proteins other than HSP70 were concerned with the augmentation of colony-forming ability and thermo- and radiation-resistance (Ibuki et al. 1998). Takahashi and Ohnishi (2009) have shown that NO radicals are an initiator of radiation- and heat-resistance induced by low dose pre-irradiation. They have also demonstarted association with p53 functioning (Takahashi and Ohnishi 2009). Other authors reported that conditioning doses (0.25 Gy or 0.5 Gy) and subsequent exposure to 8 Gy caused significant increase in the survival of mice compared to irradiated control (Tiku and Kale 2004). Adaptive response to ionizing radiation involves DNA repair mechanisms and induced proteins may enhance this repair (Wolff 1996). However according to Wouters and Skarsgard (1997) the radiation-induced increase in radiation-resistance observed in HT-29 cell line is distinct from the adaptive

response. Concidering that hypericin not show genotoxicity (Diwu and Lown 1994, Miadokova et al. 2009) and cell killing mechanism after PDT is not at the chromosom level (Halkiotis et al. 1999), therefore resistance to hypericin mediated-PDT involves other mechanisms then resistance to radiation, for example antioxidant adaptive response. Activation of antioxidant adaptive response to ALA-mediated PDT was demonstrated in lymphocytes (Casas et al. 2002).

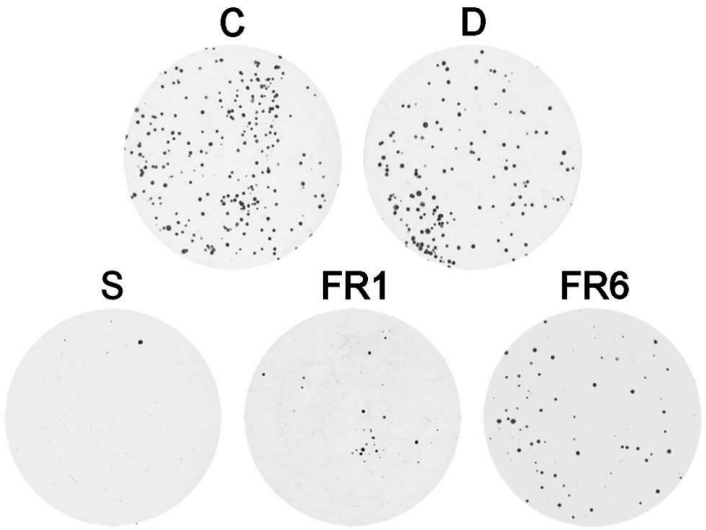

Figure 10. Colony-forming assay of HT-29 cells. Cells were harvested 24 h after hypericin photoactivation. The results are presented as a representative photo of three independent experiments. (C) control cells, (D) hypericin under dark conditions, (S) single light dose 12 $J.cm^{-2}$, fractionated light dose 1+11 $J.cm^{-2}$ with a 1 h (FR1) or 6 h (FR6) dark pause between the two light doses.

4.5 Duration of a dark pause affects PDT-mediated ROS level induced by second light dose

Detection of intracellular levels of ROS revealed shortly after the first illumination steady remission within first hour, although 6 h after PDT, the ROS level was found to be raised significantly. Dark conditions did not affect ROS level significantly when compared to untreated control (Fig. 11). The second elevation of ROS level observed 6 h after the first illumination might be secondary consequence of the ROS induced by PDT, a phenomenon known as "(ROS-induced)-ROS release" (RIRR). This fact demonstrated in mitochondria of cardiac myocytes resulted from MPT induction was considered as a general mechanism independent of the signaling ROS source (Zorov et al. 2000). The study of oxidative metabolism changes after different light delivery regimes revealed that resistant group (FR6) kept shortly after PDT, steady ROS level achieved already tightly before the lethal dose application, whereas further delivery regimes (S, FR1) resulted in markedly elevated ROS production (Fig. 12). We have observed that illumination of cells at the time of a basal ROS concentration (Fig. 11; 1 $J.cm^{-2}$ 1 h) resulted in its significant increasing (Fig. 12; FR1 0.5 h) whereas the upraised ROS level shortly before the second illumination (Fig. 11; 1 $J.cm^{-2}$ 6 h) did not rose dramatically after PDT (Fig. 12; FR6 0.5 h). Decreased ROS production and cytotoxicity after fractionated PDT was observed also by Oberdanner et al. (2005). They suggested that the dark intervals during irradiation allowed the glutathione reductase to regenerate reduced glutathione (GSH), thereby

cells were less susceptible to ROS produced by PDT compared with continuous irradiation. Although we did not analyze glutathione involvement, we predict that it might play a role in management of ROS level in cells irradiated by second light dose after 6 h long dark pause. Taking into concideration that glutathione reductase was found to recycle GSH within 1 minute of dark interval (Oberdanner et al 2005), it could be difficult to explain increase of ROS 6 h after sub-lethal PDT if glutathione reductase is implicated. Though, later analyses (3 or 24 h) showed barely induced levels in all studied experimental groups (Fig. 12). It follows that pre-sensitization and the timing of

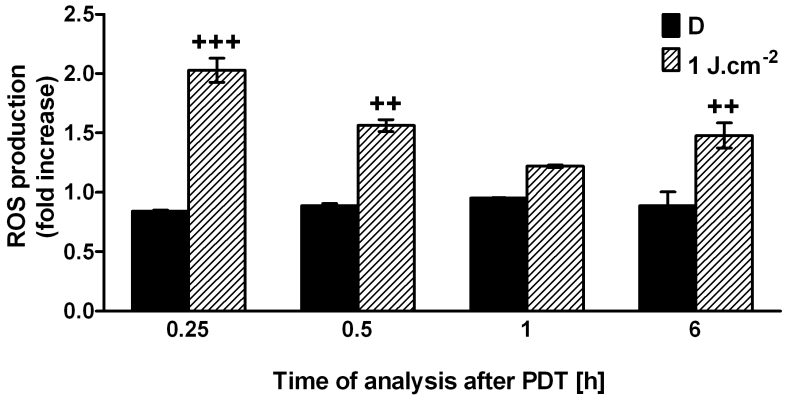

Figure 11. The effect of a sub-lethal dose 1 J.cm^{-2} on ROS production in HT-29 cells. Cells were harvested and evaluated 0.25, 0.5, 1 and 6 h after hypericin photoactivation. The results are the mean ± SD of three independent experiments presented as a ratio to untreated control. Statistical significance is expressed as follows: photoactivated (1 J.cm^{-2}) versus not photoactivated (D) (+) on the significance level $p<0.01$ (++); $p<0.001$ (+++). (D) hypericin under dark conditions.

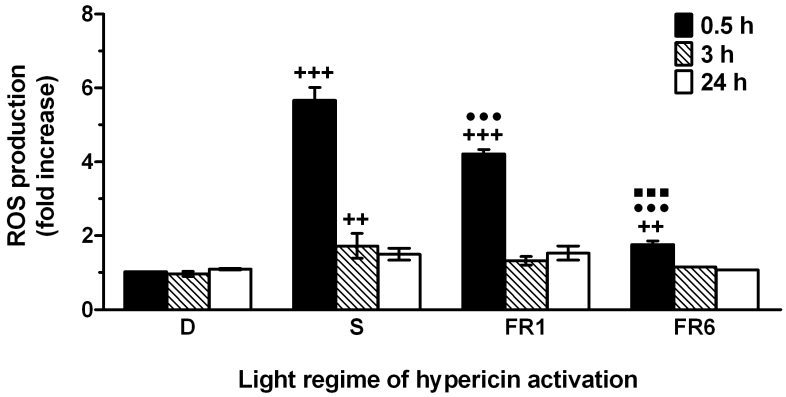

Figure 12. The effect of a single (12 J. cm^{-2}) and fractionated (1 + 11 J.cm^{-2}) light delivery on ROS production in HT-29 cells. Cells were harvested and evaluated 0.5, 3 and 24 h after hypericin-mediated photodynamic treatment. The results are the mean ± SD of three independent experiments presented as a ratio to control. Statistical significance is expressed as follows: experimental groups versus untreated control (+); fractionated light delivery versus single light delivery (●); fractionated light delivery with a 6 h versus 1 h dark pause (■) on the significance level $p<0.05$ (●); $p<0.01$ (++); $p<0.001$ (+++ or ●●● or ■■■). (D) hypericin under dark conditions, (S) single light dose 12 J.cm^{-2}, fractionated light dose 1+11 J.cm^{-2} with a 1 h (FR1) or 6 h (FR6) dark pause between the two light doses.

a second illumination could decrease photocytotoxic effect of PDT mediated through restricted ROS production. According to Huygens et al. (2005), acutely induced oxygen depletion rather than a lack of photosensitizer rendered tumour cells less sensitive to the photodynamic action of hypericin. They have reported that failure in hypericin-mediated PDT with spheroids can only by overcome with hyperoxygenation (Huygens et al 2005). However, sub-lethal light dose is not able to induce extensive hypoxia, further 6 h dark pause is sufficient for re-oxygenation of treated cells. Therefore, we assume that restricted ROS production is not due to oxygen depletion mediated by a sub-lethal light dose during a dark pause. Loss of the intracellular hypericin during a dark pause could be another factor contributing to decreased PDT effect of protracted fractionated light delivery.

4.6 Pre-sensitization did not affect physiological elimination of hypericin, however light administration regime affects hypericin elimination after lethal dose

Another possible explanation of decreased ROS production could be reduction in intracellular concentration of hypericin during a dark interval. Detection of hypericin intracellular levels after first sub-lethal light dose (Fig. 13) proved that there was a steady decrease, which was found to be significant 6 h after PDT. This drop was in compliance with a physiological elimination of hypericin, similar to hypericin-treated cells under dark conditions (D). Although, extended time of a dark interval reduced hypericin content, indeed 80% of hypericin content measured at 1 h dark pause was available and susceptible to second photoactivation. Decreased hypericin content to 90% of the original value during 3 h dark pause was reported by Paba et al. (2001) in human histiocytic lymphoma U937 cells and 20 h-dark interval reduced hypericin content to less than 75% of the hypericin present at 3 h in human endometrial carcinoma HEC1-B cells (Varriale et al. 2002). Resistance to second light dose occurred in all cases, although hypericin content was relatively high at time of the second illumination. Therefore in our opinion reduced hypericin content could result in decreased ROS production and thus partially contribute to decreased photocytotoxic effect of fractionated PDT.

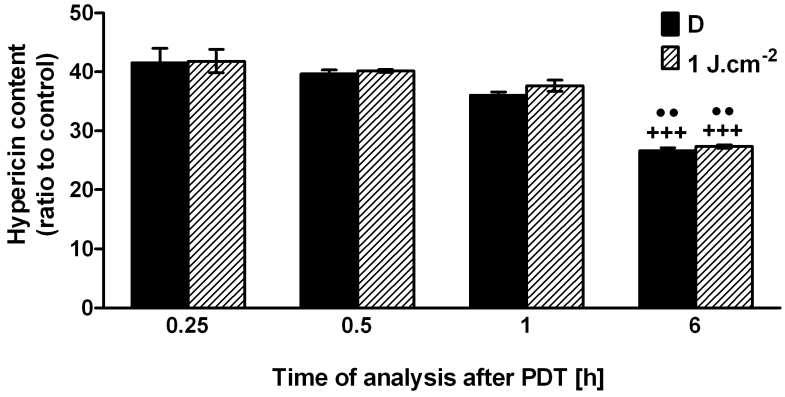

Figure 13. Determination of hypericin intracellular levels in HT-29 cells within a dark pause after first sub-lethal dose 1 J.cm^{-2}. Cells were harvested and evaluated 0.25, 0.5, 1 and 6 h after hypericin photoactivation. The results are the means ± SD of three independent experiments presented as a ratio to control. Statistical significance is expressed as follows: photoactivated (1 J.cm^{-2}) or not photoactivated (D) hypericin (0.5, 1 and 6 h) versus (0.25 h) (+); (6 h) versus (1 h) (●) on the significance level $p<0.01$ (●●); $p<0.001$ (+++). (D) hypericin under dark conditions.

Though, administration of single lethal light dose decelerated hypericin elimination by cells significantly when applied without pre-sensitization (Fig. 14; S) on the other hand, this effect was partially or completely abolished in pre-sensitized groups drug transport function might increase hypericin content in HT-29 cells. Hypericin was also found to increase activity and expression of drug efflux transporters in HT-29 cells when applied by itself, without light activation. It is therefore liable that lethal light dose induced massive destruction and inhibited efflux pumps alongs, thus slowed down rate of hypericin efflux from the cells and prolonged retention of hypericin in the cells in contrary with not photoactivated hypericin. Hypericin is more photostable than most sensitizers used in PDT, including mTHPC and Photofrin, the photobleaching seems to be not oxygen dependent, and singlet oxygen probably plays insignificant role (Uzdensky et al. 2002). These findings together with prolonged retention of photosensitized hypericin in the treated tissue may predetermine hypericin as a suitable photosensitizer for a multiple high-dose fractionation with short dark intervals between light fractions. In summary, a drop of intracellular hypericin content is influenced by a length of a dark pause and photodynamic light regime. Even though, changes of hypericin content before second light dose application (Fig. 13) may partially contribute to lower ROS production and thus decreased photocytotoxic effect of fractionated PDT. On the bases of following findings, it seems that different molecular events participate on resistance development in HT-29 cells *in vitro.*

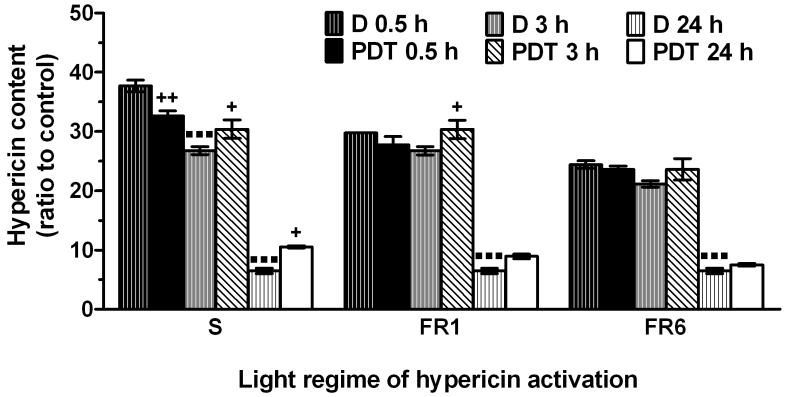

Figure 14. Determination of hypericin intracellular levels in HT-29 cells illuminated with a single (12 J. cm^{-2}) and fractionated (1 + 11 $J.cm^{-2}$) light delivery. Cells were harvested and evaluated 0.5, 3 and 24 h after PDT. The results are the means ± SD of three independent experiments presented as a ratio to control. Statistical significance is expressed as follows: single or fractionated light delivery versus not photoactivated (D) hypericin (+); not photoactivated hypericin (3 h or 24 h) versus (0.5 h) (▪) on the significance level $p<0.05$ (+); $p<0.01$ (++); $p<0.001$ (▪▪▪). (PDT) photodynamic treatment, (D) hypericin under dark conditions, (S) single light dose 12 $J.cm^{-2}$, fractionated light dose 1+11 $J.cm^{-2}$ with a 1 h (FR1) or 6 h (FR6) dark pause between the two light doses.

4.7 Sub-lethal photodynamic treatment induced NF-κB activity

It is well known that low levels of ROS may function as second messengers activating pathways that protect cells against apoptotic stimuli (Chandra et al. 2000). Since NF-κB is often considered to be a ROS-responsive transcription factor (Chandra et al. 2000, Janssen-Heininger et al. 2000) also shown to be implicated in a cancer cell responses to photodynamic therapy (Legrand-Poels et al. 1995), we employed HT-29 cells transfected with a nuclear transcription factor (NF-κB) luciferase reporter

construct in our experiments. Induction of NF-κB activity after sub-lethal dose of 1 J.cm^{-2} was verified in stably transfected HT-29 cells (clone #3 and clone #93) by luciferase reporter activity executed 0, 0.5, 1, 3 and 6 h after PDT (Fig. 15a, b). Both tested clones indicated insignificant changes within first hour, however later on, the NF-κB activity was identically induced 3 and 6 h after PDT in both models. Significantly increased luciferase activity in a later time after sub-lethal dose indicate that pre-sensitized cells prepared themselves during a longer dark period by provoking NF-κB activity and timing of the second light dose before or after NF-κB activation could be crucial for the fate of cancer cell. Since NF-κB is known as redox-regulated protein coupled with cell proliferation, transformation, and tumour development (Legrand-Poels et al. 1995), our results indicate that pre-sensitized cells activated NF-κB transcription activity that resulted in resistance. Independently of us the same finding has been reported by Chen et al. (2009) who have demonstrated that low level laser therapy (LLLT) not only enhanced mitochondrial respiration, but also activated the

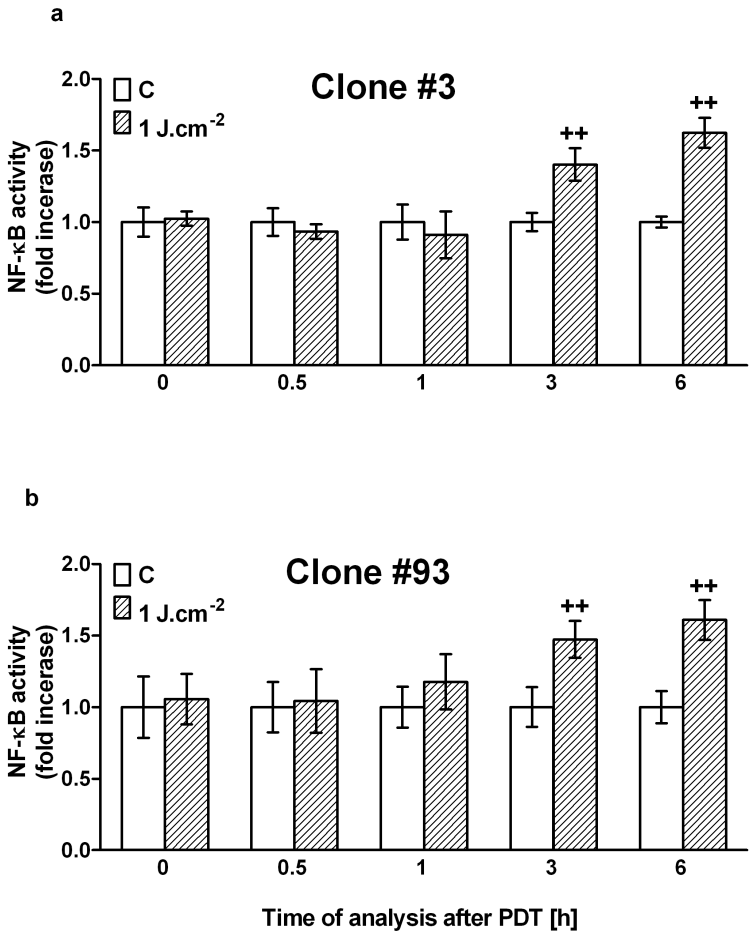

Figure 15. NF-κB binding activity (expressed as a relative luciferase activity) of two HT-29 clones #3 (a) and #93 (b) with pBIIX-LUC construct after treatment with sub-lethal dose 1 J.cm^{-2}. Cells were lysed 0, 0.25, 0.5, 1, 3 and 6 h after PDT. The results are the mean ± SD of three independent experiments presented as a ratio to untreated control. Statistical significance is expressed as follows: sub-lethal light dose versus untreated control (+) on the significance level $p<0.01$ (++). (C) control cells.

redox-sensitive transcription factor NF-κB by generating ROS as signalling molecules in embryonic fibroblasts of transgenic NF-κB luciferase reporter mice. Even significant activation of NF-κB has been observed for fluencies higher than 0.003 J.cm^{-2} (Chen et al. 2009). Although low-dose photodynamic effect differs from photobiomodulatory effect of low level laser therapy by the using of photosensitizing drug, both approaches lead to low-level ROS-mediated activation of NF-κB, eventually influencing long-term cell behaviour such as proliferation and survival. Taking into consideration published reports we have demonstrated for the first time possible implication of NF-κB in photo-resistance to fractionated PDT. Although the biological effects of low doses were described mainly in context of radiation- or heat-induced adaptive cell response (Shadley et al. 1987, Yoshida et al. 1993), we have shown that even low light doses make cells less sensitive to second light exposure. It was suggested that other stress stimuli may induce NF-κB activity through the ROS signalling. For example induction of NF-κB was shown after low-dose ionizing radiation that involved a reactive oxygen intermediate signalling pathway (Mohan and Meltz 1994). Lower doses of ionizing radiation, 0.25-2.0 Gy, were capable of inducing expression of NF-κB in human lymphoblastoid cells (Prasad et al. 1994). It follows that pro-survival pathway initiated by NF-κB seems to be responsible not only for the radiation-adaptive response in cells but also photo-adaptive cells response that resulted in resistance to second light exposure. Therefore it is liable that any exposure of treated site to light prior to regular treatment could affect efficiency of photodynamic therapy and targeted inhibition of NF-κB pathway may prevent resistance to therapy.

4.8 Even sub-lethal light dose increased whole protein expression that altered the timing of a second photodynamic treatment

Expressions of NF-κB p65, p50 and p105, Mcl-1, IκB-α, HSP70, GRP94 and clusterin-α (Fig. 16) were detected 1 and 6 h after the first sub-lethal light dose (SLD; 1 J.cm^{-2}) or 24 h after administration of a single lethal light dose (S, 12 J.cm^{-2}) and two unequal doses (1+11 J.cm^{-2}) separated by 1 or 6 h of a dark pause (FR1 or FR6). Apart from activation of NF-κB transcription activity our hypothesis concerning implication of NF-κB is also supported by increased levels of proteins whose genes are under its transcription control (increased level of NF-κB subunits p65, p50 and a precursor form of p50; p150, IκB-α and anti-apoptotic Mcl-1 protein detected 6 h after sub-lethal light dose). Even though phosphorylation and degradation of IκB is an important step for NF-κB releasing from complex with IκB, translocation from cytoplasm to nucleus and binding to DNA (Jobin et al. 1997, Wang et al. 2000), in our experimental model NF-κB activation has occurred without degradation of IκB. Therefore our results are in agreement with a study reporting altered regulation of IκB-α degradation and activation of NF-κB activity which can occur independently of IκB degradation in human colonic epithelial cells HT-29 (Jobin et al. 1997, Wang et al. 2000).

Similarly, induction of heat shock protein HSP70, occurrence of GRP94 multimers and elevation of clusterin-α already 1 h after hypericin activation confirmed onset of oxidative stress response in pre-sensitized cells. Analysis 24 h after lethal light doses (S, FR1, FR6) revealed interesting differences in levels of HSP70 and especially in GRP94 multimerization and clusterin-α expression (Fig. 16). Whereas single lethal light dose administration (S) and FR1 group demonstrated similar pattern, the fractionated administration separated by a 6 h dark pause showed significantly abolished clusterin-α level as well as suppressed occurrence of HSP70 and GRP94 multimers and slightly elevated IκB-α together with p50 and p65 subunits of NF-κB. We have also shown dose dependent increased expression of GRP94 accompanied with

a dose dependent formation of high molecular GRP94 multimers. Although, homotypic oligomerization of GPR94 protein as well as formation of high molecular multimers were described in a connection with bis-ANS and heat shock induced stress (Wassenberg et al. 2000), we presume that photodynamic therapy with hypericin may have a similar effect to GRP94 in a light dose- and photodynamic protocol-dependent manner. Our assumption supports also gradually increased amount of GRP94 multimers induced by the scale of light doses from 1 to 12 J.cm^{-2} as well as marked expression of clusterin-α and HSP70 (Fig. 17). These results are in conformity with MTT assay (Fig. 4) where 4 J.cm^{-2} could be regarded as threshold light dose that cause oxidative stress. This resulted in decreased metabolic activity and increased production of GRP94 multimers and clusterin-α. Since GRP94 protein is localized exclusively in endoplasmic reticulum, it indicates the role of ER in stress response to hypericin-mediated PDT. Our work describes for the first time multimerisation of GRP94 in a connection with PDT-mediated stress response.

Another protein related to ER is clusterin-α. Oxidative stress induced by sub-lethal light dose increased level of ~40 kDa clusterin subunit whereas a lethal light dose (Fig. 16; S, FR1) significantly altered expression of clusterin towards higher molecular forms of clusterin-α indicating the involvement of clusterin in extensive defence stress response, evidently reduced in resistant group. In summary, we have shown altered expression of proteins in a light dose dependent manner and depending on the light delivery regime of photodynamic protocol.

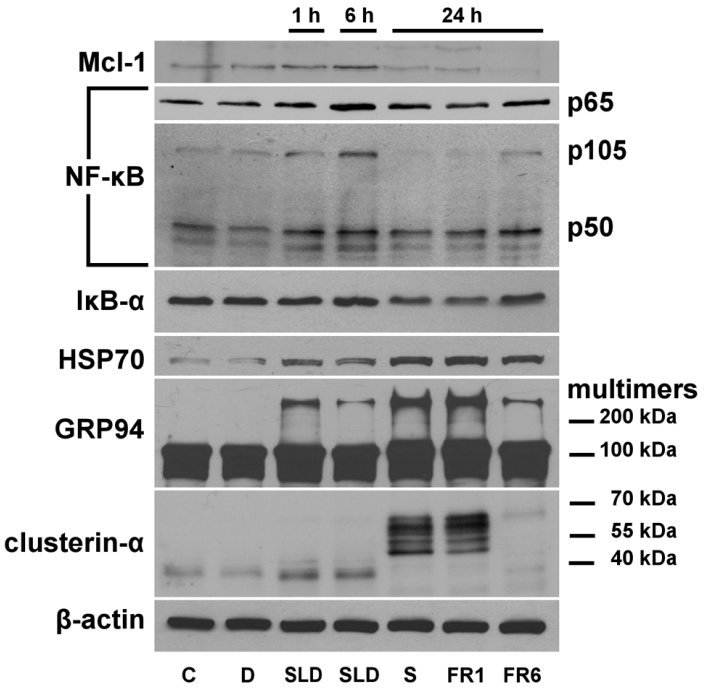

Figure 16. Western blot analysis of Mcl-1, NF-κB p65, p50 and p105, IκB-α, HSP70, GRP94, clusterin-α and β-actin proteins 1 or 6 h after hypericin photoactivation with a sub-lethal dose (1 J.cm^{-2}) or 24 h after single (12 J. cm-2) and fractionated (1 + 11 J.cm-2) light deliveries application. The results are presented as a representative photo of three independent experiments. (C) control cells, (D) hypericin under dark conditions, (SLD) sub-lethal light dose 1 J.cm^{-2} (S) single light delivery 12 J.cm^{-2}, fractionated light delivery 1+11 J.cm^{-2} with a 1 h (FR1) or 6 h (FR6) dark pause between the two light doses.

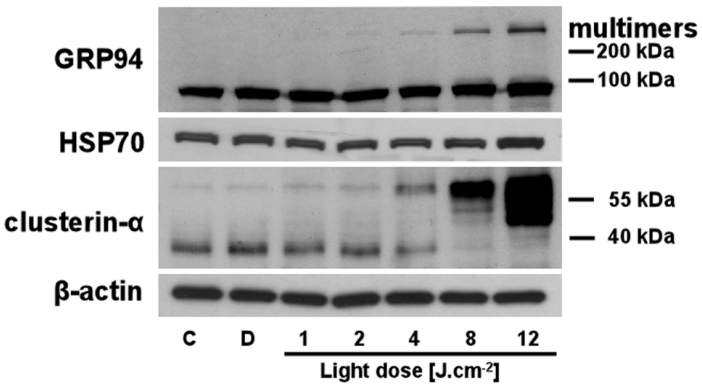

Figure 17. Western blot analysis of GRP94, HSP70, clusterin-α and β-actin proteins 24 h after hypericin photoactivation with 1, 2, 4, 8 or 12 J.cm^{-2}. The results are presented as a representative photo of three independent experiments. (C) control cells, (D) hypericin under dark conditions.

The inhibition of HSP90 protein family as well as its member GRP94 did not confirme any important role in the resistance to fractionated light delivery with 6 h-dark pause between the two unequal light doses even though higher concentration of geldanamycin was applied (Fig. 18). The results of Western blot analysis (Fig. 16) and of HSP90 inhibition complement one another. Similarly as in the case of dark conditions, geldanamycin demonstrated the same effect on resistant group (FR6) (Fig. 18). However, the implication of HSP90 proteins manifested both single (S) and fractionated light delivery regime with a 1 h dark pause (FR1) when higher concentration of geldanamycin was applied. It follows that although HSP90 proteins as

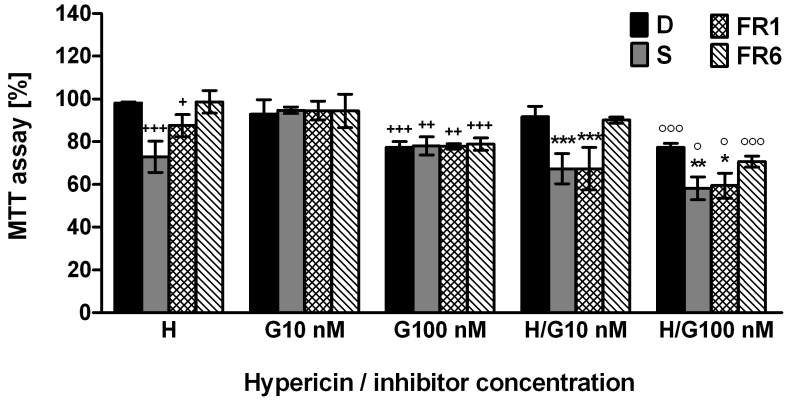

Figure 18. The effect of GRP94 and HSP90 proteins inhibition by geldanamycin on survival of HT-29 cells 24 h after hypericin mediated photodynamic treatment with a single (12 J. cm^{-2}) and fractionated (1 + 11 J.cm^{-2}) light deliveries. The results are the mean ± SD of three independent experiments presented as percentage of untreated control. Statistical significance is expressed as follows: monotherapies versus untreated control (+); combination therapy versus monotherapy with geldanamycin (*); combination therapy versus monotherapy with hypericin (○) on the significance level $p<0.05$ (+ or * or ○); $p<0.01$ (++ or **); $p<0.001$ (+++ or *** or ○○○). (H) hypericin, (G) geldanamycin, (C) control cells, (D) hypericin under dark conditions, (S) single light dose 12 J.cm^{-2}, fractionated light dose 1+11 J.cm^{-2} with a 1 h (FR1) or 6 h (FR6) dark pause between the two light doses.

well as GRP94 assist to overcome overscaled stress conditions and the absence of HSP90 or GRP94 functions intensified cell damage, doesn't play role in resistance to fractionated PDT.

4.9 Inhibition of p38 MAPK did not enhanced effect of hypericin-mediated PDT

Inhibition of p38 mitogen-activated protein kinases (MAPK) slightly decreased survival of cells irradiated with single or fractionated light deliveries, however not significantly in comparison with monotherapies with hypericin (Fig. 19). We noticed that changes in cell survival of inhibited cells were manifested by cytotoxic effect of hypericin itself. Inhibition of p38 MAPK did not abolished resistance of pre-sensitized cells to the second lethal light dose and p38 MAPK inhibition remained the same trend of hypericin-mediated photocytotoxic effect for all light delivery regimes. Contrary to our results Chan et al. (2009) have reported enhanced cell death induced with hypericin-mediated PDT by the chemical inhibition of p38 MAPKs in HK-1 nasopharyngeal carcinoma (NPC) cells. It was also shown that PDT activated p38 MAPKs through the production of singlet oxygen (Chan et al. 2009). Other authors reported that hypericin-mediated PDT of cancer cells also promoted a sustained activation of the p38 MAPK cascade, which resulted in the stabilization of the cyclooxygenase-2 (COX-2) transcript and in a rapid increase in COX-2 protein expression levels (Hendrickx et al. 2003). In spite of the evidences about p38 MAPK activation with PDT, inhibition of p38 MAPK did not enhanced hypericin-mediated photodynamic effect in our experimental model. On the other side, since pretreatment of HT-29 cells with rofecoxib and SC-560, selective inhibitors of COX-2 and COX-1, attenuated the impact of hypericin-mediated PDT in a time-dependent manner (Kleban et al. 2006) it could indicate that p38 MAPK – COX-2 is not crucial survival pathway for HT-29 cells.

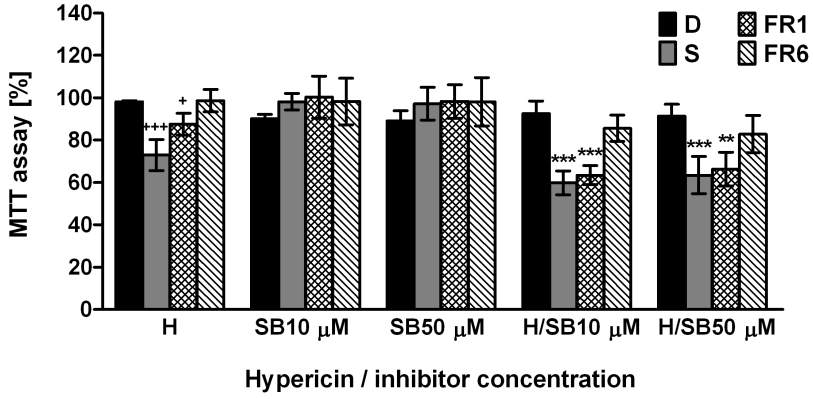

Figure 19. The effect of p38 MAPK inhibitor SB202190 on survival of HT-29 cells 24 h after hypericin mediated photodynamic treatment with a single (12 J.cm^{-2}) or fractionated (1 + 11 J.cm^{-2}) light deliveries. The results are the mean ± SD of three independent experiments presented as percentage of untreated control. Statistical significance is expressed as follows: monotherapy versus untreated control (+); combined therapy versus monotherapy with SB202190 (*); on the significance level $p<0.05$ (+); $p<0.01$ (**); $p<0.001$ (+++ or ***). (H) hypericin, (SB) p38 MAPK inhibitor SB202190, (C) control cells, (D) hypericin under dark conditions, (S) single light dose 12 J.cm^{-2}, fractionated light dose 1+11 J.cm^{-2} with a 1 h (FR1) or 6 h (FR6) dark pause between the two light doses.

5 CONCLUSIONS

Our research focused on the study of different effects of single and fractionated light delivery regimes in photodynamic therapy with hypericin on HT-29 adenocarcinoma cells *in vitro* revealed following findings:

- two-fold illumination scheme with equal or unequal light doses doesn't enhance cytotoxic effect of photodynamic therapy with hypericin in HT-29 adenocarcinoma cells

- hypericn-mediated photocytotoxic effect on HT-29 cells is reduced by light fractionation with a longer dark pause between two unequal light doses and is light dose- and photodynamic protocol-dependent

- a sub-lethal light dose alters ROS levels, protein expression and makes cells resistant to the effect of second illumination depending on its timing

- duration of a dark pause significantly decreases hypericin content that may result in decreased ROS production after second illumination and thus partially contribute to decreased cytotoxic effect of fractionated PDT

- possible implication of NF-κB in photo-resistance of HT-29 adenocarcinoma cells to fractionated delivery with a longer dark pause between two unequal light doses

- the role of p38 MAPK in resistance to fractionated PDT with hypericin is insignificant in our experimental model

- since any exposure of cancer cells to light prior to proper therapy could make them less sensitive to photodynamic treatment with hypericin, this finding could be useful in practice and together with targeted inhibition of NF-κB pathway could prevent resistance to photodynamic therapy

- although two-fold light fractionation with hypericin is not suitable therapeutic approach we assume that a high photo-stability and prolonged retention of hypericin in the light-treated cells may indicate its successful application in a high-dose multi-fraction PDT with dark intervals reduced bellow 1 h

6 ACKNOWLEDGEMENTS

I would like to express my thanks to my both supervisors, Prof. RNDr. Peter Fedoročko, CSc. from Pavol Jozef Šafárik University in Košice in Slovakia who reposaled me and accepted me in his work group where he get me freedom to actualize my ideas and supported my research. I am obliged to him for a lot of chances which enriched me, for his human approach and because he got a feeling for me, and Prof. Giuseppe Palumbo from Università di Napoli "FEDERICO II" in Italy who accepted my request for fellowship and it was an honour to me spent 6 months in his research group and acquire a part of the results to my dissertation. I would like to thank him for inspiration and his helpfulness to overcome difficulties.

Since I started to work in laboratory, my colleagues have been very helpful and I hope that I can tell, they became my friends, therefore I would like to thank to RNDr. Jaromír Mikeš, PhD. and RNDr. Veronika Sačková, PhD. for close co-operation and a lot of inspiring dialogues. The words of thanks belong also to all collective of employees and doctorate students in the work group of Prof. Fedoročko for their help. Also I would like to thank to my Italian colleagues Dr. Angela Chiaviello, PhD. and Dr. Elvira Crescenzi, PhD. and Dr. Roberta deMattia who helped me to manage my research fellowship in Naples. Although they don't anticipate it, to know them significantly influenced me and acquired experiences enriched my dissertation thesis and personal life.

I would like to thank Prof. Giancarlo Vecchio who let me attend Italian Doctorate program under his supervision.

I would like to express my great thanks to my family, my parents and my sister who gave me the opportunity follow my way, who supported me, trusted me and thanks to them I found strength to overcome all difficulties and start again.

This dissertation was supported by the following grants and grant agencies:

Slovak Research and Development Agency

- **APVT-20-003704** Hypericum perforatum L.: Genetic aspects of hypericin synthesis and its photocytotoxic effects.
- **APVV-0321-07** Hypericum spp. as a source of bioactive substances with anticancer activity.
- **APVV-0001-07** Centres for Research and Teaching Excellence: Centre for Signalome Research.

Scientific Grant Agency of the Ministry of Education of the Slovak Republic and the Slovak Academy of Science

- **VEGA MŠ SR a SAV 1/2329/05** The role of lipid mediators in hypericin-modulated proliferation and apoptosis of tumour cells.
- **VEGA MŠ SR a SAV 1/0240/08** Impact of cell membrane (phospho)lipid content variation on proliferation and cell death of colon epithelial cells in model cancer therapy.

International Scientific and Technological Co-operation

- **MVTS Bil/ČR/SR-75/06** Effect of phospholipids metabolism modulation on tumor cell proliferation and apoptosis in interaction with cytotoxic drugs.

Internal grant system for young researchers of Pavol Jozef Šafárik University in Košice, Slovakia

- **VVGS/UPJŠ/24/09-10** The role of nuclear transcription factor NF-κB and clusterin in the resistance of HT-29 colon cancer cells to fractionated regime of hypericin activation.

7 REFERENCES

Agarwal ML, Clay ME, Harvey EJ, Evans HH, Antunez AR, Oleinick NL. Photodynamic therapy induces rapid cell death by apoptosis in L5178Y mouse lymphoma cells. Cancer Res 1991; 51:5993-5996.

Agostinis P, Vantieghem A, Merlevede W, de Witte PA. Hypericin in cancer treatment: more light on the way. Int J Biochem Cell Biol 2002; 34:221-241.

Albert D, Zundorf I, Dingermann T, Muller WE, Steinhilber D, Werz O. Hyperforin is a dual inhibitor of cyclooxygenase-1 and 5-lipoxygenase. Biochem Pharmacol 2002; 64:1767-1775.

Aldrian S, Trautinger F, Frohlich I, Berger W, Micksche M, Kindas-Mugge I. Overexpression of Hsp27 affects the metastatic phenotype of human melanoma cells in vitro. Cell Stress Chaperones 2002; 7:177-185.

Ananthan J, Goldberg AL, Voellmy R. Abnormal proteins serve as eukaryotic stress signals and trigger the activation of heat shock genes. Science 1986; 232:522-524.

Anholt H, Moan J. Fractionated treatment of CaD2 tumors in mice sensitized with aluminium phthlocyanine tetrasulfonate. Cancer Lett 1992; 61:263-267.

Araki S, Israel S, Leskov KS, Criswell TL, Beman M, Klokov DY, Sampalth L, Reinicke KE, Cataldo E, Mayo LD, Boothman DA. Clusterin proteins: stress-inducible polypeptides with proposed functions in multiple organ dysfunction. BJR Suppl 2005; 27:106-113.

Ascencio M, Estevez JP, Delemer M, Farine MO, Collinet P, Mordon S. Comparison of continuous and fractionated illumination during hexaminolaevulinate-photodynamic therapy. Photodiagnosis Photodyn Ther 2008; 5:210-216.

Babilas P, Schacht V, Liebsch G, Wolfbeis OS, Landthaler M, Szeimies RM, Abels C. Effects of light fractionation and different fluence rates on photodynamic therapy with 5-aminolaevulinic acid in vivo. Br J Cancer 2003; 88:1462-1469.

Bagatell R, Whitesell L. Altered Hsp90 function in cancer: a unique therapeutic opportunity. Mol Cancer Ther 2004; 3:1021-1030.

Baldwin AS. Control of oncogenesis and cancer therapy resistance by the transcription factor NF-kappaB. J Clin Invest 2001; 107:241-246.

Barberi-Heyob M, Vedrine PO, Merlin JL, Millon R, Abecassis J, Poupon MF, Guillemin F. Wild-type p53 gene transfer into mutated p53 HT29 cells improves sensitivity to photodynamic therapy via induction of apoptosis. Int J Oncol 2004; 24:951-958.

Basso AD, Solit DB, Chiosis G, Giri B, Tsichlis P, Rosen N. Akt forms an intracellular complex with heat shock protein 90 (Hsp90) and Cdc37 and is destabilized by inhibitors of Hsp90 function. J Biol Chem 2002; 277:39858-39866.

Beere HM, Wolf BB, Cain K, Mosser DD, Mahboubi A, Kuwana T, Tailor P, Morimoto RI, Cohen GM, Green DR. Heat-shock protein 70 inhibits apoptosis by preventing recruitment of procaspase-9 to the Apaf-1 apoptosome. Nat Cell Biol 2000; 2:469-475.

Beere HM, Green DR. Stress management - heat shock protein-70 and the regulation of apoptosis. Trends Cell Biol 2001; 11:6-10.

Bellnier DA, Gollnick SO, Camacho SH, Greco WR, Cheney RT. Treatment with the tumor necrosis factor-alpha-inducing drug 5,6-dimethylxanthenone-4-acetic acid enhances the antitumor activity of the photodynamic therapy of RIF-1 mouse tumors. Cancer Res 2003; 63:7584-7590.

Blank M, Mandel M, Keisari Y, Meruelo D, Lavie G. Enhanced ubiquitinylation of heat shock protein 90 as a potential mechanism for mitotic cell death in cancer cells induced with hypericin. Cancer Res 2003; 63:8241-8247.

Blank M, Lavie G, Mandel M, Hazan S, Orenstein A, Meruelo D, Keisari Y. Antimetastatic activity of the photodynamic agent hypericin in the dark. Int J Cancer 2004; 111:596-603.

Blant SA, Woodtli A, Wagnieres G, Fontolliet C, van den Bergh H, Monnier P. In vivo fluence rate effect in photodynamic therapy of early cancers with tetra(m-hydroxyphenyl)chlorin. Photochem Photobiol 1996; 64:963-968.

Borgatti P, Martelli AM, Bellacosa A, Casto R, Massari L, Capitani S, Neri LM. Translocation of Akt/PKB to the nucleus of osteoblast-like MC3T3-E1 cells exposed to proliferative growth factors. FEBS Lett 2000; 477:27-32.

Brancho D, Tanaka N, Jaeschke A, Ventura JJ, Kelkar N, Tanaka Y, Kyuuma M, Takeshita T, Flavell RA, Davis RJ. Mechanism of p38 MAP kinase activation in vivo. Genes Dev 2003; 17:1969-1978.

Brockman H, Haschad MN, Maier K, Pohl F. Hypericin, the photodynamically active pigment from Hypericum perforatum. Naturwiss; 27:550-555

Bruey JM, Ducasse C, Bonniaud P, Ravagnan L, Susin SA, Diaz-Latoud C, Gurbuxani S, Arrigo AP, Kroemer G, Solary E, Garrido C. Hsp27 negatively regulates cell death by interacting with cytochrome c. Nat Cell Biol 2000; 2:645-652.

Brunet A, Bonni A, Zigmond MJ, Lin MZ, Juo P, Hu LS, Anderson MJ, Arden KC, Blenis J, Greenberg ME. Akt promotes cell survival by phosphorylating and inhibiting a Forkhead transcription factor. Cell 1999; 96:857-868.

Burkey BF, deSilva HV, Harmony JA. Intracellular processing of apolipoprotein J precursor to the mature heterodimer. J Lipid Res 1991; 32:1039-1048.

Buytaert E, Callewaert G, Hendrickx N, Scorrano L, Hartmann D, Missiaen L, Vandenheede JR, Heirman I, Grooten J, Agostinis P. Role of endoplasmic reticulum depletion and multidomain proapoptotic BAX and BAK proteins in shaping cell death after hypericin-mediated photodynamic therapy. Faseb J 2006a; 20:756-758.

Buytaert E, Callewaert G, Vandenheede JR, Agostinis P. Deficiency in apoptotic effectors Bax and Bak reveals an autophagic cell death pathway initiated by photodamage to the endoplasmic reticulum. Autophagy 2006b; 2:238-240.

Calabrese EJ, Baldwin LA. Defining hormesis. Hum Exp Toxicol 2002; 21:91-97.

Cardone MH, Roy N, Stennicke HR, Salvesen GS, Franke TF, Stanbridge E, Frisch S, Reed JC. Regulation of cell death protease caspase-9 by phosphorylation. Science 1998; 282:1318-1321.

Casas A, Perotti C, Fukuda H, del CBAM. Photodynamic therapy of activated and resting lymphocytes and its antioxidant adaptive response. Lasers Med Sci 2002; 17:42-50.

Cavarga I, Brezani P, Fedorocko P, Miskovsky P, Bobrov N, Longauer F, Rybarova S, Mirossay L, Stubna J. Photoinduced antitumour effect of hypericin can be enhanced by fractionated dosing. Phytomedicine 2005; 12:680-683.

Crnolatac I, Huygens A, van Aerschot A, Busson R, Rozenski J, de Witte PA. Synthesis, in vitro cellular uptake and photo-induced antiproliferative effects of lipophilic hypericin acid derivatives. Bioorg Med Chem 2005; 13:6347-6353.

Curnow A, McIlroy BW, Postle-Hacon MJ, MacRobert AJ, Bown SG. Light dose fractionation to enhance photodynamic therapy using 5-aminolevulinic acid in the normal rat colon. Photochem Photobiol 1999; 69:71-76.

Curnow A, Haller JC, Bown SG. Oxygen monitoring during 5-aminolaevulinic acid induced photodynamic therapy in normal rat colon. Comparison of continuous and fractionated light regimes. J Photochem Photobiol B 2000; 58:149-155.

Datta SR, Brunet A, Greenberg ME. Cellular survival: a play in three Akts. Genes Dev 1999; 13:2905-2927.

Davies KJ. The broad spectrum of responses to oxidants in proliferating cells: a new paradigm for oxidative stress. IUBMB Life 1999; 48:41-47.

Davis RJ. Signal transduction by the JNK group of MAP kinases. Cell 2000; 103:239-252.

de Bruijn HS, van der Veen N, Robinson DJ, Star WM. Improvement of systemic 5-aminolevulinic acid-based photodynamic therapy in vivo using light fractionation with a 75-minute interval. Cancer Res 1999; 59:901-904.

de Bruijn HS, van der Ploeg-van den Heuvel A, Sterenborg HJ, Robinson DJ. Fractionated illumination after topical application of 5-aminolevulinic acid on normal skin of hairless mice: the influence of the dark interval. J Photochem Photobiol B 2006; 85:184-190.

de Bruijn HS, de Haas ER, Hebeda KM, van der Ploeg-van den Heuvel A, Sterenborg HJ, Neumann HA, Robinson DJ. Light fractionation does not enhance the efficacy of

methyl 5-aminolevulinate mediated photodynamic therapy in normal mouse skin. Photochem Photobiol Sci 2007; 6:1325-1331.

de Witte P, Agostinis P, Van Lint J, Merlevede W, Vandenheede JR. Inhibition of epidermal growth factor receptor tyrosine kinase activity by hypericin. Biochem Pharmacol 1993; 46:1929-1936.

Deschesnes RG, Huot J, Valerie K, Landry J. Involvement of p38 in apoptosis-associated membrane blebbing and nuclear condensation. Mol Biol Cell 2001; 12:1569-1582.

Devauchelle V, Essabbani A, De Pinieux G, Germain S, Tourneur L, Mistou S, Margottin-Goguet F, Anract P, Migaud H, Le Nen D, Lequerre T, Saraux A, Dougados M, Breban M, Fournier C, Chiocchia G. Characterization and functional consequences of underexpression of clusterin in rheumatoid arthritis. J Immunol 2006; 177:6471-6479.

Diwu Z, Lown JW. Phototherapeutic potential of alternative photosensitizers to porphyrins. Pharmacol Ther 1994; 63:1-35.

Dolmans DE, Kadambi A, Hill JS, Flores KR, Gerber JN, Walker JP, Borel Rinkes IH, Jain RK, Fukumura D. Targeting tumor vasculature and cancer cells in orthotopic breast tumor by fractionated photosensitizer dosing photodynamic therapy. Cancer Res 2002; 62:4289-4294.

Dorion S, Berube J, Huot J, Landry J. A short lived protein involved in the heat shock sensing mechanism responsible for stress-activated protein kinase 2 (SAPK2/p38) activation. J Biol Chem 1999; 274:37591-37597.

Dougherty TJ, Gomer CJ, Henderson BW, Jori G, Kessel D, Korbelik M, Moan J, Peng Q. Photodynamic therapy. J Natl Cancer Inst 1998; 90:889-905.

Dreher D, Junod AF. Role of oxygen free radicals in cancer development. Eur J Cancer 1996; 32A:30-38.

Du K, Montminy M. CREB is a regulatory target for the protein kinase Akt/PKB. J Biol Chem 1998; 273:32377-32379.

Dutta R, Inouye M. GHKL, an emergent ATPase/kinase superfamily. Trends Biochem Sci 2000; 25:24-28.

Ehrenberg B, Anderson JL, Foote CS. Kinetics and yield of singlet oxygen photosensitized by hypericin in organic and biological media. Photochem Photobiol 1998; 68:135-140.

Evans S, Matthews W, Perry R, Fraker D, Norton J, Pass HI. Effect of photodynamic therapy on tumor necrosis factor production by murine macrophages. J Natl Cancer Inst 1990; 82:34-39.

Fanger GR, Gerwins P, Widmann C, Jarpe MB, Johnson GL. MEKKs, GCKs, MLKs, PAKs, TAKs, and tpls: upstream regulators of the c-Jun amino-terminal kinases? Curr Opin Genet Dev 1997; 7:67-74.

Fehr MJ, Carpenter SL, Wannemuehler Y, Petrich JW. Roles of oxygen and photoinduced acidification in the light-dependent antiviral activity of hypocrellin A. Biochemistry 1995; 34:15845-15848.

Fiers W, Beyaert R, Declercq W, Vandenabeele P. More than one way to die: apoptosis, necrosis and reactive oxygen damage. Oncogene 1999; 18:7719-7730.

Filippa N, Sable CL, Hemmings BA, Van Obberghen E. Effect of phosphoinositide-dependent kinase 1 on protein kinase B translocation and its subsequent activation. Mol Cell Biol 2000; 20:5712-5721.

Finkel T. Redox-dependent signal transduction. FEBS Lett 2000; 476:52-54.

Fritsch C, Goerz G, Ruzicka T. Photodynamic therapy in dermatology. Arch Dermatol 1998; 134:207-214.

Furre IE, Shahzidi S, Luksiene Z, Moller MT, Borgen E, Morgan J, Tkacz-Stachowska K, Nesland JM, Peng Q. Targeting PBR by hexaminolevulinate-mediated photodynamic therapy induces apoptosis through translocation of apoptosis-inducing factor in human leukemia cells. Cancer Res 2005; 65:11051-11060.

Gabai VL, Meriin AB, Mosser DD, Caron AW, Rits S, Shifrin VI, Sherman MY. Hsp70 prevents activation of stress kinases. A novel pathway of cellular thermotolerance. J Biol Chem 1997; 272:18033-18037.

Gabai VL, Yaglom JA, Volloch V, Meriin AB, Force T, Koutroumanis M, Massie B, Mosser DD, Sherman MY. Hsp72-mediated suppression of c-Jun N-terminal kinase is implicated in development of tolerance to caspase-independent cell death. Mol Cell Biol 2000; 20:6826-6836.

Gerner EW, Schneider MJ. Induced thermal resistance in HeLa cells. Nature 1975; 256:500-502.

Gibson SL, VanDerMeid KR, Murant RS, Raubertas RF, Hilf R. Effects of various photoradiation regimens on the antitumor efficacy of photodynamic therapy for R3230AC mammary carcinomas. Cancer Res 1990; 50:7236-7241.

Gottesman MM, Fojo T, Bates SE. Multidrug resistance in cancer: role of ATP-dependent transporters. Nat Rev Cancer 2002; 2:48-58.

Grammatikakis N, Vultur A, Ramana CV, Siganou A, Schweinfest CW, Watson DK, Raptis L. The role of Hsp90N, a new member of the Hsp90 family, in signal transduction and neoplastic transformation. J Biol Chem 2002; 277:8312-8320.

Granville DJ, Levy JG, Hunt DW. Photodynamic therapy induces caspase-3 activation in HL-60 cells. Cell Death Differ 1997; 4:623-628.

Granville DJ, Carthy CM, Jiang H, Shore GC, McManus BM, Hunt DW. Rapid cytochrome c release, activation of caspases 3, 6, 7 and 8 followed by Bap31 cleavage in HeLa cells treated with photodynamic therapy. FEBS Lett 1998; 437:5-10.

Granville DJ, Jiang H, McManus BM, Hunt DW. Fas ligand and TRAIL augment the effect of photodynamic therapy on the induction of apoptosis in JURKAT cells. Int Immunopharmacol 2001; 1:1831-1840.

Guay J, Lambert H, Gingras-Breton G, Lavoie JN, Huot J, Landry J. Regulation of actin filament dynamics by p38 map kinase-mediated phosphorylation of heat shock protein 27. J Cell Sci 1997; 110 (Pt 3):357-368.

Gurevich AI, Dobrynin VN, Kolosov MN, Popravko SA, Riabova ID. [Antibiotic hyperforin from Hypericum perforatum L]. Antibiotiki 1971; 16:510-513.

Hadjur C, Richard MJ, Parat MO, Jardon P, Favier A. Photodynamic effects of hypericin on lipid peroxidation and antioxidant status in melanoma cells. Photochem Photobiol 1996; 64:375-381.

Halkiotis K, Yova D, Pantelias G. In vitro evaluation of the genotoxic and clastogenic potential of photodynamic therapy. Mutagenesis 1999; 14:193-198.

Han J, Lee JD, Bibbs L, Ulevitch RJ. A MAP kinase targeted by endotoxin and hyperosmolarity in mammalian cells. Science 1994; 265:808-811.

Hanlon JG, Adams K, Rainbow AJ, Gupta RS, Singh G. Induction of Hsp60 by Photofrin-mediated photodynamic therapy. J Photochem Photobiol B 2001; 64:55-61.

Hansen RK, Parra I, Hilsenbeck SG, Himelstein B, Fuqua SA. Hsp27-induced MMP-9 expression is influenced by the Src tyrosine protein kinase yes. Biochem Biophys Res Commun 2001; 282:186-193.

Hayes SA, Huang X, Kambhampati S, Platanias LC, Bergan RC. p38 MAP kinase modulates Smad-dependent changes in human prostate cell adhesion. Oncogene 2003; 22:4841-4850.

Hedges JC, Dechert MA, Yamboliev IA, Martin JL, Hickey E, Weber LA, Gerthoffer WT. A role for p38(MAPK)/HSP27 pathway in smooth muscle cell migration. J Biol Chem 1999; 274:24211-24219.

Helmbrecht K, Zeise E, Rensing L. Chaperones in cell cycle regulation and mitogenic signal transduction: a review. Cell Prolif 2000; 33:341-365.

Henderson BW, Gollnick SO, Snyder JW, Busch TM, Kousis PC, Cheney RT, Morgan J. Choice of oxygen-conserving treatment regimen determines the inflammatory response and outcome of photodynamic therapy of tumors. Cancer Res 2004; 64:2120-2126.

Hendrickx N, Volanti C, Moens U, Seternes OM, de Witte P, Vandenheede JR, Piette J, Agostinis P. Up-regulation of cyclooxygenase-2 and apoptosis resistance by p38 MAPK in hypericin-mediated photodynamic therapy of human cancer cells. J Biol Chem 2003; 278:52231-52239.

Ho YF, Wu MH, Cheng BH, Chen YW, Shih MC. Lipid-mediated preferential localization of hypericin in lipid membranes. Biochim Biophys Acta 2009; 1788:1287-1295.
Holden C. Treating AIDS with worts. Science 1991; 254:522.
Hostanska K, Reichling J, Bommer S, Weber M, Saller R. Hyperforin a constituent of St John's wort (Hypericum perforatum L.) extract induces apoptosis by triggering activation of caspases and with hypericin synergistically exerts cytotoxicity towards human malignant cell lines. Eur J Pharm Biopharm 2003; 56:121-132.
Hua Z, Gibson SL, Foster TH, Hilf R. Effectiveness of delta-aminolevulinic acid-induced protoporphyrin as a photosensitizer for photodynamic therapy in vivo. Cancer Res 1995; 55:1723-1731.
Huang Y, Sadee W. Membrane transporters and channels in chemoresistance and -sensitivity of tumor cells. Cancer Lett 2006; 239:168-182.
Humphreys DT, Carver JA, Easterbrook-Smith SB, Wilson MR. Clusterin has chaperone-like activity similar to that of small heat shock proteins. J Biol Chem 1999; 274:6875-6881.
Huot J, Lambert H, Lavoie JN, Guimond A, Houle F, Landry J. Characterization of 45-kDa/54-kDa HSP27 kinase, a stress-sensitive kinase which may activate the phosphorylation-dependent protective function of mammalian 27-kDa heat-shock protein HSP27. Eur J Biochem 1995; 227:416-427.
Huot J, Houle F, Spitz DR, Landry J. HSP27 phosphorylation-mediated resistance against actin fragmentation and cell death induced by oxidative stress. Cancer Res 1996; 56:273-279.
Huot J, Houle F, Rousseau S, Deschesnes RG, Shah GM, Landry J. SAPK2/p38-dependent F-actin reorganization regulates early membrane blebbing during stress-induced apoptosis. J Cell Biol 1998; 143:1361-1373.
Huygens A, Kamuhabwa AR, Van Laethem A, Roskams T, Van Cleynenbreugel B, Van Poppel H, Agostinis P, De Witte PA. Enhancing the photodynamic effect of hypericin in tumour spheroids by fractionated light delivery in combination with hyperoxygenation. Int J Oncol 2005; 26:1691-1697.
Hyzd'alova M, Hofmanova J, Pachernik J, Vaculova A, Kozubik A. The interaction of butyrate with TNF-alpha during differentiation and apoptosis of colon epithelial cells: Role of NF-kappa B activation. Cytokine 2008; 44:33-43.
Chaloupka R, Obsil T, Plasek J, Sureau F. The effect of hypericin and hypocrellin-A on lipid membranes and membrane potential of 3T3 fibroblasts. Biochim Biophys Acta 1999; 1418:39-47.
Chan PS, Koon HK, Wu ZG, Wong RN, Lung ML, Chang CK, Mak NK. Role of p38 MAPKs in hypericin photodynamic therapy-induced apoptosis of nasopharyngeal carcinoma cells. Photochem Photobiol 2009; 85:1207-1217.
Chandra J, Samali A, Orrenius S. Triggering and modulation of apoptosis by oxidative stress. Free Radic Biol Med 2000; 29:323-333.
Chang L, Karin M. Mammalian MAP kinase signalling cascades. Nature 2001; 410:37-40.
Chapman PM. Defining hormesis: comments on Calabrese and Baldwin (2002). Hum Exp Toxicol 2002; 21:99-101; discussion 113-104.
Chen G, Cao P, Goeddel DV. TNF-induced recruitment and activation of the IKK complex require Cdc37 and Hsp90. Mol Cell 2002; 9:401-410.
Chen CH, Tsai JL, Wang YH, Lee CL, Chen JK, Huang MH. Low-level laser irradiation promotes cell proliferation and mRNA expression of type I collagen and decorin in porcine Achilles tendon fibroblasts in vitro. J Orthop Res 2009; 27:646-650.
Chen YR, Tan TH. The c-Jun N-terminal kinase pathway and apoptotic signaling (review). Int J Oncol 2000; 16:651-662.
Chretien P, Landry J. Enhanced constitutive expression of the 27-kDa heat shock proteins in heat-resistant variants from Chinese hamster cells. J Cell Physiol 1988; 137:157-166.
Chu ZL, McKinsey TA, Liu L, Gentry JJ, Malim MH, Ballard DW. Suppression of tumor necrosis factor-induced cell death by inhibitor of apoptosis c-IAP2 is under NF-kappaB control. Proc Natl Acad Sci U S A 1997; 94:10057-10062.

Ibuki Y, Hayashi A, Suzuki A, Goto R. Low-dose irradiation induces expression of heat shock protein 70 mRNA and thermo- and radio-resistance in myeloid leukemia cell line. Biol Pharm Bull 1998; 21:434-439.

Iinuma S, Schomacker KT, Wagnieres G, Rajadhyaksha M, Bamberg M, Momma T, hasan T. In vivo fluence rate and fractionation with two photosensitizers in orthotopic rat tumor model. Cancer Res 1999; 59:6164-6170.

Jaattela M, Wissing D, Bauer PA, Li GC. Major heat shock protein hsp70 protects tumor cells from tumor necrosis factor cytotoxicity. Embo J 1992; 11:3507-3512.

Jaattela M. Escaping cell death: survival proteins in cancer. Exp Cell Res 1999; 248:30-43.

Janssen-Heininger YM, Poynter ME, Baeuerle PA. Recent advances towards understanding redox mechanisms in the activation of nuclear factor kappaB. Free Radic Biol Med 2000; 28:1317-1327.

Jendzelovsky R, Mikes J, Koval J, Soucek K, Prochazkova J, Kello M, Sackova V, Hofmanova J, Kozubik A, Fedorocko P. Drug efflux transporters, MRP1 and BCRP, affect the outcome of hypericin-mediated photodynamic therapy in HT-29 adenocarcinoma cells. Photochem Photobiol Sci 2009; DOI:10.1039/b9pp00086k in press.

Ji Z, Yang G, Shahzidi S, Tkacz-Stachowska K, Suo Z, Nesland JM, Peng Q. Induction of hypoxia-inducible factor-1alpha overexpression by cobalt chloride enhances cellular resistance to photodynamic therapy. Cancer Lett 2006; 244:182-189.

Jobin C, Haskill S, Mayer L, Panja A, Sartor RB. Evidence for altered regulation of I kappa B alpha degradation in human colonic epithelial cells. J Immunol 1997; 158:226-234.

Joiner MC, Lambin P, Malaise EP, Robson T, Arrand JE, Skov KA, Marples B. Hypersensitivity to very-low single radiation doses: its relationship to the adaptive response and induced radioresistance. Mutat Res 1996; 358:171-183.

Kalka K, Merk H, Mukhtar H. Photodynamic therapy in dermatology. J Am Acad Dermatol 2000; 42:389-413; quiz 414-386.

Kane LP, Shapiro VS, Stokoe D, Weiss A. Induction of NF-kappaB by the Akt/PKB kinase. Curr Biol 1999; 9:601-604.

Kascakova S, Refregiers M, Jancura D, Sureau F, Maurizot JC, Miskovsky P. Fluorescence spectroscopic study of hypericin-photosensitized oxidation of low-density lipoproteins. Photochem Photobiol 2005; 81:1395-1403.

Kerr JF, Wyllie AH, Currie AR. Apoptosis: a basic biological phenomenon with wide-ranging implications in tissue kinetics. Br J Cancer 1972; 26:239-257.

Kleban J, Szilardiova B, Mikes J, Horvath V, Sackova V, Brezani P, Hofmanova J, Kozubik A, Fedorocko P. Pre-treatment of HT-29 cells with 5-LOX inhibitor (MK-886) induces changes in cell cycle and increases apoptosis after photodynamic therapy with hypericin. J Photochem Photobiol B 2006; 84:79-88.

Klionsky DJ. The molecular machinery of autophagy: unanswered questions. J Cell Sci 2005; 118:7-18.

Korbelik M, Sun J, Cecic I, Serrano K. Adjuvant treatment for complement activation increases the effectiveness of photodynamic therapy of solid tumors. Photochem Photobiol Sci 2004; 3:812-816.

Korbelik M. PDT-associated host response and its role in the therapy outcome. Lasers Surg Med 2006; 38:500-508.

Kyriakis JM, Avruch J. pp54 microtubule-associated protein 2 kinase. A novel serine/threonine protein kinase regulated by phosphorylation and stimulated by poly-L-lysine. J Biol Chem 1990; 265:17355-17363.

Lambert H, Charette SJ, Bernier AF, Guimond A, Landry J. HSP27 multimerization mediated by phosphorylation-sensitive intermolecular interactions at the amino terminus. J Biol Chem 1999; 274:9378-9385.

Landry J, Bernier D, Chretien P, Nicole LM, Tanguay RM, Marceau N. Synthesis and degradation of heat shock proteins during development and decay of thermotolerance. Cancer Res 1982; 42:2457-2461.

Landry J, Chretien P, Laszlo A, Lambert H. Phosphorylation of HSP27 during development and decay of thermotolerance in Chinese hamster cells. J Cell Physiol 1991; 147:93-101.

Landry J, Huot J. Regulation of actin dynamics by stress-activated protein kinase 2 (SAPK2)-dependent phosphorylation of heat-shock protein of 27 kDa (Hsp27). Biochem Soc Symp 1999; 64:79-89.

Lavie G, Valentine F, Levin B, Mazur Y, Gallo G, Lavie D, Weiner D, Meruelo D. Studies of the mechanisms of action of the antiretroviral agents hypericin and pseudohypericin. Proc Natl Acad Sci U S A 1989; 86:5963-5967.

Lavoie JN, Lambert H, Hickey E, Weber LA, Landry J. Modulation of cellular thermoresistance and actin filament stability accompanies phosphorylation-induced changes in the oligomeric structure of heat shock protein 27. Mol Cell Biol 1995; 15:505-516.

Lee JC, Laydon JT, McDonnell PC, Gallagher TF, Kumar S, Green D, McNulty D, Blumenthal MJ, Heys JR, Landvatter SW, et al. A protein kinase involved in the regulation of inflammatory cytokine biosynthesis. Nature 1994; 372:739-746.

Lee KW, Kim MS, Kang NJ, Kim DH, Surh YJ, Lee HJ, Moon A. H-Ras selectively up-regulates MMP-9 and COX-2 through activation of ERK1/2 and NF-kappaB: an implication for invasive phenotype in rat liver epithelial cells. Int J Cancer 2006; 119:1767-1775.

Legrand-Poels S, Bours V, Piret B, Pflaum M, Epe B, Rentier B, Piette J. Transcription factor NF-kappa B is activated by photosensitization generating oxidative DNA damages. J Biol Chem 1995; 270:6925-6934.

Leskov KS, Klokov DY, Li J, Kinsella TJ, Boothman DA. Synthesis and functional analyses of nuclear clusterin, a cell death protein. J Biol Chem 2003; 278:11590-11600.

Li GC, Werb Z. Correlation between synthesis of heat shock proteins and development of thermotolerance in Chinese hamster fibroblasts. Proc Natl Acad Sci U S A 1982; 79:3218-3222.

Lindquist S. The heat-shock response. Annu Rev Biochem 1986; 55:1151-1191.

Lindquist S, Craig EA. The heat-shock proteins. Annu Rev Genet 1988; 22:631-677.

Luo Y, Kessel D. Initiation of apoptosis versus necrosis by photodynamic therapy with chloroaluminum phthalocyanine. Photochem Photobiol 1997; 66:479-483.

Martin KR, Barrett JC. Reactive oxygen species as double-edged swords in cellular processes: low-dose cell signaling versus high-dose toxicity. Hum Exp Toxicol 2002; 21:71-75.

Martinez-Poveda B, Quesada AR, Medina MA. Hypericin in the dark inhibits key steps of angiogenesis in vitro. Eur J Pharmacol 2005; 516:97-103.

Matroule JY, Volanti C, Piette J. NF-kappaB in photodynamic therapy: discrepancies of a master regulator. Photochem Photobiol 2006; 82:1241-1246.

Melnick J, Aviel S, Argon Y. The endoplasmic reticulum stress protein GRP94, in addition to BiP, associates with unassembled immunoglobulin chains. J Biol Chem 1992; 267:21303-21306.

Meriin AB, Yaglom JA, Gabai VL, Zon L, Ganiatsas S, Mosser DD, Zon L, Sherman MY. Protein-damaging stresses activate c-Jun N-terminal kinase via inhibition of its dephosphorylation: a novel pathway controlled by HSP72. Mol Cell Biol 1999; 19:2547-2555.

Miadokova E, Chalupa I, Vlckova V, Sevcovicova A, Nadova S, Kopaskova M, Hercegova A, Gasperova P, Alfoldiova L, Komjatiova M, Csanyiova Z, Galova E, Cellarova E, Vlcek D. Genotoxicity and antigenotoxicity evaluation of non-photoactivated hypericin. Phytother Res 2009.

Miccoli L, Beurdeley-Thomas A, De Pinieux G, Sureau F, Oudard S, Dutrillaux B, Poupon MF. Light-induced photoactivation of hypericin affects the energy metabolism of human glioma cells by inhibiting hexokinase bound to mitochondria. Cancer Res 1998; 58:5777-5786.

Mikes J, Kleban J, Sackova V, Horvath V, Jamborova E, Vaculova A, Kozubik A, Hofmanova J, Fedorocko P. Necrosis predominates in the cell death of human colon adenocarcinoma HT-29 cells treated under variable conditions of photodynamic therapy with hypericin. Photochem Photobiol Sci 2007; 6:758-766.

Miskovsky P, Sureau F, Chinsky L, Turpin PY. Subcellular distribution of hypericin in human cancer cells. Photochem Photobiol 1995; 62:546-549.

Mitchel RE, Jackson JS, McCann RA, Boreham DR. The adaptive response modifies latency for radiation-induced myeloid leukemia in CBA/H mice. Radiat Res 1999; 152:273-279.

Mitra S, Cassar SE, Niles DJ, Puskas JA, Frelinger JG, Foster TH. Photodynamic therapy mediates the oxygen-independent activation of hypoxia-inducible factor 1alpha. Mol Cancer Ther 2006; 5:3268-3274.

Mlkvy P, Messmann H, Pauer M, Stewart JC, Millson CE, MacRobert AJ, Bown SG. Distribution and photodynamic effects of meso-tetrahydroxyphenylchlorin (mTHPC) in the pancreas and adjacent tissues in the Syrian golden hamster. Br J Cancer 1996; 73:1473-1479.

Mohan N, Meltz ML. Induction of nuclear factor kappa B after low-dose ionizing radiation involves a reactive oxygen intermediate signaling pathway. Radiat Res 1994; 140:97-104.

Morimoto RI. Cells in stress: transcriptional activation of heat shock genes. Science 1993; 259:1409-1410.

Mosmann T. Rapid colorimetric assay for cellular growth and survival: application to proliferation and cytotoxicity assays. J Immunol Methods 1983; 65:55-63.

Mosser DD, Kotzbauer PT, Sarge KD, Morimoto RI. In vitro activation of heat shock transcription factor DNA-binding by calcium and biochemical conditions that affect protein conformation. Proc Natl Acad Sci U S A 1990; 87:3748-3752.

Mosser DD, Martin LH. Induced thermotolerance to apoptosis in a human T lymphocyte cell line. J Cell Physiol 1992; 151:561-570.

Mosser DD, Caron AW, Bourget L, Denis-Larose C, Massie B. Role of the human heat shock protein hsp70 in protection against stress-induced apoptosis. Mol Cell Biol 1997; 17:5317-5327.

Mosser DD, Caron AW, Bourget L, Meriin AB, Sherman MY, Morimoto RI, Massie B. The chaperone function of hsp70 is required for protection against stress-induced apoptosis. Mol Cell Biol 2000; 20:7146-7159.

Nathan DF, Vos MH, Lindquist S. In vivo functions of the Saccharomyces cerevisiae Hsp90 chaperone. Proc Natl Acad Sci U S A 1997; 94:12949-12956.

Neckers L. Hsp90 inhibitors as novel cancer chemotherapeutic agents. Trends Mol Med 2002; 8:S55-61.

Nigam SK, Goldberg AL, Ho S, Rohde MF, Bush KT, Sherman M. A set of endoplasmic reticulum proteins possessing properties of molecular chaperones includes Ca(2+)-binding proteins and members of the thioredoxin superfamily. J Biol Chem 1994; 269:1744-1749.

Nicholson KM, Anderson NG. The protein kinase B/Akt signalling pathway in human malignancy. Cell Signal 2002; 14:381-395.

Noodt BB, Berg K, Stokke T, Peng Q, Nesland JM. Different apoptotic pathways are induced from various intracellular sites by tetraphenylporphyrins and light. Br J Cancer 1999; 79:72-81.

Nylandsted J, Rohde M, Brand K, Bastholm L, Elling F, Jaattela M. Selective depletion of heat shock protein 70 (Hsp70) activates a tumor-specific death program that is independent of caspases and bypasses Bcl-2. Proc Natl Acad Sci U S A 2000; 97:7871-7876.

Oberdanner CB, Plaetzer K, Kiesslich T, Krammer B. Photodynamic treatment with fractionated light decreases production of reactive oxygen species and cytotoxicity in vitro via regeneration of glutathione. Photochem Photobiol 2005; 81:609-613.

Okazaki R, Ootsuyama A, Norimura T. Radioadaptive response for protection against radiation-induced teratogenesis. Radiat Res 2005; 163:266-270.

Olivieri G, Bodycote J, Wolff S. Adaptive response of human lymphocytes to low concentrations of radioactive thymidine. Science 1984; 223:594-597.

Ono K, Han J. The p38 signal transduction pathway: activation and function. Cell Signal 2000; 12:1-13.

Paba V, Quarto M, Varriale L, Crescenzi E, Palumbo G. Photo-activation of hypericin with low doses of light promotes apparent photo-resistance in human histiocytic lymphoma U937 cells. J Photochem Photobiol B 2001; 60:87-96.

Pandey P, Saleh A, Nakazawa A, Kumar S, Srinivasula SM, Kumar V, Weichselbaum R, Nalin C, Alnemri ES, Kufe D, Kharbanda S. Negative regulation of cytochrome c-mediated oligomerization of Apaf-1 and activation of procaspase-9 by heat shock protein 90. Embo J 2000; 19:4310-4322.

Park HS, Lee JS, Huh SH, Seo JS, Choi EJ. Hsp72 functions as a natural inhibitory protein of c-Jun N-terminal kinase. Embo J 2001; 20:446-456.

Park J, English DS, Wannemuehler Y, Carpenter S, Petrich JW. The role of oxygen in the antiviral activity of hypericin and hypocrellin. Photochem Photobiol 1998; 68:593-597.

Parsell DA, Lindquist S. The function of heat-shock proteins in stress tolerance: degradation and reactivation of damaged proteins. Annu Rev Genet 1993; 27:437-496.

Pe MB, Ikeda H, Inokuchi T. Tumour destruction and proliferation kinetics following periodic, low power light, haematoporphyrin oligomers mediated photodynamic therapy in the mouse tongue. Eur J Cancer B Oral Oncol 1994; 30B:174-178.

Perovic S, Muller WE. Pharmacological profile of hypericum extract. Effect on serotonin uptake by postsynaptic receptors. Arzneimittelforschung 1995; 45:1145-1148.

Piper PW. The Hsp90 chaperone as a promising drug target. Curr Opin Investig Drugs 2001; 2:1606-1610.

Pogue BW, Hasan T. A theoretical study of light fractionation and dose-rate effects in photodynamic therapy. Radiat Res 1997; 147:551-559.

Pogue BW, Braun RD, Lanzen JL, Erickson C, Dewhirst MW. Analysis of the heterogeneity of pO2 dynamics during photodynamic therapy with verteporfin. Photochem Photobiol 2001; 74:700-706.

Pogue BW, Sheng C, Benevides J, Forcione D, Puricelli B, Nishioka N, Hasan T. Protoporphyrin IX fluorescence photobleaching increases with the use of fractionated irradiation in the esophagus. J Biomed Opt 2008; 13:034009.

Prasad AV, Mohan N, Chandrasekar B, Meltz ML. Activation of nuclear factor kappa B in human lymphoblastoid cells by low-dose ionizing radiation. Radiat Res 1994; 138:367-372.

Randow F, Seed B. Endoplasmic reticulum chaperone gp96 is required for innate immunity but not cell viability. Nat Cell Biol 2001; 3:891-896.

Redmond RW, Kochevar IE. Spatially resolved cellular responses to singlet oxygen. Photochem Photobiol 2006; 82:1178-1186.

Ris HB, Altermatt HJ, Nachbur B, Stewart JC, Wang Q, Lim CK, Bonnett R, Althaus U. Effect of drug-light interval on photodynamic therapy with meta-tetrahydroxyphenylchlorin in malignant mesothelioma. Int J Cancer 1993; 53:141-146.

Robinson DJ, de Bruijn HS, van der Veen N, Stringer MR, Brown SB, Star WM. Fluorescence photobleaching of ALA-induced protoporphyrin IX during photodynamic therapy of normal hairless mouse skin: the effect of light dose and irradiance and the resulting biological effect. Photochem Photobiol 1998; 67:140-149.

Robinson DJ, de Bruijn HS, de Wolf WJ, Sterenborg HJ, Star WM. Topical 5-aminolevulinic acid-photodynamic therapy of hairless mouse skin using two-fold illumination schemes: PpIX fluorescence kinetics, photobleaching and biological effect. Photochem Photobiol 2000; 72:794-802.

Robinson DJ, de Bruijn HS, Star WM, Sterenborg HJ. Dose and timing of the first light fraction in two-fold illumination schemes for topical ALA-mediated photodynamic therapy of hairless mouse skin. Photochem Photobiol 2003; 77:319-323.

Rodrigues NR, Rowan A, Smith ME, Kerr IB, Bodmer WF, Gannon JV, Lane DP. p53 mutations in colorectal cancer. Proc Natl Acad Sci U S A 1990; 87:7555-7559.

Roe SM, Prodromou C, O'Brien R, Ladbury JE, Piper PW, Pearl LH. Structural basis for inhibition of the Hsp90 molecular chaperone by the antitumor antibiotics radicicol and geldanamycin. J Med Chem 1999; 42:260-266.

Romashkova JA, Makarov SS. NF-kappaB is a target of AKT in anti-apoptotic PDGF signalling. Nature 1999; 401:86-90.

Rouse J, Cohen P, Trigon S, Morange M, Alonso-Llamazares A, Zamanillo D, Hunt T, Nebreda AR. A novel kinase cascade triggered by stress and heat shock that stimulates MAPKAP kinase-2 and phosphorylation of the small heat shock proteins. Cell 1994; 78:1027-1037.

Russell LB, Russell WL. An analysis of the changing radiation response of the developing mouse embryo. J Cell Physiol Suppl 1954; 43:103-149.

Sackova V, Kulikova L, Mikes J, Kleban J, Fedorocko P. Hypericin-mediated photocytotoxic effect on HT-29 adenocarcinoma cells is reduced by light fractionation with longer dark pause between two unequal light doses. Photochem Photobiol 2005; 81:1411-1416.

Sackova V, Fedorocko P, Szilardiova B, Mikes J, Kleban J. Hypericin-induced photocytotoxicity is connected with G2/M arrest in HT-29 and S-phase arrest in U937 cells. Photochem Photobiol 2006; 82:1285-1291.

Saleh A, Srinivasula SM, Balkir L, Robbins PD, Alnemri ES. Negative regulation of the Apaf-1 apoptosome by Hsp70. Nat Cell Biol 2000; 2:476-483.

Santana P, Pena LA, Haimovitz-Friedman A, Martin S, Green D, McLoughlin M, Cordon-Cardo C, Schuchman EH, Fuks Z, Kolesnick R. Acid sphingomyelinase-deficient human lymphoblasts and mice are defective in radiation-induced apoptosis. Cell 1996; 86:189-199.

Santilli G, Aronow BJ, Sala A. Essential requirement of apolipoprotein J (clusterin) signaling for IkappaB expression and regulation of NF-kappaB activity. J Biol Chem 2003; 278:38214-38219.

Sasaki MS. On the reaction kinetics of the radioadaptive response in cultured mouse cells. Int J Radiat Biol 1995; 68:281-291.

Sasaki MS, Ejima Y, Tachibana A, Yamada T, Ishizaki K, Shimizu T, Nomura T. DNA damage response pathway in radioadaptive response. Mutat Res 2002; 504:101-118.

Sattler S, Schaefer U, Schneider W, Hoelzl J, Lehr CM. Binding, uptake, and transport of hypericin by Caco-2 cell monolayers. J Pharm Sci 1997; 86:1120-1126.

Separovic D, Pink JJ, Oleinick NA, Kester M, Boothman DA, McLoughlin M, Pena LA, Haimovitz-Friedman A. Niemann-Pick human lymphoblasts are resistant to phthalocyanine 4-photodynamic therapy-induced apoptosis. Biochem Biophys Res Commun 1999; 258:506-512.

Shadley JD, Afzal V, Wolff S. Characterization of the adaptive response to ionizing radiation induced by low doses of X rays to human lymphocytes. Radiat Res 1987; 111:511-517.

Shen HR, Spikes JD, Kopecekova P, Kopecek J. Photodynamic crosslinking of proteins. I. Model studies using histidine- and lysine-containing N-(2-hydroxypropyl)methacrylamide copolymers. J Photochem Photobiol B 1996; 34:203-210.

Schafer C, Clapp P, Welsh MJ, Benndorf R, Williams JA. HSP27 expression regulates CCK-induced changes of the actin cytoskeleton in CHO-CCK-A cells. Am J Physiol 1999; 277:C1032-1043.

Schell MT, Spitzer AL, Johnson JA, Lee D, Harris HW. Heat shock inhibits NF-kB activation in a dose- and time-dependent manner. J Surg Res 2005; 129:90-93.

Schempp CM, Simon-Haarhaus B, Termeer CC, Simon JC. Hypericin photo-induced apoptosis involves the tumor necrosis factor-related apoptosis-inducing ligand (TRAIL) and activation of caspase-8. FEBS Lett 2001; 493:26-30.

Schempp CM, Kirkin V, Simon-Haarhaus B, Kersten A, Kiss J, Termeer CC, Gilb B, Kaufmann T, Borner C, Sleeman JP, Simon JC. Inhibition of tumour cell growth by hyperforin, a novel anticancer drug from St. John's wort that acts by induction of apoptosis. Oncogene 2002; 21:1242-1250.

Schoonbroodt S, Piette J. Oxidative stress interference with the nuclear factor-kappa B activation pathways. Biochem Pharmacol 2000; 60:1075-1083.

Schreck R, Rieber P, Baeuerle PA. Reactive oxygen intermediates as apparently widely used messengers in the activation of the NF-kappa B transcription factor and HIV-1. Embo J 1991; 10:2247-2258.

Sim HG, Lau WK, Olivo M, Tan PH, Cheng CW. Is photodynamic diagnosis using hypericin better than white-light cystoscopy for detecting superficial bladder carcinoma? BJU Int 2005; 95:1215-1218.

Simizu S, Osada H. Mutations in the Plk gene lead to instability of Plk protein in human tumour cell lines. Nat Cell Biol 2000; 2:852-854.

Singh G, Espiritu M, Shen XY, Hanlon JG, Rainbow AJ. In vitro induction of PDT resistance in HT29, HT1376 and SK-N-MC cells by various photosensitizers. Photochem Photobiol 2001; 73:651-656.

Sitnik TM, Hampton JA, Henderson BW. Reduction of tumour oxygenation during and after photodynamic therapy in vivo: effects of fluence rate. Br J Cancer 1998; 77:1386-1394.

Spikes JD, Shen HR, Kopeckova P, Kopecek J. Photodynamic crosslinking of proteins. III. Kinetics of the FMN- and rose bengal-sensitized photooxidation and intermolecular crosslinking of model tyrosine-containing N-(2-hydroxypropyl)methacrylamide copolymers. Photochem Photobiol 1999; 70:130-137.

Strocchi P, Smith MA, Perry G, Tamagno E, Danni O, Pession A, Gaiba A, Dozza B. Clusterin up-regulation following sub-lethal oxidative stress and lipid peroxidation in human neuroblastoma cells. Neurobiol Aging 2006; 27:1588-1594.

Subjeck JR, Sciandra JJ, Chao CF, Johnson RJ. Heat shock proteins and biological response to hyperthermia. Br J Cancer Suppl 1982; 5:127-131.

Sureau F, Miskovsky P, Chinsky L, Turpin PY. Hypericin-mediated cell photosensitization involves an intracellular pH decrease. J AM Cem 1996; 118:9484-9487.

Takahashi A, Kondo N, Inaba H, Uotani K, Kiyohara Y, Ohnishi K, Ohnishi T. Radiation-induced apoptosis in scid mice spleen after low dose irradiation. Adv Space Res 2003; 31:1569-1573.

Takahashi A, Ohnishi T. A low dose: pre-irradiation induces radio- and heat-resistance via HDM2 and NO radicals, and is associated with p53 functioning. Advances in Space Research 2009; 43:1185-1192.

Takahashi I, Nakanishi S, Kobayashi E, Nakano H, Suzuki K, Tamaoki T. Hypericin and pseudohypericin specifically inhibit protein kinase C: possible relation to their antiretroviral activity. Biochem Biophys Res Commun 1989; 165:1207-1212.

Tang J, Colacino JM, Larsen SH, Spitzer W. Virucidal activity of hypericin against enveloped and non-enveloped DNA and RNA viruses. Antiviral Res 1990; 13:313-325.

Tempel K, Schleifer S. Adaptive response of the chicken embryo to low doses of x-irradiation. Radiat Environ Biophys 1995; 34:177-183.

Thomas C, MacGill RS, Miller GC, Pardini RS. Photoactivation of hypericin generates singlet oxygen in mitochondria and inhibits succinoxidase. Photochem Photobiol 1992; 55:47-53.

Thomas C, Pardini RS. Oxygen dependence of hypericin-induced phototoxicity to EMT6 mouse mammary carcinoma cells. Photochem Photobiol 1992; 55:831-837.

Thong PS, Watt F, Ren MQ, Tan PH, Soo KC, Olivo M. Hypericin-photodynamic therapy (PDT) using an alternative treatment regime suitable for multi-fraction PDT. J Photochem Photobiol B 2006; 82:1-8.

Tcherkasskaya O, Uversky VN. Denatured collapsed states in protein folding: example of apomyoglobin. Proteins 2001; 44:244-254.
Tiku AB, Kale RK. Adaptive response and split-dose effect of radiation on the survival of mice. J Biosci 2004; 29:111-117.
Togashi H, Uehara M, Ikeda H, Inokuchi T. Fractionated photodynamic therapy for a human oral squamous cell carcinoma xenograft. Oral Oncol 2006; 42:526-532.
Tong Z, Singh G, Rainbow AJ. Sustained activation of the extracellular signal-regulated kinase pathway protects cells from photofrin-mediated photodynamic therapy. Cancer Res 2002; 62:5528-5535.
Tsuruo T. Mechanisms of multidrug resistance and implications for therapy. Jpn J Cancer Res 1988; 79:285-296.
Tsuruo T, Naito M, Tomida A, Fujita N, Mashima T, Sakamoto H, Haga N. Molecular targeting therapy of cancer: drug resistance, apoptosis and survival signal. Cancer Sci 2003; 94:15-21.
Uehara M, Inokuchi T, Sano K, Sekine J, Ikeda H. Cell kinetics of mouse tumour subjected to photodynamic therapy--evaluation by proliferating cell nuclear antigen immunohistochemistry. Oral Oncol 1999; 35:93-97.
Ueno AM, Vannais DB, Gustafson DL, Wong JC, Waldren CA. A low, adaptive dose of gamma-rays reduced the number and altered the spectrum of S1- mutants in human-hamster hybrid AL cells. Mutat Res 1996; 358:161-169.
Usuda J, Chiu SM, Azizuddin K, Xue LY, Lam M, Nieminen AL, Oleinick NL. Promotion of photodynamic therapy-induced apoptosis by the mitochondrial protein Smac/DIABLO: dependence on Bax. Photochem Photobiol 2002; 76:217-223.
Utsumi T, Okuma M, Kanno T, Takehara Y, Yoshioka T, Fujita Y, Horton AA, Utsumi K. Effect of the antiretroviral agent hypericin on rat liver mitochondria. Biochem Pharmacol 1995; 50:655-662.
Uzdensky AB, Ma LW, Iani V, Hjortland GO, Steen HB, Moan J. Intracellular localisation of hypericin in human glioblastoma and carcinoma cell lines. Lasers Med Sci 2001; 16:276-283.
Uzdensky AB, Iani V, Ma LW, Moan J. Photobleaching of hypericin bound to human serum albumin, cultured adenocarcinoma cells and nude mice skin. Photochem Photobiol 2002; 76:320-328.
van der Veen N, van Leengoed HL, Star WM. In vivo fluorescence kinetics and photodynamic therapy using 5-aminolaevulinic acid-induced porphyrin: increased damage after multiple irradiations. Br J Cancer 1994; 70:867-872.
Vanden Berghe T, Kalai M, van Loo G, Declercq W, Vandenabeele P. Disruption of HSP90 function reverts tumor necrosis factor-induced necrosis to apoptosis. J Biol Chem 2003; 278:5622-5629.
Vantieghem A, Xu Y, Declercq W, Vandenabeele P, Denecker G, Vandenheede JR, Merlevede W, de Witte PA, Agostinis P. Different pathways mediate cytochrome c release after photodynamic therapy with hypericin. Photochem Photobiol 2001; 74:133-142.
Varnes ME, Chiu SM, Xue LY, Oleinick NL. Photodynamic therapy-induced apoptosis in lymphoma cells: translocation of cytochrome c causes inhibition of respiration as well as caspase activation. Biochem Biophys Res Commun 1999; 255:673-679.
Varriale L, Coppola E, Quarto M, Veneziani BM, Palumbo G. Molecular aspects of photodynamic therapy: low energy pre-sensitization of hypericin-loaded human endometrial carcinoma cells enhances photo-tolerance, alters gene expression and affects the cell cycle. FEBS Lett 2002; 512:287-290.
Volloch V, Gabai VL, Rits S, Sherman MY. ATPase activity of the heat shock protein hsp72 is dispensable for its effects on dephosphorylation of stress kinase JNK and on heat-induced apoptosis. FEBS Lett 1999; 461:73-76.
Wada T, Penninger JM. Mitogen-activated protein kinases in apoptosis regulation. Oncogene 2004; 23:2838-2849.

Wang B, Ohyama H, Nose T, Itsukaichi H, Nakajima T, Yukawa O, Odaka T, Tanaka K, Kojima E, Yamada T, Hayata I. Adaptive response in embryogenesis: I. Dose and timing of radiation for reduction of prenatal death and congenital malformation during the late period of organogenesis. Radiat Res 1998; 150:120-122.

Wang JM, Chao JR, Chen W, Kuo ML, Yen JJ, Yang-Yen HF. The antiapoptotic gene mcl-1 is up-regulated by the phosphatidylinositol 3-kinase/Akt signaling pathway through a transcription factor complex containing CREB. Mol Cell Biol 1999; 19:6195-6206.

Wang Q, Kim S, Wang X, Evers BM. Activation of NF-kappaB binding in HT-29 colon cancer cells by inhibition of phosphatidylinositol 3-kinase. Biochem Biophys Res Commun 2000; 273:853-858.

Wassenberg JJ, Reed RC, Nicchitta CV. Ligand interactions in the adenosine nucleotide-binding domain of the Hsp90 chaperone, GRP94. II. Ligand-mediated activation of GRP94 molecular chaperone and peptide binding activity. J Biol Chem 2000; 275:22806-22814.

Webber J, Leeson B, Fromm D, Kessel D. Effects of photodynamic therapy using a fractionated dosing of mono-L-aspartyl chlorin e6 in a murine tumor. J Photochem Photobiol B 2005; 78:135-140.

Widmann C, Gibson S, Jarpe MB, Johnson GL. Mitogen-activated protein kinase: conservation of a three-kinase module from yeast to human. Physiol Rev 1999; 79:143-180.

Wolff S. Aspects of the adaptive response to very low doses of radiation and other agents. Mutat Res 1996; 358:135-142.

Wong P, Pineault J, Lakins J, Taillefer D, Leger J, Wang C, Tenniswood M. Genomic organization and expression of the rat TRPM-2 (clusterin) gene, a gene implicated in apoptosis. J Biol Chem 1993; 268:5021-5031.

Wouters BG, Skarsgard LD. Low-dose radiation sensitivity and induced radioresistance to cell killing in HT-29 cells is distinct from the "adaptive response" and cannot be explained by a subpopulation of sensitive cells. Radiat Res 1997; 148:435-442.

Wyld L, Reed MW, Brown NJ. Differential cell death response to photodynamic therapy is dependent on dose and cell type. Br J Cancer 2001; 84:1384-1386.

Xiao Z, Halls S, Dickey D, Tulip J, Moore RB. Fractionated versus standard continuous light delivery in interstitial photodynamic therapy of dunning prostate carcinomas. Clin Cancer Res 2007; 13:7496-7505.

Xue LY, Chiu SM, Azizuddin K, Joseph S, Oleinick NL. The death of human cancer cells following photodynamic therapy: apoptosis competence is necessary for Bcl-2 protection but not for induction of autophagy. Photochem Photobiol 2007; 83:1016-1023.

Yoshida N, Imada H, Kunugita N, Norimura T. Low dose radiation-induced adaptive survival response in mouse spleen T-lymphocytes in vivo. J Radiat Res (Tokyo) 1993; 34:269-276.

You M, Ku PT, Hrdlickova R, Bose HR, Jr. ch-IAP1, a member of the inhibitor-of-apoptosis protein family, is a mediator of the antiapoptotic activity of the v-Rel oncoprotein. Mol Cell Biol 1997; 17:7328-7341.

Zacal N, Espiritu M, Singh G, Rainbow AJ. Increased BNip3 and decreased mutant p53 in cisplatin-sensitive PDT-resistant HT29 cells. Biochem Biophys Res Commun 2005; 331:648-657.

Zeisser-Labouebe M, Lange N, Gurny R, Delie F. Hypericin-loaded nanoparticles for the photodynamic treatment of ovarian cancer. Int J Pharm 2006; 326:174-181.

Zha J, Harada H, Yang E, Jockel J, Korsmeyer SJ. Serine phosphorylation of death agonist BAD in response to survival factor results in binding to 14-3-3 not BCL-X(L). Cell 1996; 87:619-628.

Zong WX, Edelstein LC, Chen C, Bash J, Gelinas C. The prosurvival Bcl-2 homolog Bfl-1/A1 is a direct transcriptional target of NF-kappaB that blocks TNFalpha-induced apoptosis. Genes Dev 1999; 13:382-387.

Zorov DB, Filburn CR, Klotz LO, Zweier JL, Sollott SJ. Reactive oxygen species (ROS)-induced ROS release: a new phenomenon accompanying induction of the mitochondrial permeability transition in cardiac myocytes. J Exp Med 2000; 192:1001-1014.

Zou J, Guo Y, Guettouche T, Smith DF, Voellmy R. Repression of heat shock transcription factor HSF1 activation by HSP90 (HSP90 complex) that forms a stress-sensitive complex with HSF1. Cell 1998; 94:471-480.

Web sources:
http://ppathw3.cals.cornell.edu/glossary/Defs_R.htm
http://www.doh.wa.gov/notify/other/glossary.htm
http://www.nci.nih.gov/dictionary/?CdrID=416100

Photochemistry and Photobiology, 2005, 81: 1411–1416

Hypericin-mediated Photocytotoxic Effect on HT-29 Adenocarcinoma Cells Is Reduced by Light Fractionation with Longer Dark Pause Between Two Unequal Light Doses

Veronika Sačková, Lucia Kuliková, Jaromír Mikeš, Ján Kleban and Peter Fedoročko*

Institute of Biology and Ecology, Faculty of Sciences, P. J. Šafárik University, Košice, Slovakia

Received 5 May 2005; accepted 15 June 2005; published online 16 June 2005 DOI: 10.1562/2005-05-05-RA-514

ABSTRACT

The present study demonstrates the *in vitro* effect of hypericin-mediated PDT with fractionated light delivery. Cells were photosensitized with unequal light fractions separated by dark intervals (1 or 6 h). We compared the changes in viability, cell number, survival, apoptosis and cell cycle on HT-29 cells irradiated with a single light dose (12 J/cm^2) to the fractionated light delivery (1 + 11 J/cm^2) 24 and 48 h after photodynamic treatment. We found that a fractionated light regime with a longer dark period resulted in a decrease of hypericin cytotoxicity. Both cell number and survival were higher after light sensitization with a 6-h dark interval. DNA fragmentation occurred after a single light-dose application, but in contrast no apoptotic DNA formation was detected with a 6-h dark pause. After fractionation the percentage of cells in the G1 phase of the cell cycle was increased, while the proportion of cells in the G2 phase decreased as compared to a single light-dose application, *i.e.* both percentage of cells in the G1 and G2 phase of the cell cycle were near control levels. We presume that the longer dark interval after the irradiation of cells by first light dose makes them resistant to the effect of the second illumination. These findings confirm that the light application scheme together with other photodynamic protocol components is crucial for the photocytotoxicity of hypericin.

INTRODUCTION

Photodynamic therapy (PDT) is a cancer treatment mode based on the light activation of a photosensitizer preferentially localized in tumor tissue with subsequent reactive oxygen species production that causes photochemically induced cell death. The antitumoral effect of PDT depends on the photodynamic protocol used. Responses to photodynamic treatment depend on the photosensitizer used, the illumination conditions, the oxygenation status of the tissue and the type of cells involved (1).

Recently, modifications in light illumination scheme have been introduced on the standard photodynamic protocol (single-dose photosensitizer, single-dose light) to maximize the therapeutic effect of PDT, for example by reducing the fluence rate to improve oxygenation (2–4) or by fractionated drug administration (5–7).

Light fractionation is a relatively new approach to light delivery in which the photosensitizer is exposed to light disrupted at a particular point for a period of darkness to increase the efficacy of photodynamic therapy in tumor destruction (8–10). A number of animal studies have demonstrated that the response to PDT after systemic ALA administration can be improved by the use of light fractionation with either a short-term (2, 3, 9) or a long-term interval (11). Enhanced photodynamic effects on tumor cell killing using fractionated laser light have been described (12). A fractionated illumination scheme in which a cumulative fluence of 100 J/cm^2 was delivered in two equal light fractions separated by a dark interval of 2 h considerably increased the efficacy of 5-aminolevulinic acid (ALA)-PDT (13). It has been hypothesized that splitting the light dose into fractions by interrupting illumination for a certain time allows the treatment site to be reoxygenated, which results in increased generation of singlet oxygen and thus a greater PDT effect (14–16). In contrast, less or no effect was achieved by dividing the illumination in photodynamic therapy with mTHPC on a normal colon and a transplantable tumor in rats (17). Babilas *et al*. (18) found fractionated PDT with ALA to be unsuccessful in clinical PDT.

Photoactivation of hypericin with low doses of light-induced apparent photoresistance in human histiocytic lymphoma U937 cells (19). Low-energy pre-sensitization caused enhanced phototolerance of hypericin-loaded HEC1-B cells (20). Photodynamic treatment with fractionated light led to decreased production of reactive oxygen species and cytotoxicity *in vitro* via regeneration of glutathione (21).

In the present study, we demonstrate the *in vitro* effect of hypericin-mediated photodynamic therapy (PDT) with fractionated light delivery. We compared the effects of hypericin treatment on tumor cell viability, cell number, survival, apoptosis and cell cycle in a HT-29 cell line irradiated with a single light dose (12 J/cm^2) with its effects after fractionated light delivery (1 + 11 J/cm^2 with 1 or 6-h dark interval).

MATERIALS AND METHODS

Cell culture. A human colon adenocarcinoma cell line HT-29 (ATCC, Rockville, MD) was cultured in RPMI-1640 medium supplemented with

* To whom correspondence should be addressed: Institute of Biology and Ecology, Faculty of Sciences, P.J. Šafárik University, Moyzesova 11, 041 65 Košice, Slovakia. Fax: ++421-55-6222124; e-mail: fedvox@kosice.upjs.sk

Abbreviations: FCS, fetal calf serum; HT-29, human colon adenocarcinoma cell line; MTT, 3-(4,5-dimethylthiazol-2-yl)-2,5-diphenyl tetrazolium bromide; PBS, phosphate-buffered saline; PDT, photodynamic therapy; TBE, Tris-Borat-EDTA.

Table 1. Cytotoxicity of hypericin after various light-irradiation schemes

Light dose (J/cm)	Dark pause (h)	Cytotoxicity (MTT assay evaluated 24 h after PDT)
3 + 3 *vs* 6	1	NS*
	6	NS
6 + 6 *vs* 12	1	NS
	6	NS
1 + 11 *vs* 12	1	NS
	6	$P < 0.001$
1 *vs* 0 (control)	1	NS**
	6	NS***

* NS—not significantly.
** 1 h after PDT.
*** 6 h after PDT.

10% fetal calf serum (FCS) and antibiotics (penicillin 100 U/mL, streptomycin 100 μg/mL and amphotericin 25 μg/mL; Invitrogen Co., Carlsbad, CA). For determination of survival, 2×10^4 cells/well were seeded into 96 wells, and for evaluation of hypericin content, tumor cell viability, cell number, apoptosis and cell cycle, 6×10^5 cells/well were seeded into 6 well microplates. Cells were maintained at 37°C in a humidified 5% CO_2 atmosphere and protected from light constantly after hypericin treatment.

Hypericin treatment. Cells were incubated 16 h with different concentrations (2×10^{-8} *M*, 4×10^{-8} *M*, 6×10^{-8} *M*) of HPLC-grade hypericin (AppliChem, Darmstadt, Germany) in dark conditions, following irradiation with a single light dose (12 J/cm^2) or fractionated light doses (1 + 11 J/cm^2). The dark intervals between the two light fraction deliveries were 1 or 6 h. The control group received a medium with serum without hypericin. Before light application, the medium was replaced with fresh medium with 10% FCS.

Cell photosensitization. The cells were irradiated in hypericin-free medium by placing the microplates on a plastic diffuser sheet above a set of nine L18W/30 lamps (Osram, Berlin, Germany) with maximum emission between 530 and 620 nm (the absorption peak of hypericin is 595 nm). At the surface of the diffuser, the uniform fluence rate was 4.4 mW/cm^2.s and the temperature did not exceed 37°C. Light dose (12 J/cm^2, 11 J/cm^2 and 1 J/cm^2) was calculated by multiplying the fluence rate by the time.

Quantification of cell viability and cell number. At defined incubation times after hypericin photoactivation (24 and 48 h) eosin vital dye (0.15%) exclusion assay was used to determine both cell viability and cell number (microscopically). The viability was expressed as the percentage of live cells out of the total number of cells. Cell number was assessed by counting live cells in a Bürker chamber.

MTT assay. MTT (3-(4,5-dimethylthiazol-2-yl)-2,5-diphenyl tetrazolium bromide (Sigma Chemicals Co., St. Louis, MO) assay was performed to evaluate the survival of cultured cells as previously reported (22). The amount of dye extracted was quantified by absorbance measurements at 584 nm (FLUOstar Optima, BMG Labtechnologies GmbH, Offenburg, Germany) and expressed as a percentage of the dye extracted from untreated control cells ([OD value of treated cells/mean OD value of control cells] × 100%).

DNA fragmentation analysis. For DNA preparation 10^6–10^7 cells were harvested, pelleted and incubated with cold lysis buffer (10 mM TRIS pH 7.5; 1 mM EDTA pH 8; 0.2% Triton X-100) for 30 min on ice. Then, RNase A (10 mg/mL) and proteinase K (25 mg/mL, Amresco Inc., Solon, OH) were added and incubated for 30 min at 37°C. The DNA was precipitated with isopropanol and 5 *M* NaCl at –20°C overnight, centrifuged and resuspended in TE buffer (10 m*M* TRIS pH 7.5; 1 m*M* EDTA pH 8). DNA was analyzed by electrophoresis on 1% TBE agarose gel stained with ethidium bromide (25 μg) and visualized by UV light.

Morphological analysis by fluorescent microscopy. Adherent and floating cells were stained together by dual Hoechst 33342/propidium iodide viable staining. Native slides were evaluated by fluorescent microscope (Nikon, Eclipse 400, Japan) as a percentage of apoptotic cells from total number of minimum 300 cells.

Cell cycle analysis. For the DNA content determination, cells were harvested, washed with phosphate-buffered saline (PBS) and fixed with 70% ice cold ethanol at –20°C. Fixed cells were centrifuged, washed with PBS and stained with staining solution (5 mg/mL propidium iodide, 10 mg/mL RNase A and 10% Triton X-100 in PBS). Then samples were kept in dark conditions for 30 min and measured on a flow cytometer (FACS Calibur, Becton Dickinson, San Diego, CA). For each sample, 15 000 cells were evaluated and the sample flow rate during analysis did not exceed 200–300 cells per s. The data obtained were analyzed using the Cell Quest Pro software. Cells characterized by a smaller fluorescence than the G1 peak were considered as apoptotic cells (sub-G1 population).

Hypericin fluorescence. Cell extracts were prepared as described previously (1). Intracellular hypericin content was quantified by measuring fluorescence emission in FLUOstar Optima before the second irradiation and expressed as percentage of the fluorescence at time 0 (before irradiation) (Fig. 6).

Statistical analysis. Data were processed by GraphPadPrism (GraphPad Software Inc., San Diego, CA) and statistically analyzed using one-way ANOVA followed by Tukey's multiple comparison test.

RESULTS

Our preliminary studies together with the results presented here (Table 1) showed the different cytotoxic effect (MTT assay) of photodynamic treatment using the various light irradiation schemes and the importance of dark interval duration within a light fractionation scheme on the photocytotoxicity of hypericin. Based on this screening, in later experiments, we compared the effects of hypericin treatment on tumor cell viability, cell number, survival, apoptosis and cell cycle in a HT-29 cell line irradiated with a single light dose (12 J/cm^2) with its effects after fractionated light delivery (1 + 11 J/cm^2) separated by dark intervals 1 or 6 h.

Cell viability and cell number

Single light delivery (12 J/cm^2) vs control. The activation of hypericin (6×10^{-8} *M*) by a single light dose caused a non-significant decrease of cell viability (about 12%) compared with the untreated control. Treatments with lower drug concentrations resulted in cell viability similar to control (difference of 3%, data not shown). In contrast, cell number was reduced to 60% of control value after treatment with 4×10^{-8} *M* hypericin and to 40% of control value after 6×10^{-8} *M* hypericin treatment (Fig. 1a,b).

Fractionated light delivery (1 + 11 J/cm^2) vs control. Only minimal nonsignificant decrease of cell viability was observed after treatment with 6×10^{-8} *M* hypericin when fractionated light delivery with 1 or 6-h dark interval between light fractions was applied, compared with that of control cells (data not shown). The number of cells treated with 4×10^{-8} *M* or 6×10^{-8} *M* hypericin was reduced from 60% to 35% (at 48 h post-treatment) of the control group when the light regime of 1 + 11 J/cm^2 illumination was separated by a 1 h dark period. A dark period of 6 h in the fractionated illumination scheme reduced cell number not significantly (Fig. 1a,b).

Fractionated light delivery (1 +11 J/cm^2) vs single light delivery (12 J/cm^2). The cell viability slightly decreased when a fractionated light regime with a 1 h break between the 2 doses was used, whereas a slight increase was found with a 6-h break (data not shown). A 1-h dark pause between fractionated light deliveries induced the same effect as from single irradiation (decline to 30–40% of control). However, hypericin (6×10^{-8} *M*) activation with 2 light fractions separated by a dark interval of 6 h caused only slight decline of cell number (90% of control), *i.e.* by 50% more than after a single light dose after 24 h (Fig. 1a,b).

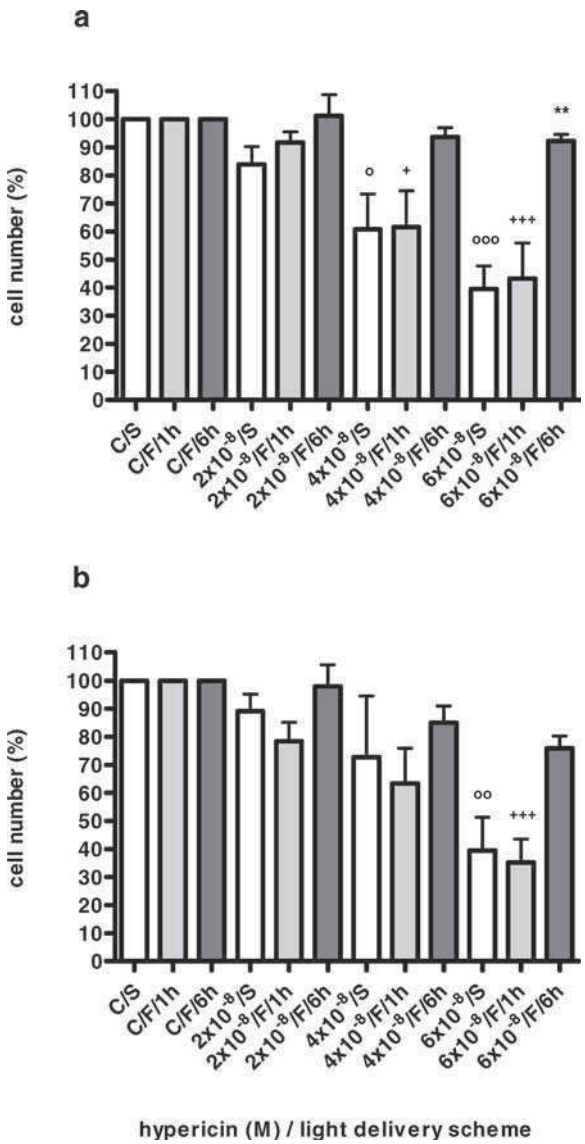

Figure 1. HT-29 cell numbers 24 h (a) and 48 h (b) after hypericin-mediated photodynamic treatment with both single light-dose and fractionated irradiation scheme. Results are expressed as relative cell numbers related to control groups. The results are the means ± SEM of three independent experiments. Single light delivery vs control (°), fractionated light delivery vs control ($^{+}$) and fractionated light delivery vs single light delivery (*) were statistically compared ($^{+}$ or $^{\circ}P < 0.05$, $^{\circ\circ}$ or $^{**}P < 0.01$, $^{+++}$ or $^{\circ\circ\circ}P < 0.001$). (C) control, (S) single light dose, (F) fractionated light dose.

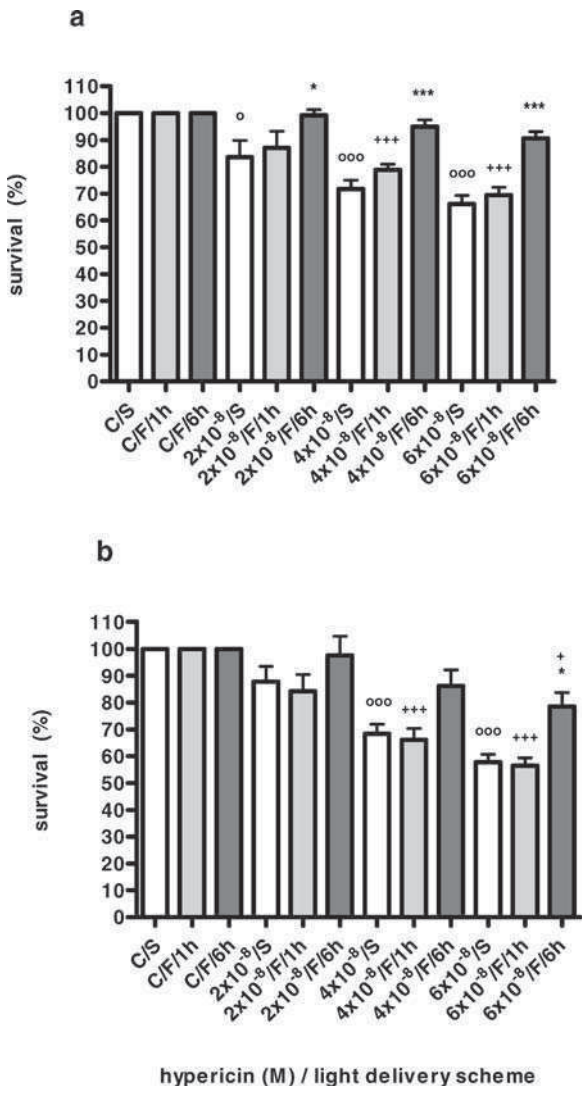

Figure 2. Survival of HT-29 cells 24 h (a) and 48 h (b) after hypericin-mediated photodynamic treatment with both single light dose and fractionated irradiation scheme. The results are the means ± SEM of four independent experiments. Single light delivery vs control (°), fractionated light delivery vs control ($^{+}$) and fractionated light delivery vs single light delivery (*) were statistically compared ($^{+}$ or $^{\circ}$ or $^{*}P < 0.05$, $^{+++}$ or $^{\circ\circ\circ}$ or $^{***}P < 0.001$). (C) control, (S) single light dose, (F) fractionated light dose.

MTT assay

Single light delivery (12 J/cm^2) vs control. Treatment of HT-29 cells with all of the tested hypericin concentrations reduced survival to 85–55% of control cells (Fig. 2a,b).

Fractionated light delivery (1 +11 J/cm^2) vs control. Survival of cells irradiated with a second light dose after a pause of 1 h decreased about 15–45% in comparison with control cells. In contrast, hypericin photosensitization by 2 unequal light fractions interrupted with 6-h dark period resulted in only slight decline in cell survival after 24 h (Fig. 2a,b).

Fractionated light delivery (1 +11 J/cm^2) vs single light delivery (12 J/cm^2). Cell survival was about 15–25% higher in group hypericin-treated cells irradiated with the $1 + 11$ J/cm^2 regime with a 6-h dark pause compared with cells for which single irradiation was used for hypericin activation. Survival of cells irradiated with a second light dose after a pause of 1 h was found to be similar to the effect of a single light dose, where a 15–45% drop in comparison with control cells was observed (Fig. 2a,b).

Determination of apoptosis

Fractionated light delivery (1 + 11 J/cm^2) vs single light delivery (12 J/cm^2). Both single-dose photosensitization and fractionated photosensitization with a 1-h dark pause between 2 light doses induced apoptotic DNA fragmentation in all hypericin-loaded cells (6×10^{-8} *M*). No apoptotic DNA fragment formation was found in cells after fractionated light delivery with the longer 6-h dark interval between the 2 light doses (Fig. 3a). The same apoptotic

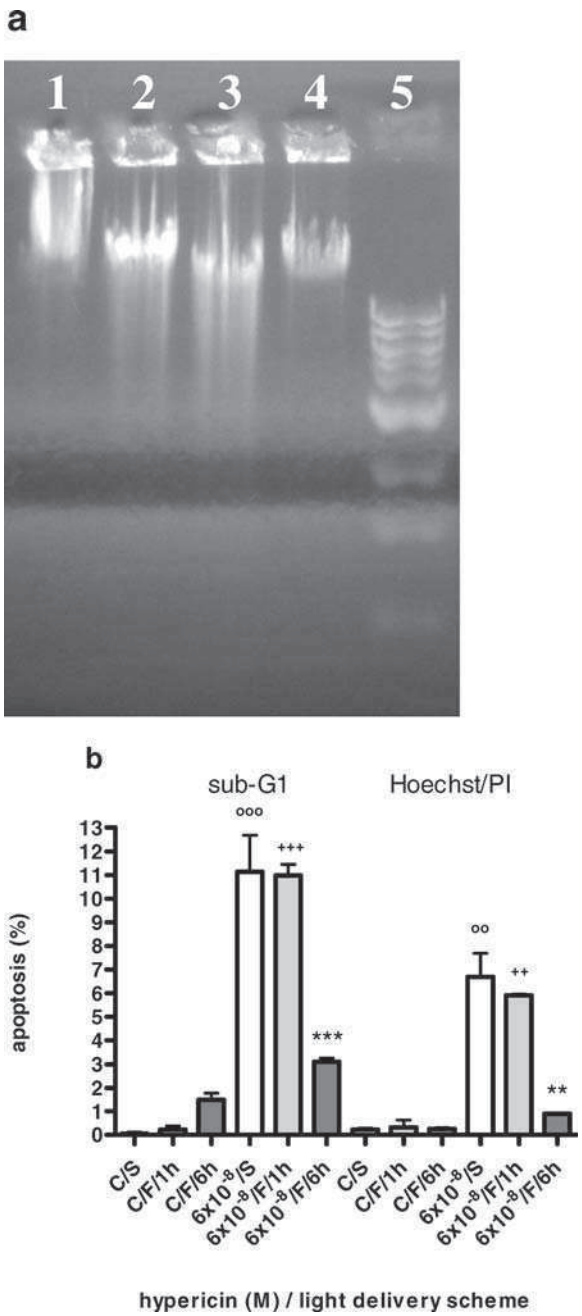

Figure 3. Determination of apoptosis in HT-29 cells 24 h after hypericin-mediated photodynamic treatment with both single light dose and fractionated irradiation scheme. (a) 1—control, 2—single light dose, 3—6×10^{-8}M/F/1h, 4—6×10^{-8}M/F/6h, 5—1 kb DNA ladder (Amresco Inc., Solon, OH). (b) The results are the means ± SEM of four independent experiments. Single light delivery vs control (°), fractionated light delivery vs control ($^{+}$) and fractionated light delivery vs single light delivery (*) were statistically compared ($^{++}$ or °° or $^{**}P < 0.01$, $^{+++}$ or °°° or $^{***}P < 0.001$). (C) control, (S) single light dose, (F) fractionated light dose.

effect was confirmed by 2 other methods: morphological analysis and sub-G1 evaluation of the nuclear fragmentation (Fig. 3b).

Cell cycle analysis

Single light delivery (12 J/cm^2) vs control. Changes in G1 phase of the cell cycle were not significant at 24 h post-treatment (data not shown). The percentage of cells in the G2 phase of the cell cycle significantly increased when cells were incubated with 6×10^{-8} *M* hypericin. Simultaneously, the percentage of cells in the G1 phase loaded with the same drug dose decreased (Figs. 4a,b and 5).

Fractionated light delivery (1 +11 J/cm^2) vs control. Changes in cell cycle after light fractionation with a 1-h dark period before the second light dose were found to be different compared with control cells when the proportion of cells in the G2 phase increased and that of G1 phase cells decreased. In contrast, a 6-h dark pause between fractionated light deliveries resulted in no changes (Figs. 4a,b and 5).

Fractionated light delivery (1 +11 J/cm^2) vs single light delivery (12 J/cm^2). The effect of a 1-h break between light deliveries was

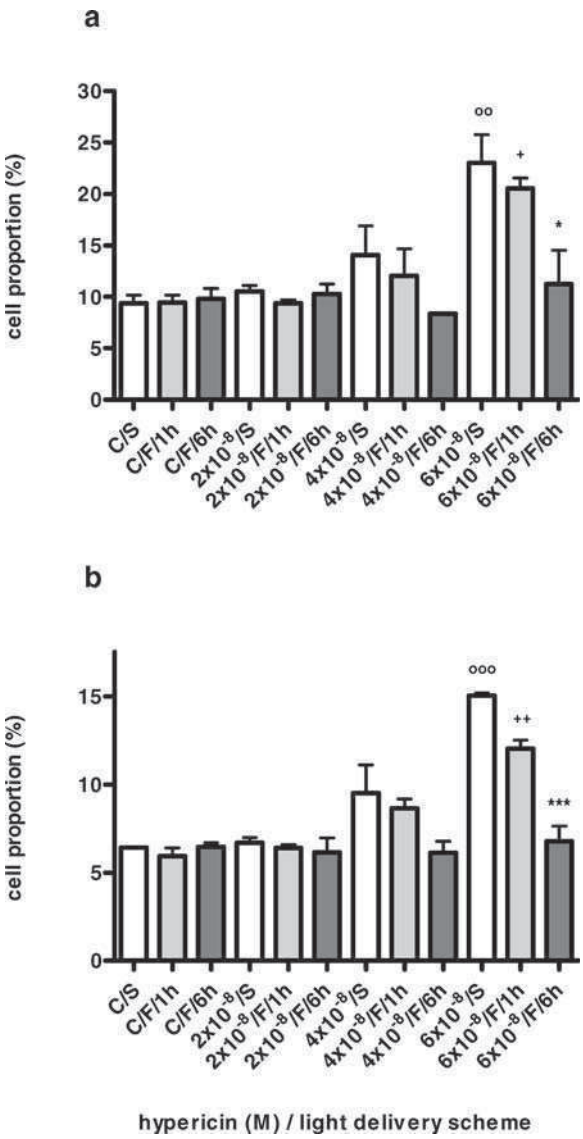

Figure 4. Proportion of HT-29 cells in the G2 phase 24 h (a) and 48 h (b) after hypericin-mediated photodynamic treatment with both single light-dose and fractionated irradiation scheme. The results are the means ± SEM of two independent experiments. Single light delivery vs control (°), fractionated light delivery vs control ($^{+}$) and fractionated light delivery vs single light delivery (*) were statistically compared ($^{+}$ or $^{*}P < 0.05$, $^{++}$ or $^{\circ\circ}P < 0.01$, °°° or $^{***}P < 0.001$). (C) control, (S) single light dose, (F) fractionated light dose.

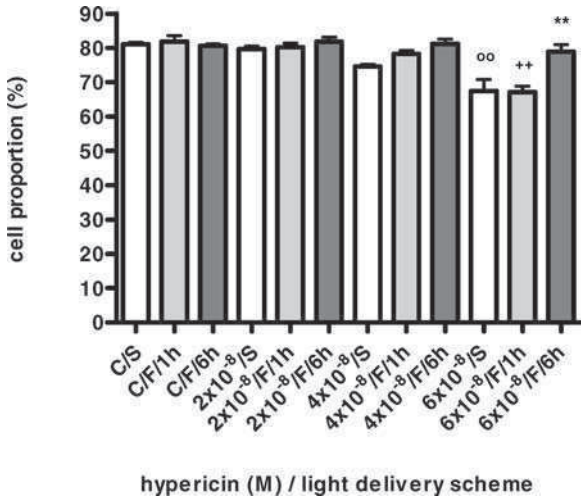

Figure 5. Proportion of HT-29 cells in the G1 phase 48 h after hypericin-mediated photodynamic treatment with both single light-dose and fractionated irradiation scheme. The results are the means ± SEM of two independent experiments. Single light delivery vs control (°), fractionated light delivery vs control ($^{+}$) and fractionated light delivery vs single light delivery (*) were statistically compared ($^{++}$ or $^{\circ\circ}$ or $^{**}P < 0.01$). (C) control, (S) single light dose, (F) fractionated light dose.

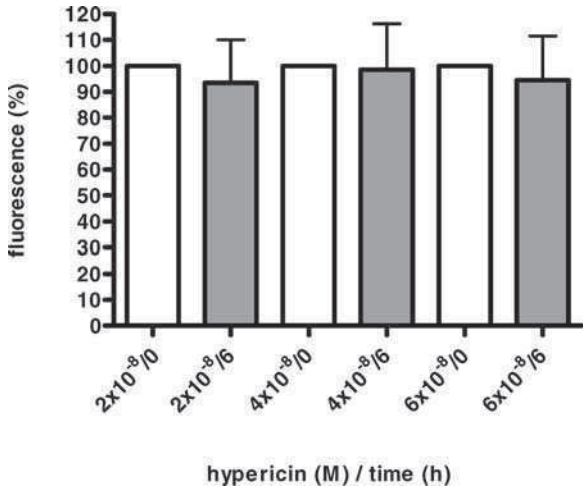

Figure 6. Fluorescence of hypericin before 1 J/cm^2 and 11 J/cm^2 irradiation. The results are the means ± SEM of two independent experiments expressed as percentages of fluorescence at time 0. (0) before irradiation and delivery of the first light dose. (6) 6 h after irradiation and before delivery of the second light dose.

almost the same as the single light-dose effect. Irradiation of hypericin-treated cells by 1 + 11 J/cm^2 with a 6-h dark pause induced a significant decrease in the percentage of G2 phase cells (to the control level) and a rise in the percentage of G1 phase cells compared with cells treated with hypericin photoactivated by single irradiation (to the control level) (Figs. 4a,b and 5).

Measurement of intracellular hypericin content confirmed that the fluorescence of hypericin remains unchanged before the second light-dose delivery (Fig. 6), therefore, reduced photocytotoxicity following fractionated irradiation with 6-h dark pause is not a result of photobleaching of hypericin.

DISCUSSION

Using fractionated light exposure to activate a photosensitive drug is a relatively new mode of light application as part of photodynamic treatment. So far there are several works reporting on comparison of single light doses with fractionated light regimes *in vivo*, producing contradictory results (9, 13, 17–18). It has been shown that the level of tissue oxygen at the treatment site is affected differently when the light dose is fractionated compared with the effect when a single light dose is employed (23). It is probable that the enhanced photodynamic effect of light fractionation is associated with reoxygenation of the treatment site during the dark period between the two light fractions, and that it is also dependent on the timing of the dark interval (3, 15–17). Enhancement of PDT by fractionation could be achieved by less rapid oxygen consumption. At lower fluence rates, the oxygen consumption rate is not fast enough to be improved by fractionation (17). It is difficult to compare individual studies because the animal model used, the photosensitive drug doses and the illumination methods are all different.

The *in vivo* and *in vitro* effects of light fractionation are completely incomparable. In contrast to *in vivo* studies, in which enhanced or no effect of fractionated irradiation was shown, the so far known *in vitro* works report either on photoresistance/photo-tolerance (19, 20) or on decreased production of reactive oxygen species and cytotoxicity via regeneration of glutathione (21).

Our preliminary studies together with the results presented here (Table 1) show the different cytotoxic effects of photodynamic treatment using the various light irradiation schemes and the importance of dark-interval duration within a light fractionation scheme as part of photodynamic treatment for its outcome related to the cytotoxic effect of hypericin on an HT-29 cell line. Comparison of the effects of hypericin treatment on tumor cell viability, cell number, cell survival, apoptosis and cell cycle after a single light-dose application (12 J/cm^2) with those after fractionated light delivery (1 + 11 J/cm^2) revealed a marked difference in all studied cellular parameters (except for viability) when the irradiation was interrupted with a longer dark period of 6 h. While fractionation with a shorter dark period induced the same cytotoxic effect on tumor cells as single-dose application, the effect of hypericin activated with light fractions separated by a dark interval of 6 h was reversed. Increased cell number and rise in metabolic activity along with an increased proportion of cells in the G1 phase of cell cycle together indicate maintained proliferation and mitochondrial function. On the other hand, the percentage of cells in the G2 phase of cell cycle decreased and no apoptotic fragmentation occurred, which is in contrast to the effects of both single-dose and fractionated light regimes. This means that the behavior of cells was similar to that of the control. The only significant change was observed in the survival of cells receiving 6×10^{-8} *M* hypericin evaluated 48 h after light sensitization, which decreased compared to that of the control. Because the fluorescence of hypericin remains unchanged before the second light-dose delivery (Fig. 6), reduced photocytotoxicity following fractionated irradiation is not a result of photobleaching or sensitizer loss from cells after the first light fraction. Our results indicate that irradiation of cells with the first light dose followed by a subsequent dark period of 6 h makes cells to resistant to the cytotoxic effect of second light dose (11 J). These findings relating to decreased cytotoxicity are in agreement with the results of the *in vitro* studies mentioned above, but the fact that different cell lines as well as

photodynamic protocols were used makes further comparison of results impossible.

Mechanisms that make cells resistant to treatment when hypericin is activated by two unequal light doses with a longer dark pause between them are the subject of our next investigation. For this time, the most probable hypothesis is that when the first light dose is sufficiently low not to induce nonreversible changes in cells, and it is followed by a longer dark period before the next light dose cells become resistant to the possible cytotoxicity of hypericin after the second light-dose application.

Acknowledgements—This study was supported by the Science and Technology Assistance Agency under contract APVT-20-003704 and by the grant agency VEGA under contract 1/2329/05. The authors are grateful to Viera Balážová for assistance with technical procedures. Thank also to Andrew J. Billingham for proofreading the manuscript.

REFERENCES

1. Vantieghem, A. (2001) *Mechanisms of Cell Death Induced by Photodynamic Therapy with Hypericin*. Leuven University Press, Leuven, Belgium.
2. Pogue, B. W. and T. Hasan (1997) A theoretical study of light fractionation and dose-rate effects in photodynamic therapy. *Radiat. Res.* **147**, 551–559.
3. Hua, Z., S. L. Gibson, T. H. Foster and R. Hilf (1995) Effectiveness of d-aminolevulinic acid-induced protoporphyrin as a photosensitizer for photodynamic therapy *in vivo*. *Cancer Res.* **55**, 1723–1731.
4. Robinson, D. J., H. S. de Bruijn, N. van der Veen, M. R. Stringer, S. B. Brown and W. M. Star (1998) Fluorescence photobleaching of ALA-induced protoporphyrin IX during photodynamic therapy of normal hairless mouse skin: the effect of light dose and irradiance and the resulting biological effect. *Photochem. Photobiol.* **67**, 140–149.
5. Dolmans, D. E., A. Kadambi, J. S. Hill, K. R. Flores, J. N. Gerber, J. P. Walker, I. H. Rinkes, R. K. Jain and D. Fukumura (2002) Targeting tumor vasculature and cancer cells in orthotopic breast tumor by fractionated photosensitizer dosing photodynamic therapy. *Cancer Res.* **62**(15), 4289–4294.
6. Webber, J., B. Leeson, D. Fromm and D. Kessel (2005) Effects of photodynamic therapy using a fractionated dosing of mono-L-aspartyl chlorin e6 in a murine tumor. *J. Photochem. Photobiol. B* **78**, 135–140.
7. Harvey, E. H., J. Webber, D. Kessel and D. Fromm (2005) Killing tumor cells: The effect of photodynamic therapy using mono-l-aspartyl chlorine and NS-398. *Am. J Surg* **189**(3), 302–305.
8. Gibson, S. L., K. R. VanDerMeid, R. S. Murant, R. F. Raubertas and R. Hilf (1990) Effects of various photoradiation regimens on the antitumor efficacy of photodynamic therapy for R3230AC mammary carcinomas. *Cancer Res.* **50**, 7236–7241.
9. Messmann, H., P. Mlkvy, G. Buonaccorsi, C. L. Davies, A. J. MacRobert and S. G. Bown (1995) Enhancement of photodynamic therapy with 5-aminolaevulinic acid induced porphyrin photosensitisation in normal rat colon by threshold and light fractionation studies. *Br. J. Cancer* **72**, 589–594.
10. Iinuma, S., K. T. Schomacker, G. Wagnieres, M. Rajadhyaksha, M. Bamberg, T. Momma and T. Hasan (1999) *In vivo* fluence rate and fractionation effects on tumor response and photobleaching: photodynamic therapy with two photosensitisers in an orthotopic rat tumor model. *Cancer Res.* **59**, 6164–6170.
11. Van der Veen, N., H. L. L. M. van Leengoed and W. M. Star (1994) *In vivo* fluorescence kinetics and photodynamic therapy using 5-aminolaevulinic acid-induced porphyrin: increased damage after multiple irradiations. *Br. J. Cancer* **70**, 867–872.
12. Muller, S., H. Walt, D. Dolber-Girdziunaite, D. Fiedler and U. Haller (1998) Enhanced photodynamic effects using fractionated laser light. *J. Photochem. Photobiol. B* **42**, 67–70.
13. Robinson, D. J., H. S. de Bruijn, W. M. Star and H. J. Sterenborg (2003) Dose and timing of the first light fraction in two-fold illumination schemes for topical ALA-mediated photodynamic therapy of hairless mouse skin. *Photochem. Photobiol.* **77**(3), 319–323.
14. Hua, Z., S. L. Gibson, T. H. Foster and R. Hilf (1995) Effectiveness of delta aminolevulinic acid-induced protoporphyrin as a photosensitiser for photodynamic therapy in vivo. *Cancer Res.* **55**, 1723–1731.
15. Robinson, D. J., H. S. de Bruijn, W. J. de Wolf, H. J. Sterenborg and W. M. Star (2000) Topical 5-aminolevulinic acid-photodynamic therapy of hairless mouse skin using two-fold illumination schemes: PpIX fluorescence kinetics, photobleaching and biological effect. *Photochem. Photobiol.* **72**, 794–802.
16. Pogue, B. W., R. D. Braun, J. L. Lanzen, C. Erickson and M. W. Dewhirst (2001) Analysis of the heterogeneity of pO_2 dynamics during photodynamic therapy with verteporfin. *Photochem. Photobiol.* **74**, 700–706.
17. Tsutsui, H., A. J. MacRobert, A. Curnow, A. Rogowska, G. Buonaccorsi, H. Kato and S. G. Bown (2002) Optimisation of illumination for photodynamic therapy with mTHPC on normal colon and a transplantable tumour in rats. *Lasers Med. Sci.* **17**(2), 101–109.
18. Babilas, P., V. Schacht, G. Liebsch, O. S. Wolfbeis, M. Landthaler, R.-M. Szeimies and C. Abels (2003) Effects of light fractionation and different fluence rates on photodynamic therapy with 5-aminolaevulinic acid in vivo. *Br. J. Cancer* **88**, 1462–1469.
19. Paba, V., M. Quarto, L. Varriale, E. Crescenzi and G. Palumbo (2001) Photo-activation of hypericin with low doses of light promotes apparent photo-resistance in human histiocytic lymphoma U937 cells. *J. Photochem. Photobiol. B* **60**, 87–96.
20. Varriale, L., E. Coppola, M. Quarto, B. M. Veneziani and G. Palumbo (2002) Molecular aspects of photodynamic therapy: low energy pre-sensitization of hypericin-loaded human endometrial carcinoma cells enhances photo-tolerance, alters gene expression and affects the cell cycle. *FEBS Letters* **512**, 287–290.
21. Oberdanner, C. B., K. Plaetzer, T. Kiesslich and B. Krammer (2005) Photodynamic treatment with fractionated light decreases production of reactive oxygen species and cytotoxicity *in vitro* via regeneration of glutathione. *Photochem. Photobiol.* (In press)
22. Mossman, T. (1983) Rapid colorimetric assay for cellular growth and survival: application to proliferation and cytotoxicity assay. *J. Immunogenet.* **21**, 235.
23. Curnow, A., J. C. Haller and S. G. Bown (2000) Oxygen monitoring during 5-aminolaevulinic acid induced photodynamic therapy in normal rat colon. Comparison of single and fractionated light regimes. *J. Photochem. Photobiol. B* **58**, 149–155.

Photochemistry and Photobiology
The official journal of the American Society of Photobiology

Possible Implication of NF-κB in Photo-Resistance of HT-29 Adenocarcinoma Cells to Fractionated Light Delivery With a Longer Dark Pause Between Two Unequal Light Doses

Journal:	*Photochemistry and Photobiology*
Manuscript ID:	Draft
Manuscript Type:	Research Article
Date Submitted by the Author:	
Complete List of Authors:	Kulikova, Lucia; Pavol Jozef Safarik University, Faculty of Science, Institute of Biology and Ecology Mikes, Jaromir; Pavol Jozef Safarik University, Faculty of Science, Institute of Biology and Ecology Hýžďalová, Martina; Institute of Biophysics AS CR Palumbo, Giuseppe; Dipartmento di Biologia e Patologia Cellulare e Molecolare "L. Califano", Università di Napoli "FEDERICO II" Fedorocko, Peter; Pavol Jozef Safarik University, Faculty of Science, Institute of Biology and Ecology
Keywords:	photodynamic therapy, hypericin, resistance, sub-lethal dose

Possible Implication of NF-κB in Photo-Resistance of HT-29 Adenocarcinoma Cells to Fractionated Light Delivery With a Longer Dark Pause Between Two Unequal Light Doses

Lucia Kuliková [1], Jaromír Mikeš [1], Martina Hýžďalová [2], Giuseppe Palumbo [3], Peter Fedoročko*[1,]

1 Institute of Biology and Ecology, Faculty of Sciences, P. J. Šafárik University, Košice, Slovakia

2 Department of Cytokinetics, Institute of Biophysics, Academy of Sciences of the Czech Republic, v.v.i., Brno, Czech Republic

3 Dipartmento di Biologia e Patologia Cellulare e Molecolare "L. Califano", Università di Napoli "FEDERICO II",Naples, Italy

*Peter Fedoročko **e-mail**: peter.fedorocko@upjs.sk

*Corresponding author email: peter.fedorocko@upjs.sk (Peter Fedoročko)

ABSTRACT

This study follows up an earlier one in which hypericin-mediated photocytotoxic effects on HT-29 adenocarcinoma cells by light fractionation with a longer dark pause between two unequal light doses were described [Sackova, A. (2005) *Photochem Photobiol*, **81**, 1411-1416]. In the present study we investigated the impact of sub-lethal light dose (1 $J.cm^{-2}$) and length of a following dark pause (1 or 6 h) on development of resistance to the effect of the second illumination (11 $J.cm^{-2}$). The use of HT-29 cells transfected with a nuclear transcription factor (NF-κB) luciferase reporter construct revealed significantly increased activity of NF-κB during a longer dark pause after 1 $J.cm^{-2}$ as well as (ROS-induced)-ROS release, decrease in hypericin content and elevated levels of NF-κB, IκB-α and Mcl-1 proteins. We demonstrated that a fractionated light regime (1+11 $J.cm^{-2}$) with a 6 h but not 1 h dark period resulted in an increase in cell proliferation activity, decrease in ROS production, hypericin content, cell membrane permeability, phosphatidilserine externalization and altered expression of HSP70, GRP94, clusterin, NF-κB, IκB-α, Mcl-1. We assume that activation of the NF-κB pathway suggests its involvement in development of photoresistance to hypericin-mediated fractionated photodynamic therapy in HT-29 cells *in vitro*.

INTRODUCTION

The cytotoxic effect of photodynamic therapy (PDT) is mediated by highly toxic reactive oxygen species (ROS) formed in tissue treated with a photosensitizing drug activated with light of appropriate wavelength in the presence of oxygen. The efficacy of PDT and subsequent mode of cell death is affected by many factors such as cell type, type of photosensitizer and its intracellular localization, light dose and its fluency rate, drug to light interval and photodynamic protocol (1-6).

Hypericin, a natural substance displaying potential as a photosensitizer for PDT, is a secondary metabolite present in *Hypericum perforatum L.* (St John's wort) (7). It is devoid of toxicity in the dark (8, 9) and genotoxic effects *in vitro* or *in vivo* (10, 11). However exhibits potent photosensitizing properties with a high singlet oxygen quantum yield (12, 13).

Efforts to improve the therapeutic effect of PDT have led to alternative approaches based on fractionationated dosing of photosensitizer (14-16) or multiple light illuminations separated with dark pauses (5, 17-29), enabling re-oxygenation in treated tissue (20, 30). In the last decade, application of light fractionation in PDT has gained increased attention from researchers and has led to the comparison of continuous and fractionated light regimes (5, 17, 19, 23, 29). Indeed, improved efficiency of fractionated light delivery has been demonstrated in various models *in vivo* (17, 19, 23, 26, 29, 30). However, the outcome of fractionated light regimes is still limited by some parameters such as distribution of photosensitizers in tissue (21), dark intervals between light doses (5, 22, 23, 27, 31) or oxygen depletion (24). In general, maintaining the tumor tissue oxygen level is crucial for PDT efficacy, and low fluency rate has also been found to improve the therapeutic outcome (2, 32, 33). Treatments such as fractionated PDT do not therefore necessarily avoid all problems. For example fractionated illumination did not enhance the efficacy of PDT using methyl 5-

aminolevulinate, but it did in the case of ALA application (21). Similarly, photo-activation of hypericin with a low light dose promoted apparent photo-resistance in U937 cells (25), just low-energy pre-sensitization of hypericin-loaded HEC1-B cells enhanced photo-tolerance (28). Increased expression of heat shock proteins (HSPs) is considered to be the basis of photo-resistance (25, 28).

Previously, we have reported hypericin-mediated photocytotoxic effects on HT-29 adenocarcinoma cells reduced by light fractionation with a longer dark pause between two unequal light doses (5). We have proceeded to investigate the relationship between dark interval and PDT response. Further study of mechanisms behind this resistance invoked by pre-sensitization with a sub-lethal light dose PDT is presented here. ROS at low levels may function as second messengers activating pathways that protect cells against apoptotic stimuli (34). Protein complex often considered to be a ROS-responsive transcription factor is NF-κB (34, 35) also shown to be implicated in cancer cell responses to photodynamic therapy (36). Analyses of ROS production, hypericin content, activity of nuclear transcription factor-κB (NF-κB), expression of selected proteins (HSP70, GRP94, clusterin, NF-κB, IκB-α, Mcl-1), changes in cell membrane permeability and externalization of phosphatidilserine have been done with aim of approaching the mechanisms behind the PDT-induced resistance. We outline the possible implication of NF-κB and describe other possible factors negatively affecting the photocytotoxic effect of fractionated light delivery with a longer dark pause.

MATERIALS AND METHODS

Cell culture. Human adenocarcinoma cell line HT-29 was purchased from American Tissue Culture Collection (ATCC, Rockville, MD). Cells were cultured in RPMI-1640 medium (Gibco, Grand Island, NY) supplemented with 10% heat-inactivated fetal calf serum (FCS;

PAA Laboratories GmbH, Linz, Austria) and antibiotics (penicillin 100 U/ml, streptomycin 100 µg/ml and amphotericin 25 µg/ml; Invitrogen Corp., Carlsbad, CA). Cells were maintained at 37 °C in a humidified 5% CO_2 atmosphere and constantly kept under dark conditions.

Experimental design. HT-29 cells ($2 \times 10^4/cm^2$) were seeded and cultivated 24 h in a complete medium with 10% FCS. Hypericin ((4,5,7,4´,5´,7´-hexahydroxy-2,2´-dimethylnaphtodiantron), HPLC grade; AppliChem GmbH, Darmstadt, Germany) of final concentration 60 nM was added and then incubated 16 h with cells in dark conditions. Prior to light application, the medium was replaced with a fresh one, free of hypericin (see Scheme 1A). The hypericin was photoactivated with a sub-lethal or lethal single light dose (1 or 12 $J.cm^{-2}$) or fractionated light doses (1 + 11 $J.cm^{-2}$) with a dark interval 1 or 6 h. The cells photoactivated with a sub-lethal light dose were analyzed 1 or 6 h after PDT. The effects of single or fractionated light regime deliveries were analyzed up to 24 h after PDT (see Scheme 1B). (SLD) sub-lethal light dose 1 $J.cm^{-2}$ (S) single light dose 12 $J.cm^{-2}$, fractionated light dose 1+11 $J.cm^{-2}$ with a 1 h (FR1) or 6 h (FR6) dark pause between the two light doses.

<Scheme 1>

Hypericin activation. The cells were irradiated in hypericin-free medium by placing cultivation dishes (TPP, Trasadingen, Switzerland) on a plastic diffuser sheet above a set of eleven L18W/30 lamps (Osram, Berlin, Germany) with maximum emission between 530 and 620 nm (the absorption peak of hypericin is ~ 600 nm). Uniform fluency rate at the surface of the diffuser was 3.15 $mW.cm^{-2}$ and the temperature did not exceed 37°C. Light dose was calculated as multiplication of fluency rate by time.

Colony forming assay. Cells were treated according to the standard protocol (Scheme 1), then harvested 24 h after single or fractionated light delivery and counted microscopically using a Bürker chamber. Equal cell numbers (500 cells per 60 mm Petri dish (TPP)) were seeded and cultivated under standard conditions for 7 days. Colonies were stained using coloured solution (40 mg methyl blue diluted in 50 ml 78% ethanol).

Detection of phosphatidilserine externalization and cell membrane permeability. For phosphatidylserine externalization and cell viability analysis an annexin V-FITC and propidium iodide (PI) double-staining kit (Bender MedSystems, Vienna, Austria) was used according to the manufacturer's instructions. The cells were treated according to the standard protocol (Scheme 1), then adherent and floating cells were harvested together 0.5, 3 and 24 h after PDT and stained with annexin V-FITC in binding buffer for 10 min, washed, stained with PI for 5 min and analyzed using the FACSCalibur flow cytometer. Results were analyzed with CellQuest Pro software. The cell populations were differentiated as living (annexin V^-/PI^-), apoptotic (annexin V^+/PI^-), secondary necrotic (annexin V^+/PI^+) or necrotic (annexin V^-/PI^+) cells. The results are presented as means ± SD of three independent experiments.

Production of ROS. The cells were treated according to the standard protocol (Scheme 1), then harvested 0.25, 0.5, 1, 6 h after a sub-lethal light dose or 0.5, 3, 24 h after single or fractionated light delivery, washed twice in phosphate-balanced salt solution (PBS), and resuspended in Hank's balanced salt solution (HBSS). Dihydrorhodamine-123 (DHR-123, Fluka, Buchs, Switzerland) was added at a final concentration of 0.2 μM, samples were then incubated for 15 min at 37 °C in 5% CO_2 atmosphere and subsequently kept on ice during

analysis. Fluorescence was analyzed using a FACSCalibur flow cytometer (Becton Dickinson, San Jose, CA) in the FL-1channel. Forward and side scatters were used to gate the viable populations of cells. CellQuestPro software (Becton Dickinson) was used to quantify the intensity of DHR-123 fluorescence in the cells, expressed as the ratio of DHR-123 fluorescence in treated cells compared to the fluorescence of untreated control cells.

Hypericin content analysis. The cells were treated according to the standard protocol (Scheme 1), then harvested 0.25, 0.5, 1, 6 h after a sub-lethal light dose or 0.5, 3, 24 h after single or fractionated light delivery, washed twice in PBS, and resuspended in HBSS. Fluorescence of hypericin was analyzed using the FACSCalibur flow cytometer in the FL-2 channel (1×10^4 cells per sample). CellQuestPro software was again used to quantify the intensity of hypericin fluorescence in the cells, expressed as the ratio of hypericin fluorescence in treated cells compared to the fluorescence of untreated control cells.

Luciferase activity assay. Luciferase reporter construct and stable cell transfection were executed as described previously (37). Stable transfected HT-29 cells were treated according to the standard protocol (Scheme 1). Cells were rinsed with PBS 0, 0.5, 1, 3, 6 h after hypericin photoactivation with a sub-lethal light dose, and lysed with 400 µl of reagent (Luciferase Assay System; Promega Corp., Madison, WI). Protein concentrations of the cell extracts were determined using detergent-compatible protein assay (BioRad Laboratories Inc., Hercules, CA). One sample at a time was diluted in equal amount of proteins and 50 µl of extract was mixed with 50 µl of luciferase substrate and luminescence was measured immediately using the FLUOstar Optima (BMG Labtechnologies GmbH, Offenburg, Germany). The luminescent signal of each sample was measured for the same period.

Western blot analysis. The cells were treated according to the standard protocol (Scheme 1), then harvested 1and 6 h after low light dose or 24 h after single or fractionated light delivery, then washed twice in cold PBS and lysed in lysis buffer (100 mM Tris-HCl, pH 7.4, 1 % SDS, 10 % glycerol and protease inhibitor cocktail P2714 (Sigma-Aldrich Corporation, St. Louis, MO) for 10 min on ice. The cell lysates were sonicated and centrifuged. Protein concentration was determined using detergent-compatible protein assay (BioRad Laboratories Inc.,). Samples were diluted in equal amounts (30 - 50 μg proteins) with 0.01 % bromphenol blue and 1% 2-mercaptoethanol, then separated with SDS-polyacrylamide gel and transferred onto nitrocellulose membrane (Advantec, Tokyo, Japan) or PVDF membrane (Millipore, Bedford, MA) in a transfer buffer containing 192 mM glycine, 25 mM Tris and 10 % methanol. The membrane was blocked in 5 % non-fat milk (or 5 % BSA) in TBS (20 mM Tris-HCl, pH=7.6; 150 mM NaCl; 0.05 % TWEEN 20, pH=7.4) for 1 h at first, and then the membrane blots were incubated 2 h at RT or overnight at 4 °C (depending on the particular antibody) with primary antibody: anti-NF-κB p65 (sc-372), anti-NF-κB p50 and p105 (sc-8414), anti-IκB-α (sc-203), anti-GRP94 (sc-1794), anti-clusterin (sc-6420), all from Santa Cruz Biotechnology, anti-Mcl-1 (#4572 Cell Signalling), anti-HSP70 (MA3-006, Affinity BioReagents). After 30 min washing in wash buffer, membranes were incubated with appropriate horseradish-conjugated secondary antibody for 1 h at RT (AntiMouse IgG-HRP, NA931 (1:3000), AntiGoat IgG-HRP (1:20 000), AntiRabbit IgG-HRP (1:20 000) (Amersham Biosciences, Buckinghamshire, UK). Detection of antibody reactivity was performed using a chemiluminescence detection kit ECL+ (Amersham Biosciences) and visualized on X-ray films (Foma Slovakia, Skycov, Slovakia). Equal sample loading was verified by immunodetection of β-actin (A5441, Sigma-Aldrich).

Statistical analysis. Data were processed with GraphPadPrism (GraphPad Software Inc., San Diego, CA) and statistically analyzed using one-way ANOVA with Tukey's multiple comparison test, and are expressed as means ± standard deviation (S. D.). Significance was evaluated at three levels; $p < 0.05$, $p < 0.01$ and $p < 0.001$.

RESULTS

The scheme of the presented experiment was chosen based on our previous study (5). The light dose of 1 J.cm^{-2} was considered as sub-lethal on the basis of our initial preliminary data (not shown) according which the light dose did not affect cell viability/survival in comparison with untreated control or hypericin treated cells. The presented data concern two aspects; cellular and subcellular events induced by sub-lethal dose of 1 J.cm^{-2} (Figures 3, 5, 7 and 8) and its consequences studied after a second lethal dose of 11 J.cm^{-2} separated by a dark pause of 1 or 6 h (Figures 1, 2, 4, 6 and 8). All the present experiments involved untreated controls as well as controls treated with hypericin and kept under dark conditions through the experiments.

Longer dark pause between two unequal light doses enhanced clonogenic potential of HT-29 cells after PDT with hypericin

Verification of resistance induced by a longer dark pause between two unequal light doses using colony-forming assay proved that pre-sensitization of HT-29 cells with a sub-lethal light dose is time-dependent. As demonstrated in Figure 1, even 1 h dark pause (FR1) shows higher clonogenic ability when compared to single lethal light dose (S). A longer pause continuing for 6 h (FR6) demonstrated much higher ability to create visible colonies, even

when compared to the FR1 group. As can be seen, hypericin under dark conditions (D) did not affect the clonogenic potential of HT-29 cells.

<Figure 1>

Longer dark pause between two unequal light doses repressed cell death in HT-29 cells after PDT with hypericin

Further analysis of phosphatidylserine externalization and cell viability (Fig. 2) in cells treated with single lethal light dose (S) or pre-sensitized with sub-lethal light dose separated by 1 h (FR1) or 6 h (FR6) dark pause, supported previous findings. In contrast to earlier analysis (Fig. 2a), significantly higher survival of the FR6 group accompanied by regress in the ratio of apoptotic and secondary necrotic cells showed 24 h after PDT (Fig. 2b).

<Figure 2>

Durations of a dark pause affects PDT-mediated ROS level induced by second light-dose

Detection of intracellular levels of reactive oxygen species (ROS) shortly after sub-lethal light dose revealed steady remission within the first hour, although 6 h after PDT, the ROS level was found to be raised significantly. Dark conditions did not affect ROS level significantly when compared to untreated control (Fig. 3). However, detection of ROS 30 min after second lethal light dose revealed significantly lower levels in both pre-sensitized groups in reciprocal proportion with time of dark pause (Fig. 4). Later analyses (3 or 24 h) showed barely induced levels.

<Figure 3>

<Figure 4>

Pre-sensitization did not affect physiological elimination of hypericin, however administration regime affects hypericin elimination after lethal dose.

Detection of hypericin intracellular levels within the first 6 h after the first sub-lethal light dose (Fig. 5) proved that there was a steady decrease, which was found to be significant 6 h after PDT. However this was in compliance with the physiological elimination of hypericin, similar to hypericin-treated cells under dark conditions (D). Although, administration of a single lethal light dose decelerated hypericin elimination by cells significantly when applied without pre-sensitization (Fig. 6, S), on the other hand, this effect was partially or completely abolished in pre-sensitized groups with 1 or 6 h dark pause (Fig. 6, FR1 or FR6).

<Figure 5>

<Figure 6>

Luciferase activity assay-Sub-lethal light dose induced NF-κB

Induction of NF-κB activity after a sub-lethal dose of 1 $J.cm^{-2}$ was verified in stably transfected HT-29 cells (clone #3 and clone #93) by luciferase reporter activity executed 0, 0.5, 1, 3 and 6 h after PDT (Fig. 7a, b). Both tested clones indicated insignificant changes

within the first hour, later on however, the NF-κB activity was identically induced 3 and 6 h after PDT in both models.

<Figure 7>

Light delivery regime altered expression of heat-shock proteins and NF-κB

Expressions of NF-κB p65, p50 and p105, Mcl-1, IκB-α, HSP70, GRP94 and clusterin-α (Fig. 8) were detected 1 and 6 h after the first sub-lethal light dose (SLD; 1 $J.cm^{-2}$) or 24 h after administration of a single lethal light dose (S, 12 $J.cm^{-2}$) and two unequal doses (1+11 $J.cm^{-2}$) separated by 1 or 6 h of dark pause (FR1 or FR6). Induction of NF-κB subunits p65, p50 and a precursor form of p50; p150, correlated with IκB-α and anti-apoptotic Mcl-1 detected 6 h after the sub-lethal dose. Similarly, induction of heat shock protein HSP70, occurrence of GRP94 multimers and elevation of clusterin-α even 1 h after hypericin activation confirmed the onset of oxidative stress response in pre-sensitized cells.

Analysis 24 h after lethal light doses (S, FR1, FR6) revealed interesting differences in HSP70, especially GRP94 multimerization and clusterin-α expression. Whereas single lethal light dose administration (S) and FR1 group demonstrated similar pattern, the fractionated administration separated by a 6 h dark pause showed significantly reduced clusterin-α levels as well as suppressed occurrence of HSP70 and GRP94 multimers and slightly elevated IκB-α together with p50 and p65 subunits of NF-κB.

<Figure 8>

DISCUSSION

As previously reported by us (5), light dose fractionation with a longer dark pause between two unequal light doses reduced hypericin-mediated photocytotoxic effects on HT-29 adenocarcinoma cells. Similar findings have been described for hypericin pre-incubated U937 and HEC1-B cells (25, 28). Although the biological effects of low doses were described mainly in the context of radiation- or heat-induced adaptive cell response (38, 39), we presume that a low sub-lethal light dose may have the same consequences in a time-dependent manner in PDT as well. We therefore examined the consequences of a sub-lethal light dose (1 $J.cm^{-2}$) and length of the following dark pause for photoresistance induced by fractionated light delivery, resulting in significant changes in all analyzed parameters.

Since the intracellular content of the photosensitizer is a limiting factor for ROS production and thus also PDT efficiency, a drop in hypericin content during a longer dark pause, due to its ability to increase activity and expression of drug efflux transporters in HT-29 cells (40) could contribute partially to decreased photocytotoxic effect of fractionated PDT. Our results indicate that increased ROS production can be induced even by sub-lethal light dose with a subsequent "(ROS-induced)-ROS release" (RIRR). This phenomenon has also been demonstrated in the mitochondria of cardiac myocytes resulting from MPT induction, and it is considered as a general mechanism independent of the signaling ROS source (34).

Considering that low level of ROS may activate pathways that protect cells against apoptotic stimuli (41) such as NF-κB, which is known as a redox-regulated protein linked with cell proliferation, transformation or tumour development (36), we therefore employed HT-29 cells transfected with a nuclear transcription factor (NF-κB) luciferase reporter construct in our experiments. Significantly increased luciferase activity at a later time after

sub-lethal dose indicates that pre-sensitized cells prepared themselves during the longer dark period by provoking NF-κB activity, and the timing of the second light dose before or after NF-κB activation could be crucial for the fate of cancer cells. Apart from stimulation of NF-κB transcription activity, this theory also supports increased levels of proteins whose genes are under its transcription control (increased level of NF-κB subunits p65, p50 and a precursor form of p50; p150, IκB-α and anti-apoptotic Mcl-1 protein detected 6 h after sub-lethal light dose as well as 24 h after second lethal dose application (apart from Mcl-1)). Even though phosphorylation and degradation of IκB is an important step for NF-κB release from the complex with IκB, translocation from cytoplasm to nucleus and binding to DNA occurred in our experimental model NF-κB activation has occurred without degradation of IκB. Our results are thus in agreement with a study reporting altered regulation of IκB-α degradation and activation of NF-κB activity which can occur independently of IκB degradation in human colonic epithelial HT-29 cells (42, 43).

Since the sub-lethal light dose did not affect cell viability in the long term when compared to control or hypericin in dark conditions (data not shown), we probed the impact of second lethal light dose timing on the resultant ability of the cells to form colonies. Apart from increased number of viable cells, resistance manifested itself also through increased clonogenic activity when a prolonged dark pause was applied.

The study of oxidative metabolism changes revealed that resistant group (FR6) kept shortly after PDT, steady ROS level was achieved already just before the lethal dose application, whereas further delivery regimes (S, FR1) resulted in markedly elevated ROS production. The results indicate that pre-sensitization and the timing of a second illumination could decrease the photocytotoxic effect of PDT mediated through restricted ROS production. Although the timing of the photodynamic protocol could contribute to reduced hypericin

content, on the basis of our findings it seems that different molecular events participate in resistance development in HT-29 cells *in vitro*.

Taking into consideration that the induction of HSPs is believed to be the basis of photo-tolerance/resistance (25, 28), we were interested in the expression of proteins playing a role in cell response to stress. Analyses revealed altered expression of proteins in a light dose dependent manner and depending on the light delivery regime of the photodynamic protocol. The expression of 94 kDa a glucose-regulated protein (GRP94), the endoplasmic reticulum paralog of HSP90 essential for proper assembly and maturation of numerous client proteins (44-46), was accompanied by proportional formation of high molecular GRP94 multimers. Although, the explanation of an unexpected band detected by GPR94 antibody was not a goal of this work, it could explain the findings of Wassenberg et all (2000). They described bis-ANS and heat shock induction of GRP94 multimerisation accompanied by a marked elevation of chaperone and peptide binding activity. In this conformation and in a concentration-dependent manner, GRP94 can undergo homotypic oligomerization leading to formation of multimers of GRP94 with high molecular weights (47). We therefore presume that photodynamic therapy with hypericin-induced oxidative stress may have a similar effect on GRP94 like heat shock, in a light dose- and photodynamic protocol-dependent manner.

In cytoprotection a role may be played by clusterin, a molecule with a chaperon-like activity, whose secretory form contributes to clearing cell debris from traumatized tissue (48, 49). The pre-secretory form of clusterin (~60 kDa) could be glycosylated and cloven into ~40 kDa α- and β-subunits which held together by disulphide bonds (50). In our case, oxidative stress induced by a sub-lethal light dose increased the level of ~40 kDa clusterin subunit, whereas a lethal light dose (S, FR1) significantly altered clusterin expression towards higher molecular forms of clusterin-α, which indicate involvement of clusterin in extensive defense stress response, not observed in the resistant group.

CONCLUSION

In summary, changes in ROS production, increased transcription activity of NF-κB, increased levels of NF-κB and Mcl-1 proteins at the moment of second light dose application support our hypothesis that the cells prepare themselves for the lethal consequences of second illumination by development of resistance. We presume that, although at the moment of second light dose administration (1 or 6 h after the sub-lethal light dose) increased level HSPs were detected, it seems that HSPs themselves are not sufficient to develop resistance in such a photodynamic protocol whereas resistance occurred when NF-κB activation was implicated. We assume therefore that activation of the NF-κB pathway may suggest its involvement in photoresistance development to a fractionated light delivery regime. Our findings do not explain the mechanism of resistance development to fractionated hypericin photoactivation in HT-29 cells *in vitro*; they do however point out another aspect of resistance in two-fold photodynamic therapy with hypericin.

Acknowledgement This study was supported by the Science and Technology Assistance Agency under contract No. VVCE-0001-07, the Scientific Grant Agency of the Ministry of Education of the Slovak Republic No. VEGA 1/0240/08, the Academy of Sciences of the Czech Republic Research Plan No. AVOZ50040507 and the Grant Agency of the Czech Republic No. 301/07/1557. The authors thank Dr. Veronika Sačková, Tünde Kissová and Dr. Karel Souček for their input to this work, and Viera Balážová for assistance with the technical procedures. Thanks also to Andrew J. Billingham for proofreading the manuscript.

REFERENCES

1. Blant, S. A., A. Woodtli, G. Wagnieres, C. Fontolliet, H. Van Den Bergh and P. Monnier (1996) In vivo fluence rate effect in photodynamic therapy of early cancers with tetra(m-hydroxyphenyl)chlorin. *Photochem Photobiol*. **64**, 963-968.

2. Henderson, B. W., S. O. Gollnick, J. W. Snyder, T. M. Busch, P. C. Kousis, R. T. Cheney and J. Morgan (2004) Choice of oxygen-conserving treatment regimen determines the inflammatory response and outcome of photodynamic therapy of tumors. *Cancer Res*. **64**, 2120-2126.

3. Noodt, B. B., K. Berg, T. Stokke, Q. Peng and J. M. Nesland (1999) Different apoptotic pathways are induced from various intracellular sites by tetraphenylporphyrins and light. *Br J Cancer*. **79**, 72-81.

4. Ris, H. B., H. J. Altermatt, B. Nachbur, J. C. Stewart, Q. Wang, C. K. Lim, R. Bonnett and U. Althaus (1993) Effect of drug-light interval on photodynamic therapy with meta-tetrahydroxyphenylchlorin in malignant mesothelioma. *Int J Cancer*. **53**, 141-146.

5. Sackova, V., L. Kulikova, J. Mikes, J. Kleban and P. Fedorocko (2005) Hypericin-mediated photocytotoxic effect on HT-29 adenocarcinoma cells is reduced by light fractionation with longer dark pause between two unequal light doses. *Photochem Photobiol*. **81**, 1411-1416.

6. Wyld, L., M. W. Reed and N. J. Brown (2001) Differential cell death response to photodynamic therapy is dependent on dose and cell type. *Br J Cancer*. **84**, 1384-1386.

7. Diwu, Z. (1995) Novel therapeutic and diagnostic applications of hypocrellins and hypericins. *Photochem Photobiol*. **61**, 529-539.

8. Fox, E., R. F. Murphy, C. L. Mccully and P. C. Adamson (2001) Plasma pharmacokinetics and cerebrospinal fluid penetration of hypericin in nonhuman primates. *Cancer Chemother Pharmacol*. **47**, 41-44.

9. Jacobson, J. M., L. Feinman, L. Liebes, N. Ostrow, V. Koslowski, A. Tobia, B. E. Cabana, D. Lee, J. Spritzler and A. M. Prince (2001) Pharmacokinetics, safety, and antiviral effects of hypericin, a derivative of St. John's wort plant, in patients with chronic hepatitis C virus infection. *Antimicrob Agents Chemother*. **45**, 517-524.

10. Miadokova, E., I. Chalupa, V. Vlckova, A. Sevcovicova, S. Nadova, M. Kopaskova, A. Hercegova, P. Gasperova, L. Alfoldiova, M. Komjatiova, Z. Csanyiova, E. Galova, E. Cellarova and D. Vlcek (2009) Genotoxicity and antigenotoxicity evaluation of non-photoactivated hypericin. *Phytother Res*.

11. Okpanyi, S. N., H. Lidzba, B. C. Scholl and H. G. Miltenburger (1990) [Genotoxicity of a standardized Hypericum extract]. *Arzneimittelforschung*. **40**, 851-855.

12. Ehrenberg, B., J. L. Anderson and C. S. Foote (1998) Kinetics and yield of singlet oxygen photosensitized by hypericin in organic and biological media. *Photochem Photobiol*. **68**, 135-140.

13. Redmond, R. W. and J. N. Gamlin (1999) A compilation of singlet oxygen yields from biologically relevant molecules. *Photochem Photobiol*. **70**, 391-475.

14. Cavarga, I., P. Brezani, P. Fedorocko, P. Miskovsky, N. Bobrov, F. Longauer, S. Rybarova, L. Mirossay and J. Stubna (2005) Photoinduced antitumour effect of hypericin can be enhanced by fractionated dosing. *Phytomedicine*. **12**, 680-683.

15. Dolmans, D. E., A. Kadambi, J. S. Hill, K. R. Flores, J. N. Gerber, J. P. Walker, I. H. Borel Rinkes, R. K. Jain and D. Fukumura (2002) Targeting tumor vasculature and cancer cells in orthotopic breast tumor by fractionated photosensitizer dosing photodynamic therapy. *Cancer Res*. **62**, 4289-4294.

16. Webber, J., B. Leeson, D. Fromm and D. Kessel (2005) Effects of photodynamic therapy using a fractionated dosing of mono-L-aspartyl chlorin e6 in a murine tumor. *J Photochem Photobiol B*. **78**, 135-140.

17. Ascencio, M., J. P. Estevez, M. Delemer, M. O. Farine, P. Collinet and S. Mordon (2008) Comparison of continuous and fractionated illumination during hexaminolaevulinate-photodynamic therapy. *Photodiagnosis Photodyn Ther*. **5**, 210-216.

18. Babilas, P., V. Schacht, G. Liebsch, O. S. Wolfbeis, M. Landthaler, R. M. Szeimies and C. Abels (2003) Effects of light fractionation and different fluence rates on photodynamic therapy with 5-aminolaevulinic acid in vivo. *Br J Cancer*. **88**, 1462-1469.

19. Curnow, A., J. C. Haller and S. G. Bown (2000) Oxygen monitoring during 5-aminolaevulinic acid induced photodynamic therapy in normal rat colon. Comparison of continuous and fractionated light regimes. *J Photochem Photobiol B*. **58**, 149-155.

20. Curnow, A., B. W. Mcilroy, M. J. Postle-Hacon, A. J. Macrobert and S. G. Bown (1999) Light dose fractionation to enhance photodynamic therapy using 5-aminolevulinic acid in the normal rat colon. *Photochem Photobiol*. **69**, 71-76.

21. De Bruijn, H. S., E. R. De Haas, K. M. Hebeda, A. Van Der Ploeg-Van Den Heuvel, H. J. Sterenborg, H. A. Neumann and D. J. Robinson (2007) Light fractionation does not enhance the efficacy of methyl 5-aminolevulinate mediated photodynamic therapy in normal mouse skin. *Photochem Photobiol Sci*. **6**, 1325-1331.

22. De Bruijn, H. S., A. Van Der Ploeg-Van Den Heuvel, H. J. Sterenborg and D. J. Robinson (2006) Fractionated illumination after topical application of 5-aminolevulinic acid on normal skin of hairless mice: the influence of the dark interval. *J Photochem Photobiol B*. **85**, 184-190.

23. De Bruijn, H. S., N. Van Der Veen, D. J. Robinson and W. M. Star (1999) Improvement of systemic 5-aminolevulinic acid-based photodynamic therapy in vivo using light fractionation with a 75-minute interval. *Cancer Res*. **59**, 901-904.

24. Huygens, A., A. R. Kamuhabwa, A. Van Laethem, T. Roskams, B. Van Cleynenbreugel, H. Van Poppel, P. Agostinis and P. A. De Witte (2005) Enhancing the photodynamic effect of hypericin in tumour spheroids by fractionated light delivery in combination with hyperoxygenation. *Int J Oncol*. **26**, 1691-1697.

25. Paba, V., M. Quarto, L. Varriale, E. Crescenzi and G. Palumbo (2001) Photo-activation of hypericin with low doses of light promotes apparent photo-resistance in human histiocytic lymphoma U937 cells. *J Photochem Photobiol B*. **60**, 87-96.

26. Pogue, B. W., C. Sheng, J. Benevides, D. Forcione, B. Puricelli, N. Nishioka and T. Hasan (2008) Protoporphyrin IX fluorescence photobleaching increases with the use of fractionated irradiation in the esophagus. *J Biomed Opt*. **13**, 034009.

27. Togashi, H., M. Uehara, H. Ikeda and T. Inokuchi (2006) Fractionated photodynamic therapy for a human oral squamous cell carcinoma xenograft. *Oral Oncol*. **42**, 526-532.

28. Varriale, L., E. Coppola, M. Quarto, B. M. Veneziani and G. Palumbo (2002) Molecular aspects of photodynamic therapy: low energy pre-sensitization of hypericin-loaded human endometrial carcinoma cells enhances photo-tolerance, alters gene expression and affects the cell cycle. *FEBS Lett*. **512**, 287-290.

29. Xiao, Z., S. Halls, D. Dickey, J. Tulip and R. B. Moore (2007) Fractionated versus standard continuous light delivery in interstitial photodynamic therapy of dunning prostate carcinomas. *Clin Cancer Res*. **13**, 7496-7505.

30. Takahashi, A. and T. Ohnishi (2009) A low dose: pre-irradiation induces radio- and heat-resistance via HDM2 and NO radicals, and is associated with p53 functioning. *Advances in Space Research*. **43**, 1185-1192.

31. Uehara, M., T. Inokuchi, K. Sano, J. Sekine and H. Ikeda (1999) Cell kinetics of mouse tumour subjected to photodynamic therapy--evaluation by proliferating cell nuclear antigen immunohistochemistry. *Oral Oncol*. **35**, 93-97.

32. Sitnik, T. M., J. A. Hampton and B. W. Henderson (1998) Reduction of tumour oxygenation during and after photodynamic therapy in vivo: effects of fluence rate. *Br J Cancer*. **77**, 1386-1394.

33. Thong, P. S., F. Watt, M. Q. Ren, P. H. Tan, K. C. Soo and M. Olivo (2006) Hypericin-photodynamic therapy (PDT) using an alternative treatment regime suitable for multi-fraction PDT. *J Photochem Photobiol B*. **82**, 1-8.

34. Chandra, J., A. Samali and S. Orrenius (2000) Triggering and modulation of apoptosis by oxidative stress. *Free Radic Biol Med*. **29**, 323-333.

35. Janssen-Heininger, Y. M., M. E. Poynter and P. A. Baeuerle (2000) Recent advances towards understanding redox mechanisms in the activation of nuclear factor kappaB. *Free Radic Biol Med*. **28**, 1317-1327.

36. Legrand-Poels, S., V. Bours, B. Piret, M. Pflaum, B. Epe, B. Rentier and J. Piette (1995) Transcription factor NF-kappa B is activated by photosensitization generating oxidative DNA damages. *J Biol Chem*. **270**, 6925-6934.

37. Hyzd'alova, M., J. Hofmanova, J. Pachernik, A. Vaculova and A. Kozubik (2008) The interaction of butyrate with TNF-alpha during differentiation and apoptosis of colon epithelial cells: Role of NF-kappa B activation. *Cytokine*. **44**, 33-43.

38. Shadley, J. D., V. Afzal and S. Wolff (1987) Characterization of the adaptive response to ionizing radiation induced by low doses of X rays to human lymphocytes. *Radiat Res*. **111**, 511-517.

39. Yoshida, N., H. Imada, N. Kunugita and T. Norimura (1993) Low dose radiation-induced adaptive survival response in mouse spleen T-lymphocytes in vivo. *J Radiat Res (Tokyo)*. **34**, 269-276.

40. Jendzelovsky, R., J. Mikes, J. Koval, K. Soucek, J. Prochazkova, M. Kello, V. Sackova, J. Hofmanova, A. Kozubik, P. Fedorocko (2009) Drug efflux transporters, MRP1 and BCRP, affect the outcome of hypericin-mediated photodynamic therapy in HT-29 adenocarcinoma cells. *Photochem Photobiol Sci*. "*in press*" **DOI: 10.1039/B9PP00086K**.

41. Zorov, D. B., C. R. Filburn, L. O. Klotz, J. L. Zweier and S. J. Sollott (2000) Reactive oxygen species (ROS)-induced ROS release: a new phenomenon accompanying induction of the mitochondrial permeability transition in cardiac myocytes. *J Exp Med*. **192**, 1001-1014.

42. Jobin, C., S. Haskill, L. Mayer, A. Panja and R. B. Sartor (1997) Evidence for altered regulation of I kappa B alpha degradation in human colonic epithelial cells. *J Immunol*. **158**, 226-234.

43. Wang, Q., S. Kim, X. Wang and B. M. Evers (2000) Activation of NF-kappaB binding in HT-29 colon cancer cells by inhibition of phosphatidylinositol 3-kinase. *Biochem Biophys Res Commun*. **273**, 853-858.

44. Melnick, J., S. Aviel and Y. Argon (1992) The endoplasmic reticulum stress protein GRP94, in addition to BiP, associates with unassembled immunoglobulin chains. *J Biol Chem*. **267**, 21303-21306.

45. Nigam, S. K., A. L. Goldberg, S. Ho, M. F. Rohde, K. T. Bush and M. Sherman (1994) A set of endoplasmic reticulum proteins possessing properties of molecular chaperones includes Ca(2+)-binding proteins and members of the thioredoxin superfamily. *J Biol Chem*. **269**, 1744-1749.

46. Randow, F. and B. Seed (2001) Endoplasmic reticulum chaperone gp96 is required for innate immunity but not cell viability. *Nat Cell Biol*. **3**, 891-896.

47. Wassenberg, J. J., R. C. Reed and C. V. Nicchitta (2000) Ligand interactions in the adenosine nucleotide-binding domain of the Hsp90 chaperone, GRP94. II. Ligand-mediated activation of GRP94 molecular chaperone and peptide binding activity. *J Biol Chem*. **275**, 22806-22814.

48. Araki, S., S. Israel, K. S. Leskov, T. L. Criswell, M. Beman, D. Y. Klokov, L. Sampalth, K. E. Reinicke, E. Cataldo, L. D. Mayo and D. A. Boothman (2005) Clusterin proteins: stress-inducible polypeptides with proposed functions in multiple organ dysfunction. *BJR Suppl*. **27**, 106-113.

49. Humphreys, D. T., J. A. Carver, S. B. Easterbrook-Smith and M. R. Wilson (1999) Clusterin has chaperone-like activity similar to that of small heat shock proteins. *J Biol Chem*. **274**, 6875-6881.

50. Burkey, B. F., H. V. Desilva and J. A. Harmony (1991) Intracellular processing of apolipoprotein J precursor to the mature heterodimer. *J Lipid Res*. **32**, 1039-1048.

FIGURE LEGENDS

Scheme 1. Experimental design. (A) Time schedule of experiments – HT-29 cells were seeded (point -40 h in the experimental time schedule) and cultivated 24 h in a complete medium and then hypericin was added (point -16 h). The medium with hypericin was removed from cells 16 h later and replaced with hypericin-free medium with subsequent activation of intracellular hypericin (point 0 h). Analyses were performed up to 6 h or up to 24 h after PDT (point +6 h or +24 h).

(B) Schedule of hypericin activation - hypericin-loaded HT-29 cells were illuminated with a single light dose (sub-lethal 1 $J.cm^{-2}$ or lethal 12 $J.cm^{-2}$ light dose) or two unequal light doses (1+11 $J.cm^{-2}$) separated by 1 h or 6 h dark pause. (S) single light delivery 12 $J.cm^{-2}$, fractionated light dose 1+11 $J.cm^{-2}$ with a 1 h (FR1) or 6 h (FR6) dark pause between the two light doses.

Figure 1. Clonogenic assay of HT-29 cells. Cells were harvested 24 h after hypericin photoactivation. The results are presented as a representative photo of three independent experiments. (C) control cells, (D) hypericin under dark conditions, (S) single light dose 12 $J.cm^{-2}$, fractionated light dose 1+11 $J.cm^{-2}$ with a 1 h (FR1) or 6 h (FR6) dark pause between the two light doses.

Figure 2. Detection of phosphatidilserine externalization and membrane permeability of HT-29 cells by dual annexin V/PI staining 3 h (a) and 24 h (b) after single (12 J. cm^{-2}) or fractionated (1 + 11 $J.cm^{-2}$) light dose. Cells were harvested and evaluated 3 or 24 h after PDT. The results are the means ± SD of three independent experiments presented as percentages of control values. Statistical significance is expressed as follows: experimental

groups versus untreated control (●); fractionated light delivery versus single light delivery (+); fractionated light delivery with a 6 h versus 1 h dark pause (□) on the significance level $p<0.05$ (● or + or □); $p<0.01$ (●● or ++); $p<0.001$ (●●●). (C) control cells, (D) hypericin under dark conditions, (S) single light dose 12 J.cm^{-2}, fractionated light dose 1+11 J.cm^{-2} with a 1 h (FR1) or 6 h (FR6) dark pause between the two light doses.

Figure 3. The effect of a sub-lethal dose 1 J.cm^{-2} on ROS production in HT-29 cells. Cells were harvested and evaluated 0.25, 0.5, 1 and 6 h after hypericin photoactivation. The results are the means ± SD of three independent experiments presented as ratios to untreated control values. Statistical significance is expressed as follows: photoactivated (1 J.cm^{-2}) versus not photoactivated hypericin (D) (+) on the significance level $p<0.01$ (++); $p<0.001$ (+++). (D) hypericin under dark conditions.

Figure 4. The effect of a single (12 J. cm^{-2}) and fractionated (1 + 11 J.cm^{-2}) light delivery on ROS production in HT-29 cells. Cells were harvested and evaluated 0.5, 3 and 24 h after hypericin-mediated photodynamic treatment. The results are the means ± SD of three independent experiments presented as ratios to control values. Statistical significance is expressed as follows: experimental groups versus untreated control (+); fractionated light delivery versus single light delivery (●); fractionated light delivery with a 6 h versus 1 h dark pause (■) on the significance level $p<0.05$ (●); $p<0.01$ (++); $p<0.001$ (+++ or ●●● or ■■■). (D) hypericin under dark conditions, (S) single light dose 12 J.cm^{-2}, fractionated light dose 1+11 J.cm^{-2} with a 1 h (FR1) or 6 h (FR6) dark pause between the two light doses.

Figure 5. Determination of hypericin intracellular levels in HT-29 cells during the dark pause after first sub-lethal dose 1 J.cm^{-2}. Cells were harvested and evaluated 0.25, 0.5, 1 and 6 h after hypericin photoactivation. The results are the means ± SD of three independent experiments presented as ratios to control values. Statistical significance is expressed as follows: photoactivated (1 J.cm^{-2}) or not photoactivated (D) hypericin (0.5, 1 and 6 h) versus (0.25 h) (+); (6 h) versus (1 h) (●) on the significance level $p<0.01$ (●●); $p<0.001$ (+++). (D) hypericin under dark conditions.

Figure 6. Determination of hypericin intracellular levels in HT-29 cells illuminated with a single (12 J. cm^{-2}) and fractionated (1 + 11 J.cm^{-2}) light delivery. Cells were harvested and evaluated 0.5, 3 and 24 h after PDT. The results are the means ± SD of three independent experiments presented as ratios to control values. Statistical significance is expressed as follows: single or fractionated light delivery versus not photoactivated (D) hypericin (+); not photoactivated hypericin (3 h or 24 h) versus (0.5 h) (■) on the significance level $p<0.05$ (+); $p<0.01$ (++); $p<0.001$ (■■■). (PDT) photodynamic treatment, (D) hypericin under dark conditions, (S) single light dose 12 J.cm^{-2}, fractionated light dose 1+11 J.cm^{-2} with a 1 h (FR1) or 6 h (FR6) dark pause between the two light doses.

Figure 7. NF-κB binding activity (expressed as relative luciferase activity) of two HT-29 clones #3 (a) and #93 (b) with pBIIX-LUC construct after treatment with sub-lethal dose 1 J.cm^{-2}. Cells were lysed 0, 0.25, 0.5, 1, 3 and 6 h after PDT. The results are the means ± SD of three independent experiments presented as ratios to untreated control values. Statistical significance is expressed as follows: sub-lethal light dose versus untreated control (+) on the significance level $p<0.01$ (++). (C) control cells.

Figure 8. Western blot analysis of Mcl-1, NF-κB p65, p50 and p105, IκB-α, HSP70, GRP94, clusterin-α and β-actin proteins 1 or 6 h after hypericin photoactivation with a sub-lethal dose (1 J.cm^{-2}) or 24 h after single (12 J. cm-2) and fractionated (1 + 11 J.cm-2) light delivery. The results are presented as a representative photo of three independent experiments. (C) control cells, (D) hypericin under dark conditions, (SLD) sub-lethal light dose 1 J.cm^{-2} (S) single light dose 12 J.cm^{-2}, fractionated light dose 1+11 J.cm^{-2} with a 1 h (FR1) or 6 h (FR6) dark pause between the two light doses.

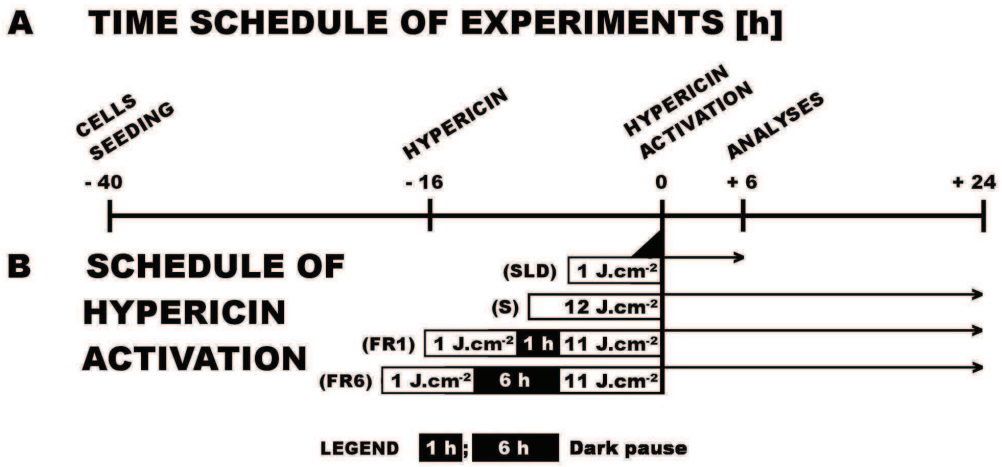

Scheme 1. Experimental design. (A) Time schedule of experiments – HT-29 cells were seeded (point -40 h in the experimental time schedule) and cultivated 24 h in a complete medium and then hypericin was added (point -16 h). The medium with hypericin was removed from cells 16 h later and replaced with hypericin-free medium with subsequent activation of intracellular hypericin (point 0 h). Analyses were performed up to 6 h or up to 24 h after PDT (point +6 h or +24 h). (B) Schedule of hypericin activation - hypericin-loaded HT-29 cells were illuminated with a single light dose (sub-lethal 1 J.cm-2 or lethal 12 J.cm-2 light dose) or two unequal light doses (1+11 J.cm-2) separated by 1 h or 6 h dark pause. (S) single light delivery 12 J.cm-2, fractionated light dose 1+11 J.cm-2 with a 1 h (FR1) or 6 h (FR6) dark pause between the two light doses.

83x39mm (600 x 600 DPI)

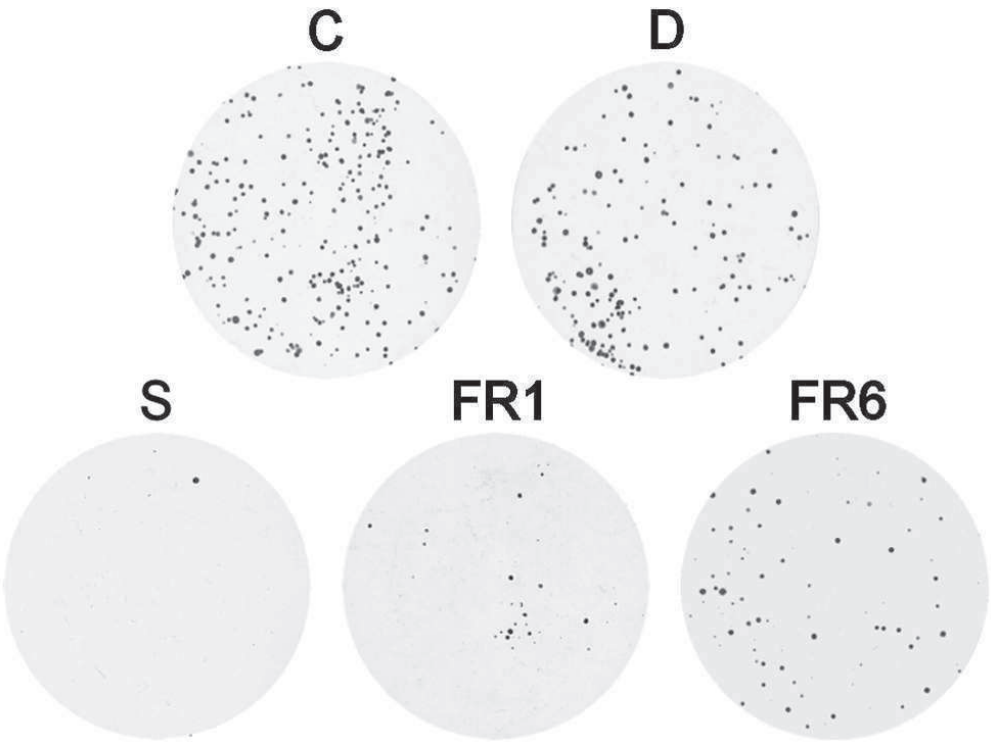

Figure 1. Clonogenic assay of HT-29 cells. Cells were harvested 24 h after hypericin photoactivation. The results are presented as a representative photo of three independent experiments. (C) control cells, (D) hypericin under dark conditions, (S) single light dose 12 J.cm-2, fractionated light dose 1+11 J.cm-2 with a 1 h (FR1) or 6 h (FR6) dark pause between the two light doses.
82x61mm (300 x 300 DPI)

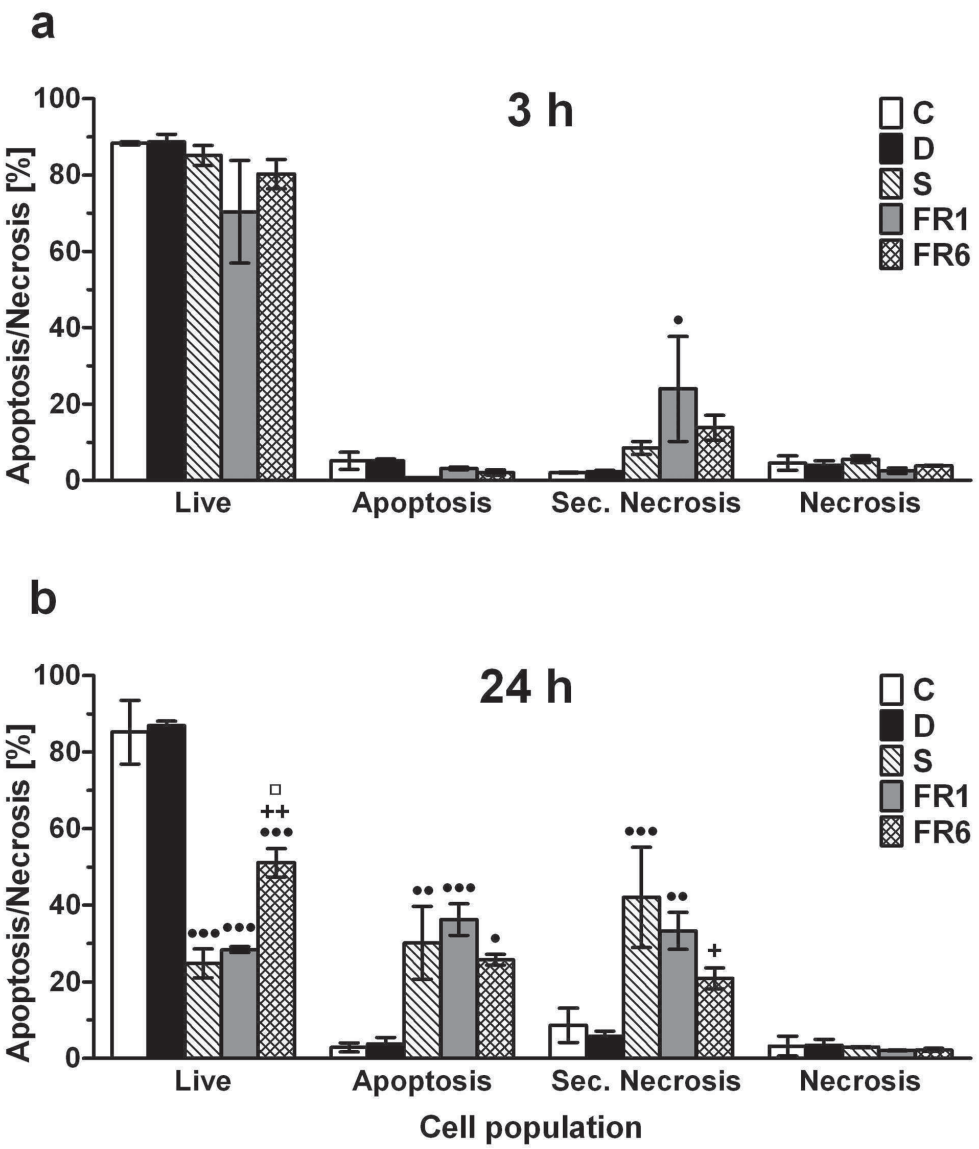

Figure 2. Detection of phosphatidilserine externalization and membrane permeability of HT-29 cells by dual annexin V/PI staining 3 h (a) and 24 h (b) after single (12 J. cm-2) or fractionated (1 + 11 J.cm-2) light dose. Cells were harvested and evaluated 3 or 24 h after PDT. The results are the means ± SD of three independent experiments presented as percentages of control values. Statistical significance is expressed as follows: experimental groups versus untreated control (•); fractionated light delivery versus single light delivery (+); fractionated light delivery with a 6 h versus 1 h dark pause (□) on the significance level $p<0.05$ (• or + or □); $p<0.01$ (•• or ++); $p<0.001$ (•••). (C) control cells, (D) hypericin under dark conditions, (S) single light dose 12 J.cm-2, fractionated light dose 1+11 J.cm-2 with a 1 h (FR1) or 6 h (FR6) dark pause between the two light doses.
83x98mm (600 x 600 DPI)

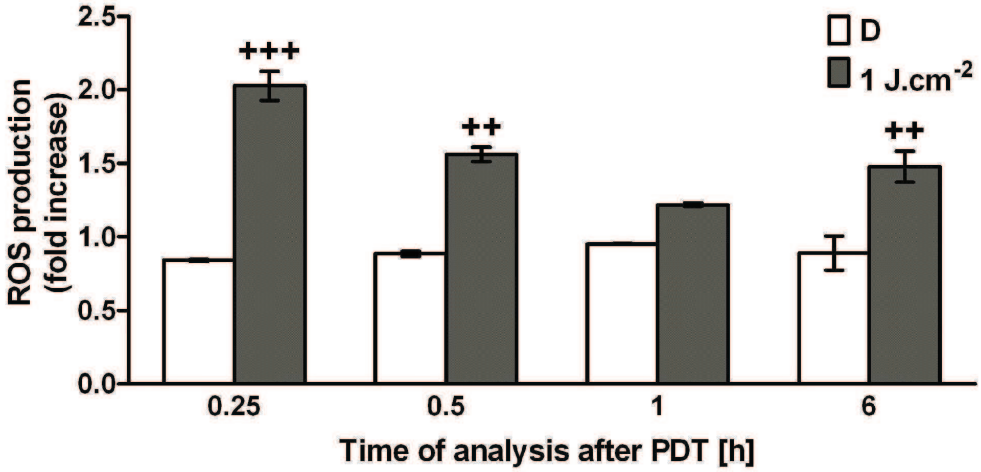

Figure 3. The effect of a sub-lethal dose 1 J.cm-2 on ROS production in HT-29 cells. Cells were harvested and evaluated 0.25, 0.5, 1 and 6 h after hypericin photoactivation. The results are the means ± SD of three independent experiments presented as ratios to untreated control values. Statistical significance is expressed as follows: photoactivated (1 J.cm-2) versus not photoactivated hypericin (D) (+) on the significance level $p<0.01$ (++); $p<0.001$ (+++). (D) hypericin under dark conditions.
83x41mm (600 x 600 DPI)

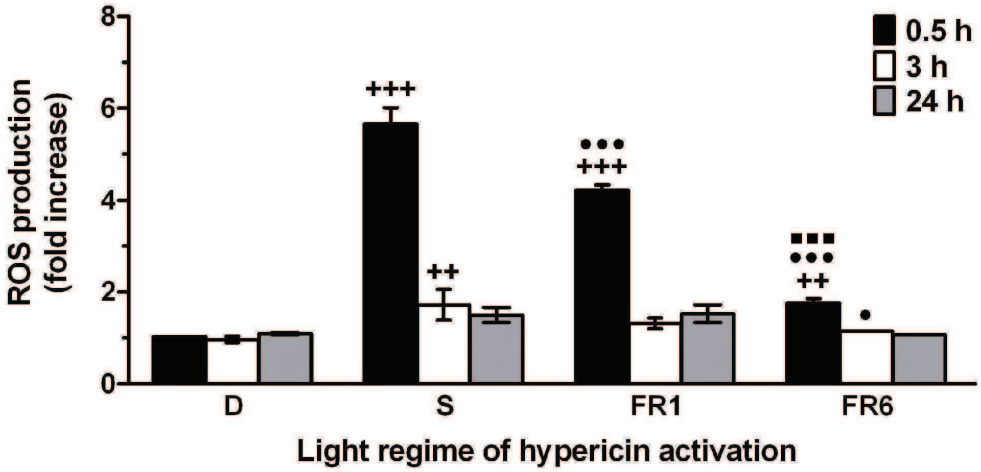

Figure 4. The effect of a single (12 J. cm-2) and fractionated (1 + 11 J.cm-2) light delivery on ROS production in HT-29 cells. Cells were harvested and evaluated 0.5, 3 and 24 h after hypericin-mediated photodynamic treatment. The results are the means ± SD of three independent experiments presented as ratios to control values. Statistical significance is expressed as follows: experimental groups versus untreated control (+); fractionated light delivery versus single light delivery (●); fractionated light delivery with a 6 h versus 1 h dark pause (■) on the significance level $p<0.05$ (●); $p<0.01$ (++); $p<0.001$ (+++ or ●●● or ■■■). (D) hypericin under dark conditions, (S) single light dose 12 J.cm-2, fractionated light dose 1+11 J.cm-2 with a 1 h (FR1) or 6 h (FR6) dark pause between the two light doses.
83x41mm (600 x 600 DPI)

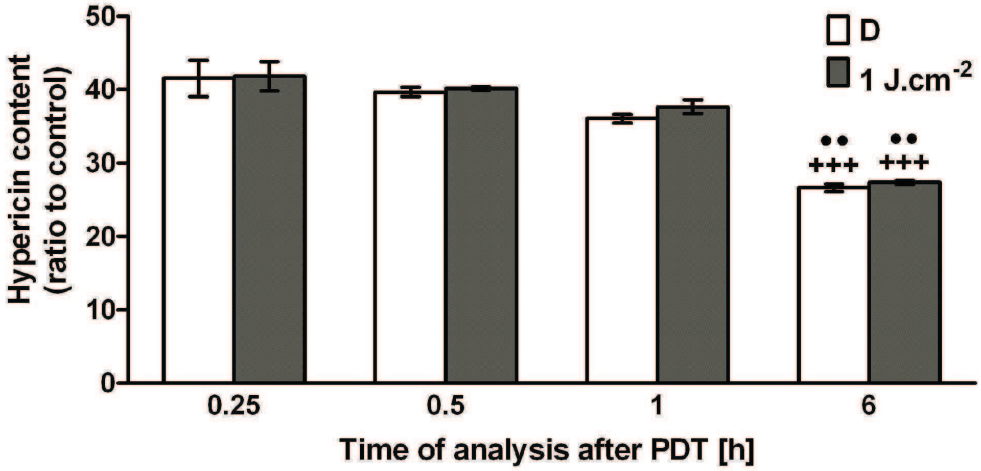

Figure 5. Determination of hypericin intracellular levels in HT-29 cells during the dark pause after first sub-lethal dose 1 J.cm-2. Cells were harvested and evaluated 0.25, 0.5, 1 and 6 h after hypericin photoactivation. The results are the means ± SD of three independent experiments presented as ratios to control values. Statistical significance is expressed as follows: photoactivated (1 J.cm-2) or not photoactivated (D) hypericin (0.5, 1 and 6 h) versus (0.25 h) (+); (6 h) versus (1 h) (●) on the significance level $p<0.01$ (●●); $p<0.001$ (+++). (D) hypericin under dark conditions.
83x41mm (600 x 600 DPI)

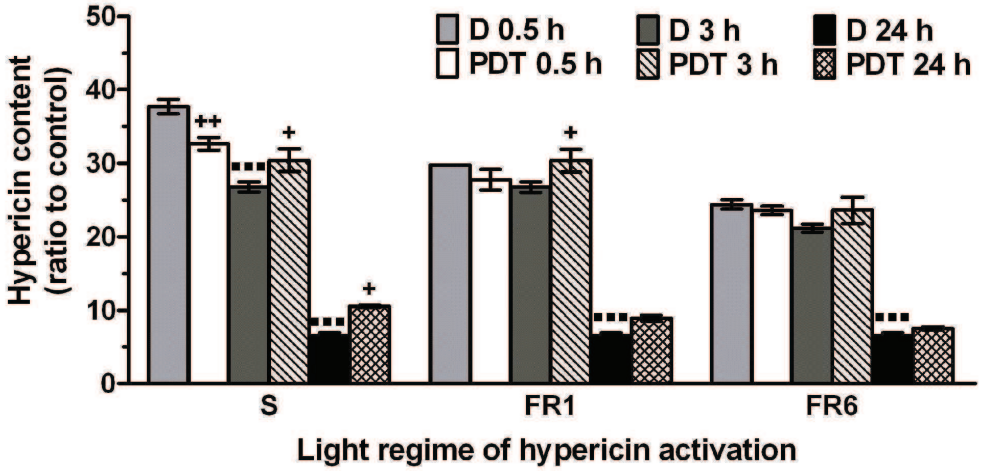

Figure 6. Determination of hypericin intracellular levels in HT-29 cells illuminated with a single (12 J. cm-2) and fractionated (1 + 11 J.cm-2) light delivery. Cells were harvested and evaluated 0.5, 3 and 24 h after PDT. The results are the means ± SD of three independent experiments presented as ratios to control values. Statistical significance is expressed as follows: single or fractionated light delivery versus not photoactivated (D) hypericin (+); not photoactivated hypericin (3 h or 24 h) versus (0.5 h) (■) on the significance level $p<0.05$ (+); $p<0.01$ (++); $p<0.001$ (■■■). (PDT) photodynamic treatment, (D) hypericin under dark conditions, (S) single light dose 12 J.cm-2, fractionated light dose 1+11 J.cm-2 with a 1 h (FR1) or 6 h (FR6) dark pause between the two light doses.
83x41mm (600 x 600 DPI)

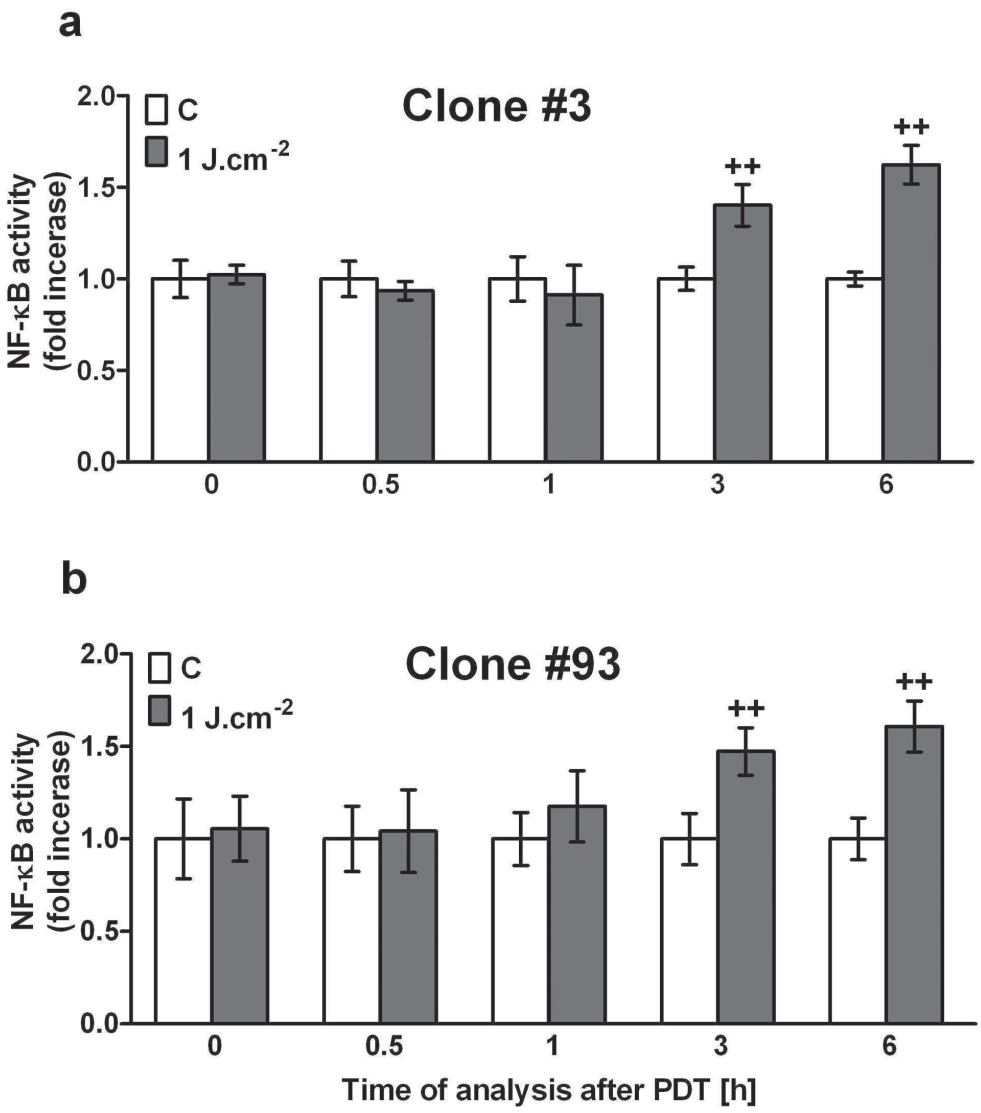

Figure 7. NF-κB binding activity (expressed as relative luciferase activity) of two HT-29 clones #3 (a) and #93 (b) with pBIIX-LUC construct after treatment with sub-lethal dose 1 J.cm-2. Cells were lysed 0, 0.25, 0.5, 1, 3 and 6 h after PDT. The results are the means ± SD of three independent experiments presented as ratios to untreated control values. Statistical significance is expressed as follows: sub-lethal light dose versus untreated control (+) on the significance level $p<0.01$ (++). (C) control cells.
83x96mm (600 x 600 DPI)

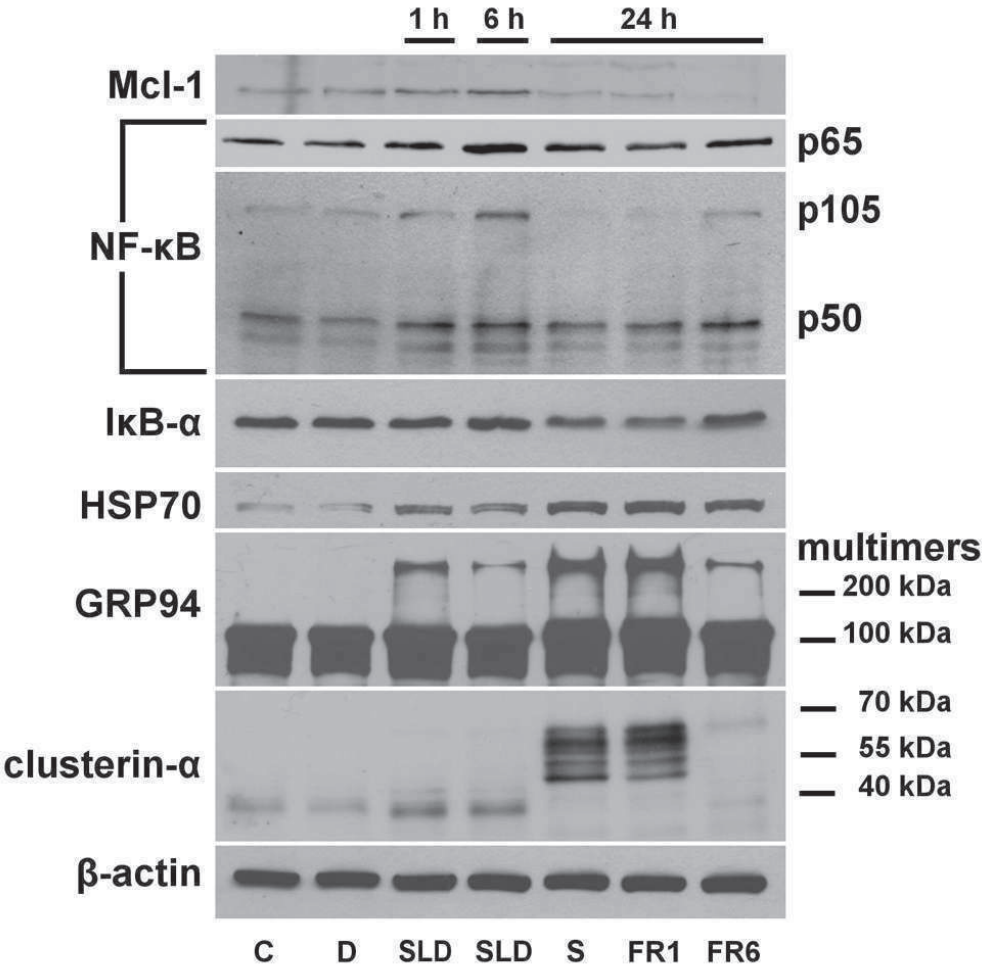

Figure 8. Western blot analysis of Mcl-1, NF-κB p65, p50 and p105, IκB-α, HSP70, GRP94, clusterin-α and β-actin proteins 1 or 6 h after hypericin photoactivation with a sub-lethal dose (1 J.cm-2) or 24 h after single (12 J. cm-2) and fractionated (1 + 11 J.cm-2) light delivery. The results are presented as a representative photo of three independent experiments. (C) control cells, (D) hypericin under dark conditions, (SLD) sub-lethal light dose 1 J.cm-2 (S) single light dose 12 J.cm-2, fractionated light dose 1+11 J.cm-2 with a 1 h (FR1) or 6 h (FR6) dark pause between the two light doses.
82x83mm (300 x 300 DPI)

The role of p53 in the efficiency of photodynamic therapy with hypericin and subsequent long-term survival of colon cancer cells

Jaromír Mikeš, Ján Koval', Rastislav Jendželovský, Veronika Sačková, Ivana Uhrinová, Martin Kello, Lucia Kuliková and Peter Fedoročko*

Received 12th June 2009, Accepted 24th July 2009
First published as an Advance Article on the web 10th September 2009
DOI: 10.1039/b9pp00021f

Photodynamic therapy with hypericin (HY-PDT) is known as an efficient modality for treatment of various cancerous and non-cancerous diseases. Although the role of p53 protein in cell death signaling is well established, relatively little is known of its impact on the efficiency of HY-PDT. Comparison of sensitivity and long-term survival of p53-null *versus* wt-p53-expressing HCT-116 cells is reported here. The lack of p53 function did not affect cell proliferation or attenuate the initial phases of programmed cell death. However, analyses of apoptosis in the final stages revealed suppression of its incidence and delayed activation of caspase-3 in p53-null cells. Significantly higher clonogenic ability, especially in hypoxia, was identified in the case of p53-null cells. Induction of Mcl-1 and Bax levels were more prominent in wt-pt53 cells. Interestingly, the level of Bcl-2 did not react to HY-PDT at all, in both cell lines. Bringing the evidence together, we prove that despite insignificant impact on overall toxicity, expression of p53 affects the clonogenic efficiency of HCT-116 cells. Since destruction of tumor tissue and its vascular system by PDT tends to lead to hypoxia, superior survival of p53-deficient tumor cells under given conditions might result in recurrence of cancer diseases.

Introduction

Photodynamic therapy (PDT) represents a flexible and versatile therapeutic approach depending on the nature of the photosensitive compound, its concentration and incubation time, on the wavelength of light radiation, fluency rate and light dose, as well as on the histological origin of tissue and oxygen pressure in it.[1] For all these reasons, the type of cell death induced by PDT depends upon many factors and their combinations.

Hypericin (HY), a naturally-occurring photosensitive compound synthesized by *Hypericum* sp. (St. John's Wort), has properties suitable for PDT.[1] The peculiar attributes of this photosensitizer are high efficiency in production of singlet oxygen[2] and superoxide anions after irradiation with light wavelength around 600 nm, and low or no toxicity in the dark.[3,4] Although HY is localized in the endoplasmic reticulum and Golgi apparatus and not in mitochondria[1] (so it should induce apoptosis with lower efficiency),[5] rapid loss of mitochondrial membrane potential, subsequent cytochrome c release, caspase-3 activation and apoptosis occur as a result of the photodynamic action of activated HY. The photosensitizing effects of HY are generally considered as oxygen-dependent.[6,7]

TP53, a tumor suppressor gene encoding a tumor protein 53 (p53), plays a central role in cellular responses and defence against DNA damage.[8] Mutations in the p53 pathway are found in nearly all types of cancers[9] and more than 50% of all cancers are reported to carry a mutant gene for p53, which is often linked to altered cellular sensitivity towards chemotherapy and radiation therapy.[10,11] In response to the stress stimuli, p53 (which normally has a low expression level) accumulates within cells due to an increase in the protein stability.[12,13] p53 integrates signals from various pathways that become activated as a result of different stimuli such as DNA damage, radiation, oxidative stress, hypoxia and oncogene activation.[14–16] Responses to the stimuli are regulated through different mechanisms but most of them are carried out *via* the ability of p53 to function as transcription factor.

In the field of PDT the dependence of cell-killing on p53 is still much debated, since papers proposing reliance[17,18] as well as no correlation[19] have been published. There is also evidence to show that induction of apoptosis (but not necrosis) may be influenced by p53 and ATM (ataxia telangiectasia mutation) even if total cell death is similar between the wild type and mutant phenotype.[20] These studies have largely been limited because the cancer cell lines employed by various researchers not only differ in their p53 status but are also likely to carry some other genetic differences in part because they were derived from different cell types or different carcinoma samples.[21]

Since one of our previous works evaluated cell death incidence evoked by HY-PDT in mut-p53 colon adenocarcinoma cells HT-29,[22] we continue here with a closer study of the effect of p53 on the sensitivity of HY-PDT, consequent cell death incidence and its role in the immediate and long-term survival of cells after PDT. In order to understand these issues, p53-null and wt-p53-expressing colon adenocarcinoma cell lines HCT-116 were chosen for the experiments presented here.

Experimental

Cell culture conditions

For the present experiments, wild type p53- (wt-p53) expressing HCT-116 cells (HCT-116 $p53^{+/+}$) were compared to the p53-null

Institute of Biology and Ecology, Faculty of Science, P.J. Šafárik University in Košice, Moyzesova 11, 040 01, Košice, Slovakia. E-mail: peter.fedorocko@upjs.sk; Fax: +421-55-6222124; Tel: +421-55-2341182

HCT-116 subline (HCT-116 p53$^{-/-}$), which was created by targeted homologous recombination[23] and was a gift from Professor Bert Vogelstein (both kindly provided by Dr Alois Kozubík, Institute of Biophysics, Brno, Czech Republic). Both cell lines were cultured in McCoy's 5A medium (Sigma-Aldrich, St. Louis, MO, USA) supplemented with 10% fetal calf serum, antibiotics (penicillin 100 U ml^{-1}, streptomycin 100 μg ml^{-1} and amphotericin 25 μg ml^{-1}; Gibco Invitrogen Corp., Carlsbad, CA, USA) and gentamycin (50 μg ml^{-1}; Sigma-Aldrich).

The cultures were maintained at 37 °C in 5% CO_2 and 95% humidity. For the experiments, cells were seeded in 96 well (1×10^4 cells per well), 6 well (1.5×10^5 cells per well) tissue culture plates or 100 mm diameter Petri dish (1×10^6 cells per dish) (TPP, Trasadingen, Switzerland). 24 h after seeding, hypericin (HPLC grade from Applichem, Darmstadt, Germany) was added into the medium for another 16 h. For the irradiation procedure, experimental groups as well as untreated controls were placed on the diffuser glass of the irradiating device (L18W/30 fluorescent tubes (Osram, Berlin, Germany)) in sequence and exposed to irradiation for specific time periods corresponding to the light dose 3.15 J cm^{-2}. Afterwards cells were cultured in the stated conditions and subsequently analyzed 8 h, 24 h or 48 h after irradiation. For hypoxic cultivation, cells were maintained at 37 °C in 5% CO_2, 1% O_2 (controlled by Proox Model 110, BioSpherix, Lacona, New York, USA) and 95% humidity.

Clonogenic assay

For clonogenic assay, cells were harvested (8 h, 24 h and 48 h after PDT treatment), counted and 500 viable cells were seeded in 6 well plates (TPP). Cells were simultaneously maintained under standard cultivation conditions as well as under the above-mentioned hypoxic conditions. Ten days later, the plates were stained with methylene blue dye (0.08% w/v) and scanned, and colonies were counted using Clono-Counter software.[24] Results were evaluated as percentages of the untreated control.

Quantification of total cell number and percentage of floating cells

Absolute numbers of cells within individual groups were evaluated by counting in a Bürker chamber or by Coulter Counter (Model ZF, Coulter Electronics Ltd, Luton, Beds., UK). Total cell number was expressed as a percentage of the untreated control. Floating cells were expressed as a percentage of the total cell number.

Morphological analysis of cell death

Morphological analysis of cell death was carried out using viable double staining with Hoechst 33342/propidium iodide or staining of fixed cells with 2-(4-amidinophenyl)-6-indolecarbamidine dihydrochloride (DAPI). At the scheduled time of analysis (24 h or 48 h after HY-PDT), total cell population was harvested (by trypsinisation of adherent and collection of medium with floating cells), centrifuged and washed once in Hank's balanced salt solution (HBSS) (Sigma-Aldrich). Subsequently, 1×10^6 cells were either fixed in cold 70% ethanol and kept at –20 °C overnight or viably stained with Hoechst 33342 (2 μg ml^{-1}) for 25 min and propidium iodide (PI) (25 μg ml^{-1}) for an additional 5 min (both Sigma-Aldrich) in darkness at RT. Viable staining was followed by washing in HBSS. Cells were then resuspended in 100 μl of HBSS, prepared as fresh specimen slides and immediately evaluated with a fluorescent microscope (Nikon Eclipse 400, Nikon Instech Co. Ltd., Kawasaki, Japan). Representative photographs of actual stainings are presented below. Ethanol fixed samples were processed as follows. The samples were stained in fixative solution by addition of DAPI (2 μg ml^{-1}) and incubated for 30 min at RT. Subsequently, cells were washed twice by centrifugation and finally resuspended in PBS. The cells were then mounted into MOWIOL 4-88 (Sigma-Aldrich) and allowed to harden for at least 24 h at 4 °C. The slides were analyzed using a Nikon Eclipse 400 fluorescent microscope and evaluated as the percentage of cells with fragmented nuclei from a total number of minimum 300 cells.

Metabolic activity of cells analyzed by MTT assay

At scheduled time points (8 h, 24 h or 48 h) after HY-PDT, MTT (3-[4,5-dimethylthiazol-2-yl]-2,5-diphenyltetrazolium bromide) was added to the cells in a 96 well plate (final concentration 0.5 mg ml^{-1}). Cells were incubated for another 4 h at 37 °C. Reaction was stopped and violet-blue crystals of insoluble formazan were dissolved by addition of sodium dodecyl sulfate (SDS) at a final concentration of 3.3%. Cells were incubated overnight at 37 °C and the absorbance ($\lambda = 584$ nm) was measured using BMG FLUOstar Optima (BMG Labtechnologies GmbH, Offenburg, Germany). Results were evaluated as percentages of the absorbance of the untreated control.

Analysis of hypericin incorporation

For analysis of HY incorporation, cells were seeded in 6 well plates and left to settle for 24 h, then incubated with HY for another 16 h. Subsequently, cells were harvested by trypsinization and the HY fluorescence was immediately analyzed using a BD FACSCalibur flow cytometer (Becton Dickinson, San Jose, CA, USA) with a 488 nm argon-ion excitation laser. The incorporation was quantified as the ratio of each experimental group to the untreated control.

Cell cycle analysis

Adherent and floating cells (5×10^5) were harvested together 24 h or 48 h after activation of HY, fixed in cold 70% ethanol and kept at –20 °C overnight. Prior to analysis, cells were washed in PBS. RNA was degraded with ribonuclease A and nuclear DNA was stained with propidium iodide (Sigma) (20 μg ml^{-1}) in Vindelov's solution at RT for 30 min. DNA content was analyzed using a BD FACSCalibur flow cytometer. The ModFit 3.0 (Verity Software House, Topsham, ME, USA) software was used to generate DNA content frequency histograms and to quantify the number of cells in the individual cell cycle phases.

Mitochondrial membrane depolarization

Adherent and floating cells (5×10^5) were harvested together 24 h after PDT, washed with HBSS, stained with 100 nmol dm^{-3} tetramethylrhodamine ethyl ester perchlorate (TMRE; Sigma-Aldrich) for at least 10 min and than analyzed using a BD FACSCalibur flow cytometer. The results are presented as means ± SD of three independent experiments together with one representative set of data. Graphical output was generated using WinMDI software.

Phosphatidylserine externalization analysis

For phosphatidylserine externalization analysis, an Annexin V-FITC/PI double-staining kit (Bender MedSystems, Vienna, Austria) was used according to the manufacturer's instructions. Adherent and floating cells (1.5×10^5) were harvested together 8 h or 24 h after PDT and stained with Annexin V-FITC in binding buffer (Bender MedSystems) for 10 min, washed, stained with PI for at least 10 min and thereafter analyzed using a BD FACSCalibur flow cytometer. Results were analyzed using CellQuest Pro software. The results are presented as means ± SD of three independent experiments together with one representative set of data. Graphical output was generated using WinMDI software.

Cell membrane fluidity analysis

For cell membrane fluidity analysis, cells were maintained in HBSS supplemented with 2% FCS during all steps of sample preparation. Adherent and floating cells (5×10^5) were harvested together 24 h after PDT, washed, stained with MC540 (5 ng ml^{-1}) for 10 min (rotating), washed twice and than analyzed using a BD FACSCalibur flow cytometer. The results are presented as means ± SD of three independent experiments together with one representative set of data. Graphical output was generated using WinMDI software.

Caspase-3 activation

Activation of caspase-3 was analyzed 8 h and 24 h after PDT using a FITC Active Caspase-3 Apoptosis Kit (BD Pharmingen, Franklin Lanes, NJ, USA, cat.# 550480) according to the manufacturer's instructions. Briefly, adherent and floating cells were harvested together, washed in cold PBS, permeabilized for 20 min on ice, washed again twice, incubated with antibody for 30 min at RT, washed and finally analyzed using a BD FACSCalibur flow cytometer. The results were evaluated as percentages of positively-stained cells and are presented as means ± SD of four independent experiments.

Western blot

For Western blot analysis, cells were scraped and lysed in Laemmli sample buffer (100 mM Tris [pH 6.8], 2% SDS, 10% glycerol). The extracts of total proteins were assayed with a DC protein assay kit (Bio-Rad Laboratories, Inc., Hercules, CA, USA) and equal protein amounts (10 μg) with 0.01% bromphenol blue and 1% mercaptoethanol were subjected to SDS-PAGE. The gels were transferred electrophoretically to polyvinylidene fluoride membranes (Millipore, Bedford, MA, USA) in a buffer containing 192 mM glycine, 25 mM Tris and 10% methanol. The membranes were blocked for 1 h in 5% non-fat milk in wash buffer (0.05% Tween-20 in 20 mM Tris [pH 7.6], 140 mM NaCl). Primary antibodies (rabbit anti-Bax, 1 : 500, sc-493; mouse anti-Bcl-2, 1 : 1000, sc-509; mouse anti-caspase-3, 1 : 500, sc-7272; rabbit anti-PARP, 1 : 500, sc-7150; Santa Cruz Biotechnology, Santa Cruz, CA, USA; mouse anti-β-actin, 1 : 6000, A5441, Sigma-Aldrich; mouse anti-HSP70, 1 : 1000; MA3-006, Affinity BioReagents, Golden, CO, USA; rabbit anti-calpain I, 1 : 500, #3189-100, BioVision, San Francisco Bay Area, CA, USA; mouse monoclonal anti-p53 (DO-1) kindly provided by Dr. Vojtešek[25]) were incubated with the blots for 2 h at RT or overnight at 4 °C. After washing, secondary antibodies coupled with horseradish peroxidase (anti-mouse IgG, 1 : 6000; anti-rabbit IgG, 1 : 6000; both Amersham Biosciences, Buckinghamshire, UK) were added for 2 h. The membranes were washed and antibody reactivity was visualized with enhanced chemiluminescence (ECL) reagent (Amersham Biosciences) against X-ray film-CP (AGFA, Gevaert N.V., Belgium). Loading was verified by detection of β-actin levels and by non-specific amidoblack protein staining.

Statistical analysis

Data were analyzed using one-way ANOVA with Tukey's post test or *t*-test and are expressed as mean ± standard deviation (S.D.). Significance levels are indicated in the legend to each particular figure.

Results

For presented experiments focused on the implication of p53 in sensitivity of colon adenocarcinoma to HY-PDT, a p53-null HCT-116 colon adenocarcinoma cell line (HCT-116 $p53^{-/-}$) was compared to HCT-116 cells expressing wild-type p53 (HCT-116 $p53^{+/+}$).

Suitable concentrations for experiments were chosen based on preliminary screening (MTT assay) with one light dose of 3.15 J cm^{-2} and HY concentrations ranging 0–150 nmol dm^{-3} (data not shown). Three concentrations (25, 50 and 75 nmol dm^{-3}) were used for all types of analyses, but in some cases only the results of 75 nmol dm^{-3} HY were significant when compared to the untreated control, and accordingly only those are presented. Analyses were performed 8, 24 or 48 h after PDT depending on the particular method.

Total cell numbers were mostly insignificant, whereas the floating cells analysis showed higher accumulation in p53 deficient cells 24 h after PDT. Analysis of total cell numbers (Fig. 1A) revealed a dose-dependent reaction to HY-PDT, which was significant in almost all groups when compared to the untreated control and therefore significance is not presented. Differences between cell lines were scarce and observed only at the lowest concentration.

In contrast, both cell lines showed significantly elevated floating cells not only when compared to the untreated control, but also compared with each other, mainly 24 h after PDT (Fig. 1B).On the other hand, analyses accomplished 48 h after PDT disclosed that only 25 nmol dm^{-3} HY and untreated controls were significant and therefore appeared to be in good correlation with the total cell number.

Cell cycle progression was significantly affected by PDT; however, both cell lines underwent mostly similar changes. Changes in cell cycle progression of both cell lines were significantly affected by HY-PDT (Table 1). The cells of both lines accumulated in the G_2/M-phase during the first 24 h after HY-PDT. The percentage of p53-null cells in the S-phase was significantly higher at this time point, but their untreated control had a similarly higher, though insignificant percentage of S-phase cells as the untreated control of wt-p53 cells. Later on, G_2/M-phase arrest declined but stayed significant and both cell lines accumulated in the S-phase. Although the trend seems to be similar, uneven distribution with significantly higher percentage of cells in the G_1-phase at

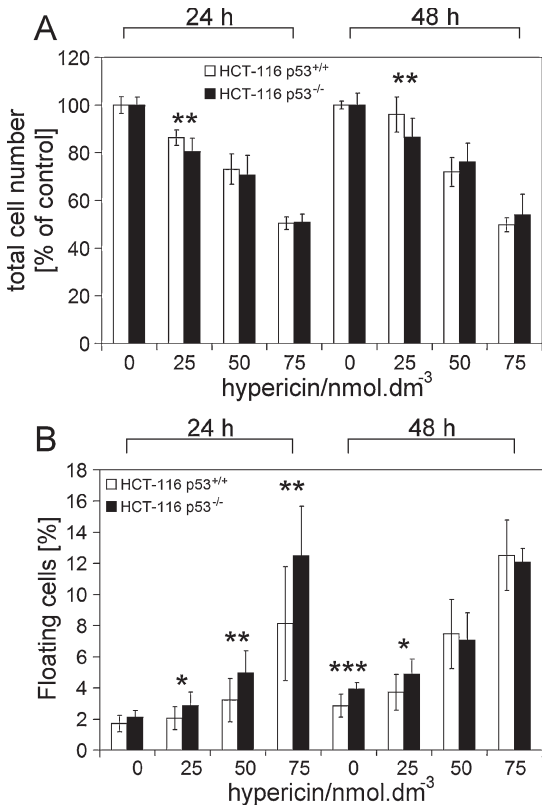

Fig. 1 Total cell numbers (A) and floating cell percentage (B) of wt-p53 (HCT-116 p53$^{+/+}$) or p53-null cells (HCT-116 p53$^{-/-}$). Cells were untreated or treated with 25, 50 and 75 nmol dm^{-3} hypericin, irradiated with 3.15 J cm^{-2} and harvested 24 or 48 h after PDT. The results (means ± S.D.) of three independent experiments are shown as the percentages of an untreated control. Statistical significance is identified as follows: $p < 0.05$ (*), $p < 0.01$ (**) and $p < 0.001$ (***) HCT-116 p53$^{+/+}$ *versus* HCT-116 p53$^{-/-}$.

the expense of the S-phase was recorded in wt-p53 cells. However, this might be the consequence of higher accumulation of p53 deficient cells in the S-phase in general. Apart from these differences, both cell lines responded to HY-PDT similarly.

Detection of phosphatidylserine externalization and cell viability by Annexin V/PI staining revealed that both cell lines underwent significant changes of cell membrane structure (Table 2), as indicated by a significant decrease in surviving cells (Annexin V$^-$/PI$^-$) and an increase in cells dedicated to programmed cell death (Annexin V$^+$/PI$^-$) in all comparisons of the untreated control to the particular experimental group. Differences between the cell lines were confined to the percentage of surviving cells (Annexin V$^-$/PI$^-$) 8 h after PDT only. Although there were some differences in the percentage of Annexin V$^+$/PI$^-$ cells 24 h after PDT, these were insignificant. Apart from these differences, the percentages of Annexin V$^+$ cells as well as surviving cells seem to be similar, and therefore there are no differences between p53 deficient *versus* p53 wild-type HCT-116 cells when considering this parameter 24 h after PDT. There was a difference in time-dependent decrease in the surviving cells percentage as there was transient resistance of HCT-116 p53$^{+/+}$ cells 8 h after PDT. From this point of view, p53 deficient cells seemed to proceed to cell death faster during the first hours after HY-PDT.

p53-deficient HCT-116 cells underwent mitochondrial membrane depolarization and membrane structure loosening more intensively 24 h after HY-PDT. Analysis of mitochondrial membrane potential ($\Delta\Psi_m$) 24 h after PDT revealed a significant decrease as a consequence of HY-PDT in both cell lines, but significantly superior $\Delta\Psi_m$ dissipation in p53-deficient cells was detected (Fig. 2A). Similarly, analysis of cell membrane loosening by MC540 24 h after irradiation revealed alterations of cell membrane structure in a significantly higher percentage of cells in both cell lines, and again the changes were more intensive in p53-deficient cells (Fig. 2B).

The percentage of cells in the final apoptotic phase was significantly lower in the p53-deficient cells. In spite of previous data indicating an insignificant or higher preference for cell death processes in the p53-null cells, the percentages of apoptotic cells in the final stages of programmed cell death, indicated as nuclear

Table 1 Cell cycle progression of wt-p53 (HCT-116 p53$^{+/+}$) or p53-null cells (HCT-116 p53$^{-/-}$). The cells were untreated or treated with 75 nmol dm^{-3} hypericin (Hyp 75), irradiated with 3.15 J cm^{-2} and harvested 24 h or 48 h after PDT. The results (means ± S.D.) of three independent experiments are shown as percentages of cells in the particular phases of the cell cycle. Statistical significance (S S.) is identified as follows: $p < 0.05$ (*) hypericin *versus* untreated control; $p < 0.05$ (●) HCT-116 p53$^{+/+}$ *versus* HCT-116 p53$^{-/-}$ and $p < 0.05$ (■) 24 h *versus* 48 h interval

			HCT-116 p53$^{+/+}$			HCT-116 p53$^{-/-}$		
Time/h	Group	CC phase	G0/G1	S	G2/M	G0/G1	S	G2/M
24	Control	Average [%]	67.09	22.16	10.75	53.48	29.41	17.11
		S.D.	±1.46	±1.6	±0.15	±9.25	±5.65	±3.58
		S S.						
24	Hyp 75	Average [%]	53.49	17.70	28.82	42.71	27.35	29.94
		S.D.	±5.58	±1.57	±4.02	±3.03	±1.99	±1.05
		S S.		●	*		●	*
48	Control	Average [%]	70.98	21.17	7.85	60.70	28.33	10.98
		S.D.	±2.97	±4.81	±1.85	±4.66	±4.03	±0.64
		S S.						
48	Hyp 75	Average [%]	47.87	33.78	18.36	40.03	37.85	22.12
		S.D.	±0.96	±1.96	±2.92	±0.45	±0.72	±1.18
		S S.	*/●	*/■	*	*/●	*/■	*/■

Table 2 Externalization of phosphatidylserine and viability of wt-p53 (HCT-116 $p53^{+/+}$) or p53-null cells (HCT-116 $p53^{-/-}$). The cells were untreated or treated with 75 nmol dm^{-3} hypericin (Hyp 75), irradiated with 3.15 J cm^{-2} and harvested 8 h or 24 h after PDT. The results (means ± S.D.) of three independent experiments are shown as percentages of cells in particular quadrants. Statistical significance (S S.) is identified as follows: $p < 0.05$ (*), $p < 0.01$ (**) or $p < 0.001$ (***) hypericin *versus* untreated control; $p < 0.05$ (●) or $p < 0.01$ (●●) HCT-116 $p53^{+/+}$ *versus* HCT-116 $p53^{-/-}$ and $p < 0.05$ (■) 8 h *versus* 24 h interval

			HCT-116 $p53^{+/+}$				HCT-116 $p53^{-/-}$			
		Annexin V	+	+	−	−	+	+	−	−
Time/h	Group	PI	−	+	−	+	−	+	−	+
8	Control	Average [%]	3.0	4.3	87.4	5.3	1.2	2.2	91.9	4.7
		S.D.	±1.4	±2.8	±1.2	±3.1	±0.9	±1.5	±1.6	±2.2
		S S.	**		***/●		*		***/●	
8	Hyp 75	Average [%]	26.9	9.9	57.8	5.4	30.0	22.3	39.6	8.1
		S.D.	±4.3	±4.9	±2.0	±2.6	±7.2	±9.8	±2.9	±4.9
		S S.	**		***/●●/■		*		***/●●	
24	Control	Average [%]	1.7	4.5	90.0	3.8	2.1	2.8	91.6	3.5
		S.D.	±1.4	±1.8	±2.2	±2.5	±0.8	±1.6	±2.8	±2.6
		S S.	*		**		*		**	
24	Hyp 75	Average [%]	32.0	32.1	31.2	4.7	45.1	24.2	28.3	2.4
		S.D.	±6.5	±11.0	±8.8	±2.3	±11.4	±12.0	±7.4	±1.2
		S S.	*		**		*		**	

fragmentation, were significantly lower both 24 and 48 h after PDT (Fig. 3). Concentration-dependent accumulation of apoptotic cells was convincingly noticeable at the highest 75 nmol dm^{-3} HY, although the trend was obvious in both cell lines also at lower concentrations.

Analysis of nuclear morphology and cellular viability reveals different tendencies for apoptotic cell death. Corresponding with the differences between cell lines determined by morphological analysis of nuclear morphology (DAPI staining; Fig. 3), floating cells (Fig. 1B) and concurrence of total cell number (Fig. 1A), the mutual analysis of nuclear morphology and cellular viability using viable staining with Hoechst 33342 and propidium iodide (Fig. 4) revealed different tendencies of cells to die by apoptosis or necrosis. Whereas in HCT-116 $p53^{+/+}$ cells prevalence of apoptotic processes with characteristic nuclear morphology is evident when detected 24 h after PDT, p53 deficient cells tended to be shifted towards necrosis.

Clonogenic assay revealed differences in survival of both cell lines either under normoxic or hypoxic conditions. For clonogenic assay, cells were harvested 8, 24 and 48 h after PDT, and subsequently 500 viable cells were seeded. The results (Fig. 5) reveal significantly higher clonogenic potential (especially under hypoxia) of p53-deficient cells harvested and seeded 8 h after HY-PDT (Fig. 5). Later on (24 and 48 h after HY-PDT), the differences between hypoxia and normoxia became insignificant, the clonogenic potential of both cell lines increased significantly with time and the differences between cell lines vanished.

Analyses of protein expression levels disclosed some interesting events in the regulation of programmed cell death (Fig. 6). We confirmed an undetectable level of protein p53-null cells, but at the same time we found its level responsive to HY-PDT in p53 wild-type-expressing cells. The photocytotoxic effect of HY stabilized p53 8 h after PDT, and led to the accumulation. Regression of p53 at 75 nmol dm^{-3} HY 24 h after PDT might indicate intensive degradation of p53 as a consequence of high dose PDT.

Cleavage of PARP was evident at 75 nmol dm^{-3} HY in both cell lines and became even more markedly pronounced in p53-deficient cells 24 h after PDT even at lower (25 and 50 nmol dm^{-3}) HY concentrations.

Interestingly, neither p53 wild-type-expressing cells nor p53-deficient cells showed any impressive caspase-3 cleavage (except p53-deficient cells 8 h, 75 nmol dm^{-3} HY-PDT). An expression of calpain did not indicate any significant changes in either cell line, too. Moreover, levels of anti-apoptotic Bcl-2 protein did not respond to HY-PDT. On the other hand, the expression of Mcl-1 was markedly induced in HCT-116 $p53^{+/+}$ cells already 8 h, and endured even 24 h after PDT. The level of Mcl-1 in p53-deficient cells was less responsive and mild as compared to wt-p53 cells. An expression of Bax, a protein involved in $\Delta\Psi_m$ depolarization, responded to HY-PDT in cells expressing wild-type p53 but was not responsive to PDT and generally minor in p53-deficient cells.

Analysis of HSP-70 level confirmed the involvement of oxidative stress in the photocytotoxic action of HY, since it responded to PDT in both lines and both analysis time-points.

Percentage of cells with activated caspase-3 detected by FCM analysis revealed time-delay of activation onset in p53-deficient cells. Percentages of cells with activated caspase-3 were detected by FCM analysis 8 and 24 h after HY-PDT (Table 3). We found differences between cell lines insignificant 24 h after HY activation, but the earlier analysis (8 h) showed us lower incidence of caspase-3^{pos} events in HCT-116 cells deficient in p53 when treated with PDT after incubation with either 50 or 75 nmol dm^{-3} HY. Although the differences were not very striking when compared to untreated control 8 h after activation, there was a significant increase in percentage of positives after treatment with 50 and 75 nmol dm^{-3} HY, though not with the 25 nmol dm^{-3} dose. Later on, when analyzed 24 h after PDT, only the PDT treatment with 75 nmol dm^{-3} HY showed significant accumulation of cells with activated caspase-3 (over 20% positive events) in comparison to untreated control as well as to previous analysis. Since a total lysate of the

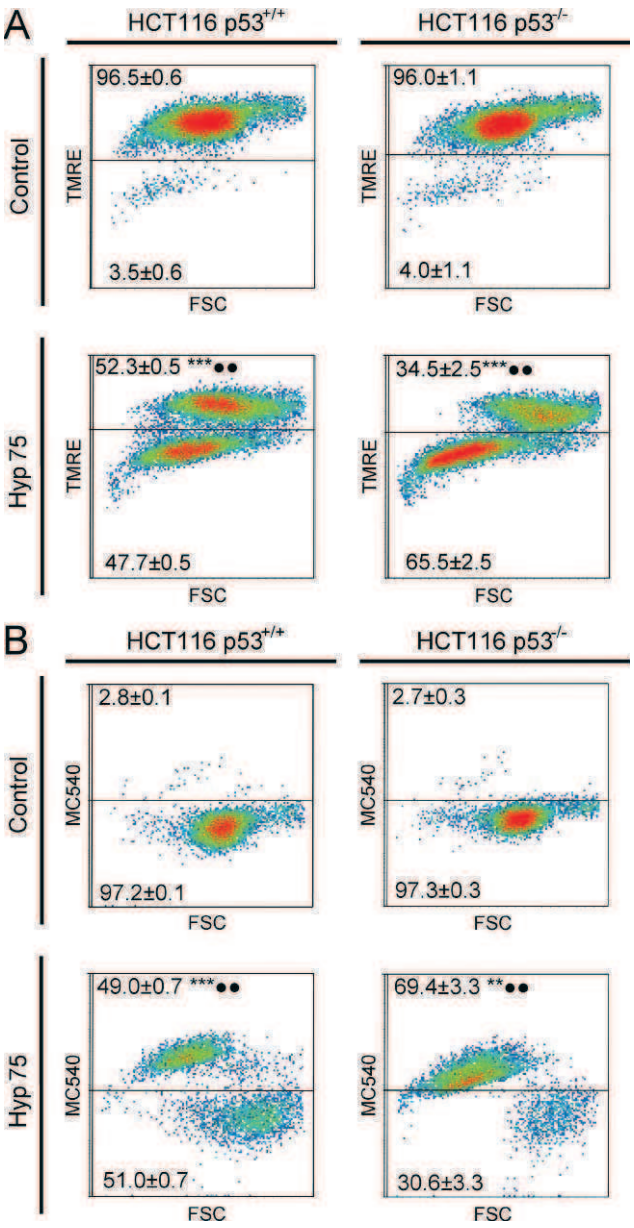

Fig. 2 Mitochondrial membrane depolarization (A) and cell membrane loosening (B) of wt-p53 (HCT-116 $p53^{+/+}$) or p53-null cells (HCT-116 $p53^{-/-}$) cells measured by TMRE and merocyanine (MC540) incorporation, respectively. The cells were untreated or treated with 75 nmol dm^{-3} hypericin (Hyp 75), irradiated with 3.15 J cm^{-2} and harvested 24 h after PDT. The results (means ± S.D.) of three independent experiments are shown as percentages of cells in particular quadrants together with one representative set of results. Statistical significance is identified as follows: $p < 0.01$ (**) or $p < 0.001$ (***) hypericin *versus* untreated control; $p < 0.01$ (●●) HCT-116 $p53^{+/+}$ *versus* HCT-116 $p53^{-/-}$.

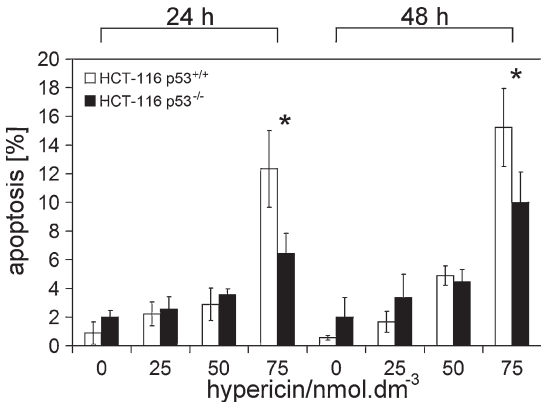

Fig. 3 Percentage of apoptotic cells analyzed *via* DAPI staining and morphological analysis of nuclear fragmentation in wt-p53 (HCT-116 $p53^{+/+}$) or p53-null cells (HCT-116 $p53^{-/-}$). Cells were untreated or treated with 25, 50 and 75 nmol dm^{-3} hypericin, irradiated with 3.15 J cm^{-2} and harvested 24 and 48 h after PDT. The results (means ± S.D.) of three independent experiments are shown as a percentage of cells with apoptotic morphology within the minimum of 300 cells. Statistical significance is identified as follows: $p < 0.05$ (*) HCT-116 $p53^{+/+}$ *versus* HCT-116 $p53^{-/-}$.

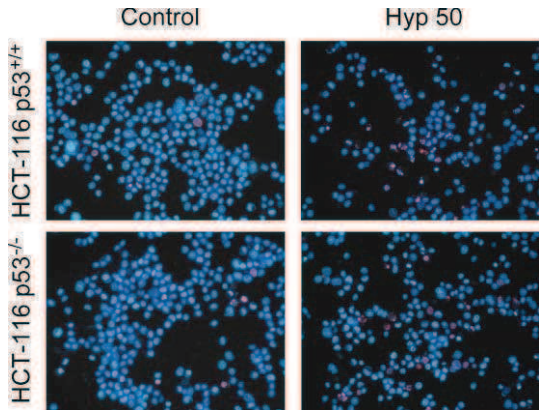

Fig. 4 Hoechst 33342/Propidium iodide staining of wt-p53 (HCT-116 $p53^{+/+}$) or p53-null cells (HCT-116 $p53^{-/-}$) 24 h after PDT. Cells were untreated or treated with 50 nmol dm^{-3} hypericin (Hyp 50), irradiated with 3.15 J cm^{-2}, harvested and stained 24 h after PDT. Cells could be recognized as vital (blue stained compact nuclei), apoptotic (blue stained fragmented nuclei), necrotic (red stained compact nuclei) and secondary necrotic (red stained fragmented nuclei). One of three independent experiments is presented herein (magnified 200×).

whole cell population (Fig. 6) did not facilitate sufficiently detailed analyses, activation of caspase-3 analyzed by FCM was used for further evaluation of activation of programmed cell death.

Discussion

In our previous study, we found necrosis to be the principal form of cell death in adenocarcinoma colon cancer cells HT-29,[22] despite the extensive range of HY-PDT doses evoked by variations in two variables: hypericin concentration and light dose. We also suggested that the mutation of TP53 in HT-29 cells leading to the stabilization of p53 protein and its consequent accumulation may play a key role in cell death signaling of these cells subjected to PDT. Our investigation of p53 as the factor possibly responsible for the drift in cell death incidence induced by PDT led to the present experiments employing a model of HCT-116 cells expressing wild-type p53 compared to the same cell line with p53 knock-out.

Summarizing our data, we can presume that proliferation of HCT-116 after HY-PDT was not dependent on status of p53. Though earlier analysis revealed a tendency of p53 null cells to detach and undergo cell death faster, later on (48 h after PDT) floating cells aligned (Fig. 1). This tendency was also indicated by intensive phosphatidyl serine externalization already 8 h after

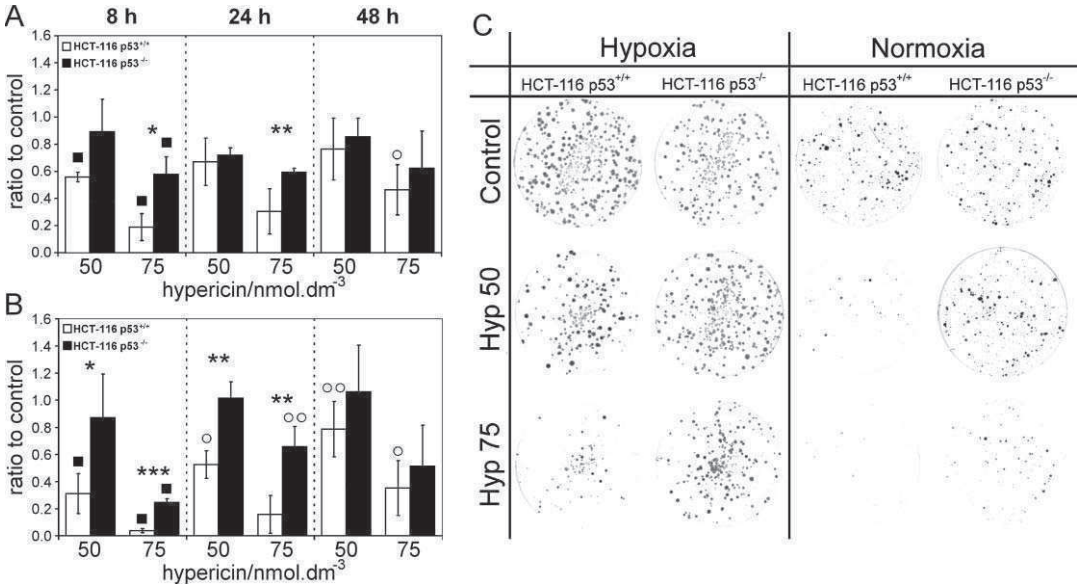

Fig. 5 Clonogenic assay of wt-p53 (HCT-116 p53$^{+/+}$) or p53-null cells (HCT-116 p53$^{-/-}$) under hypoxic (A) or normoxic (B) conditions. Cells were harvested 8, 24 or 48 h after PDT with 50 and 75 nmol dm^{-3} hypericin (Hyp 50 and Hyp 75). Representative results of cells harvested 8 h after PDT (C) is presented. The results (means ± S.D.) of three independent experiments are shown as a ratio to untreated control. Statistical significance is identified as follows: $p < 0.05$ (*) and $p < 0.01$ (**) HCT-116 p53$^{+/+}$ *versus* HCT-116 p53$^{-/-}$; $p < 0.05$ (■) hypoxia *versus* normoxia; $p < 0.05$ (○) and $p < 0.01$ (○○) 24 h/48 h *versus* 8 h time of seeding post PDT.

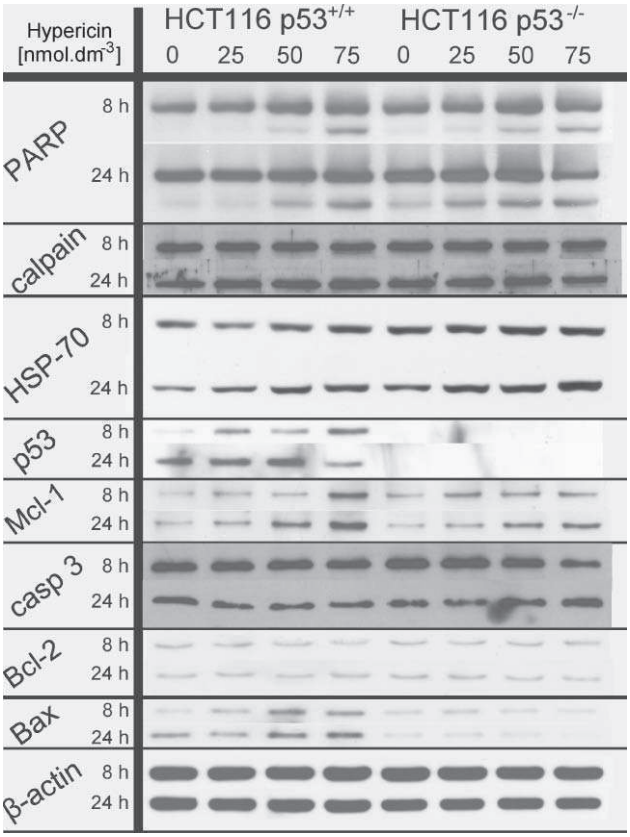

Fig. 6 Western blot analysis of PARP and caspase-3 (a procaspase) cleavage or calpain, HSP-70, p53, Mcl-1, Bcl-2, Bax and β-actin expression in wt-p53 (HCT-116 p53$^{+/+}$) or p53-null cells (HCT-116 p53$^{-/-}$). Cells were untreated or treated with 25, 50 and 75 nmol dm^{-3} hypericin, irradiated with 3.15 J cm^{-2} and harvested 8 and 24 h after PDT. One representative experiment of two is presented.

Table 3 Percentage of cells without activated caspase-3. Cells were harvested 8 h and 24 h after PDT with 25, 50 and 75 nmol dm^{-3} hypericin. Percentage of cells positive for active caspase-3 is a result of four independent experiments (mean ± S.D.). Statistical significance (S S.) is identified as follows: $p < 0.05$ (*), $p < 0.01$ (**), $p < 0.001$ (***) hypericin *versus* untreated control; $p < 0.05$ (●), $p < 0.01$(●●) HCT-116 p53$^{+/+}$ *versus* HCT-116 p53$^{-/-}$; $p < 0.01$(■■), $p < 0.001$(■■■) 8 h *versus* 24 h analysis

Time/h	HCT-116	Hyp [nmol dm^{-3}]	Average ± S.D.	S S.
8	p53$^{+/+}$	0	97.91% ± 0.32	
8	p53$^{+/+}$	25	97.13% ± 0.44	
8	p53$^{+/+}$	50	94.38% ± 1.23	*/●
8	p53$^{+/+}$	75	87.65% ± 1.66	***/●●/■■
8	p53$^{-/-}$	0	98.72% ± 0.15	
8	p53$^{-/-}$	25	98.25% ± 0.24	
8	p53$^{-/-}$	50	96.83% ± 0.69	*/●
8	p53$^{-/-}$	75	93.90% ± 1.99	*/●●/■■■
24	p53$^{+/+}$	0	95.11% ± 0.68	
24	p53$^{+/+}$	25	93.75% ± 3.17	
24	p53$^{+/+}$	50	95.42% ± 2.39	
24	p53$^{+/+}$	75	79.87% ± 2.63	***/—/■■
24	p53$^{-/-}$	0	96.95% ± 1.27	
24	p53$^{-/-}$	25	94.19% ± 2.16	
24	p53$^{-/-}$	50	92.71% ± 3.61	
24	p53$^{-/-}$	75	72.02% ± 6.73	**/—/■■■

PDT (Table 2) and further supported by a higher percentage of cells with lowered $\Delta\Psi_m$ and increased cell membrane fluidity (both in good mutual correlation, indicating close interconnection of the processes) (Fig. 2) detected 24 h after HY-PDT. However, morphological analyses (Fig. 3 and 4) revealed a prevalence of apoptotic processes with characteristic nuclear morphology in HCT-116 p53$^{+/+}$ cells and shifting towards necrosis in

p53-deficient cells. Yet, the hallmarks of oxidative stress (HSP70) and programmed cell death (PARP cleavage) were detectable in both cell lines (Fig. 6), as was the activation of caspase 3 (Table 3). Therefore it is likely that termination of the apoptotic process in HCT-116 cells is linked with the functional version of p53. Long term surival detected by clonogenic assay (Fig. 5) indicated differences between populations of viable cells harvested especially 8 h after HY-PDT. Cells deficient in p53 achieved a higher recovery rate even in spite of evidence of higher toxicity. Therefore it is possible that p53 status affects processes leading to survival of tumour cells exposed to HY-PDT.

It is well known that the p53 protein can promote apoptosis *via* transcription-independent mechanisms as well as transcriptional activation of pro-apoptotic (Bax)[26] or repression of anti-apoptotic genes.[27] Still, there is a lot of confusion about the role of p53 and its status in the efficacy of PDT. This is mostly due to the fact that PDT is generally considered as non-genotoxic, because the photosensitizers employed in PDT do not localize to the nucleus.[28] There are several studies linking induced p53 expression to higher incidence of apoptosis after ALA-PDT[29] or claiming either p53-dependent[17] or p53-independent[19] toxicity of Photofrin-PDT. The possibly hazy and scrambled nature of the results suggests that the question of the role of p53 in PDT might not have an easy and straightforward answer. Not only does p53 play a crucial role in numerous cellular processes, but moreover the phenotype of different sorts of cancer and distinct molecular and cellular mechanisms of phototoxicity induced by various photosensitizers under various conditions certainly significantly affect the overall efficacy of PDT.

The role of protein p53 in the photocytotoxicity of PDT has already been studied by several authors. Lee and colleagues[30] even studied HY-PDT in osteosarcoma cells with low *versus* high expression of p53 induced by stabilization of the protein, and they found the comparison of sensitivity between cell lines established by MTT and clonogenic assay insignificant. Likewise, phosphatidylserine externalization and mitochondrial potential dissipation exhibited similar trends in the onset and progression of programmed cell death. However, they did not present a quantitative analysis of the final stages of apoptosis. In another experiment, the dependence of the efficiency of PDT with m-THPC on *atm* and TP53 gene expression[20] demonstrated that p53 and ATM are not required for necrosis but might be required for apoptosis. In this case, genomic DNA fragmentation detected by TUNEL assay was used to analyze the final stage of the apoptotic process.

In concert with the results of Lee and colleagues,[30] we also concluded that p53 does not affect HY accumulation (data not shown) or the ability of photoactivated HY to kill tumour cells, *i.e.* its overall toxicity. We also found results of phosphatidylserine externalization 24 h after PDT insignificant, though earlier analysis (8 h) revealed some significant results in our experiment. However, since these authors did not present any quantitative analysis of the final stage of apoptosis, we could not compare our results indicating different incidence of apoptosis in our *in vitro* model of colon adenocarcinoma cells (Fig. 3). But the lower percentage of final stage apoptotic cells in p53-deficient cells correlates with m-THPC-mediated PDT in the work of Heinzelmann-Schwarz and colleagues.[20]

To bring more light to bear on the mechanism of passage along the apoptotic pathway influenced by p53 status, activation of caspase-3 was analyzed using Western blot as well as on a cellular basis using FCM (Fig. 6 and Table 3). The percentage of cells with activated caspase-3 (caspase-3^{pos}) analyzed 8 h after PDT (Table 3) was significantly enhanced in cells expressing wt-p53 when compared to control as well as to p53-deficient cells. However, considerable induction of caspase-3^{pos} cells by PDT with 75 nmol dm^{-3} HY, but no difference between cell lines 24 h after PDT, indicated that the apoptotic program was executed irrespective of p53 status, although some deceleration in p53-deficient cells was detected at the early stage (8 h). Since PARP is a substrate of caspase-3,[31] its cleavage, similar in both cell lines, is in accordance with caspase-3 activation. Though PARP cleavage did not correlate with differences in percentages of cells with apoptotic morphology of the nucleus. Therefore we consider it more as a qualitative/semiquantitative, but not a fully quantitative, indicator of the apoptotic process. And since there is some evidence of caspase-3[32] or even caspase-3, -6 and -7 independent cleavage of PARP[33] as well as a caspase- and PARP-cleavage-independent apoptotic pathway,[34,35] we might consider PARP cleavage more as a qualitative hallmark of programmed cell death.

Since PDT action is limited to a short period during photosensitizer activation by light, and subsequent cell death is a consequence of damage induced by ROS produced during activation, those cells that handle the impact of PDT may undergo a series of different changes, even those inducing resistance.[36] The significantly higher clonogenic potential of p53-deficient cells harvested 8 h and 24 h after PDT and the elapsed-time ascending trend (Fig. 5) in both cell lines indicate that the pools of viable cells seeded at those mentioned time points differed in their physiological status. Especially the 8 h harvest indicates that the population of p53-deficient cells, even though showing a lower survival rate (Annexin V/PI), contained a pool of surviving cells in different physiological condition and even when seeded in the same numbers they expressed a higher clonogenic potential. It is liable, that this population of surviving cells might be coincident with cancer stem cell subpopulations of HCT-116 cells described by Botchkina and colleagues,[37] which proved to possess higher clonogenic potential and *in vivo* tumorigenicity than the bulk population they originated from. In accordance with this presumption, cancer stem cells defined as $CD133^{+}$ are known to be highly resistant to chemotherapy[38] and their higher percentage correlates with tumor aggressiveness and clinical outcome.[39] When populations of both cell lines were harvested and seeded 48 h after PDT, the differences between them diminished.

Interestingly, harvesting and seeding cells 8 h after PDT revealed significantly higher clonogenic potential of both cell lines also under hypoxic conditions (1% O_2). These findings underline the impact of early response mechanisms (*e.g.* HIF-1[40]) on the therapeutic outcome and suggest that low-dose PDT might stimulate cell survival and induce resistant phenotype.[36] Regarding these results, it is also likely that the mechanisms linked to higher clonogenic potential under hypoxia are independent of p53 status. All told, together with analyses of phosphatidylserine externalization, $\Delta\Psi_m$ dissipation, cell membrane fluidity, total cell number and floating cells, we suggest that the programmed cell death pathway is decelerated in cells expressing wt-p53, whereas cells deficient in p53 proceeded faster to their demise. Although activation of caspase-3 seems to be an exception negating the above stated premise, as a matter of fact only a fraction of cells

with higher cell membrane fluidity, dissipated $\Delta\Psi_m$ or externalized phophatidylserine proceeded to caspase-3 activation. A higher percentage of Annexin V^+ cells compared to cells with dissipated $\Delta\Psi_m$ might also signify either preferential onset of phosphatidyl serine externalization[41] or reversibility of the process.[42,43]

As already reported by us and others, HY-PDT induces cell cycle arrest with preference at the G_2/M transition point.[22,44–46] Moreover, the protein p53 is known to affect cell cycle progression at the G_1/S transition[47] as well as the G_2/M transition point.[48] In our experiment, both cell lines underwent G_2/M arrest, however significantly higher accumulation of p53-deficient cells in the S-phase at the expense of the G_1-phase was detected 48 h after PDT. Based on these results, we suggest that accumulation of cells in the G_2/M phase of the cell cycle is not affected by p53 status, in accordance with the results of Lee and colleagues.[30] But in addition we might claim that HY-PDT induced minor accumulation at the G_1/S transition point, which was abrogated in p53-deficient cells. However justification of this event might require further study.

The crucial role in the onset of the apoptotic process is played by a wide group of anti- and pro-apoptotic proteins from the Bcl-2 family. Interestingly, an expression of Bcl-2 was not affected at all, either by p53 status or PDT (Fig. 6). On the other hand, induction of Mcl-1, another anti-apoptotic member of the Bcl-2 family, was in apparent correlation with PDT dose in the wt-p53 expressing cells. Bax, a representative of the pro-apoptotic group of the Bcl-2 family, responded to HY-PDT in the HCT-116 $p53^{+/+}$ but not $p53^{-/-}$ cells (Fig. 6). Since Mcl-1 does not inhibit Bax-mediated apoptosis,[49] induction of Bax, in spite of higher levels of Mcl-1, might be responsible for onset of apoptosis in wt-p53 cells. In contrast, the low expression of Bcl-2 together with Bax and only weaker responsiveness of Mcl-1 to increasing HY concentration were characteristic for apoptotic signaling in p53-deficient cells. This might indicate an impact of p53 status on Bcl-2 protein family signaling.

Based on the data presented here, we can predicate that our results correlate with other studies discussing this issue when considering the direct overall phototoxicity of HY-PDT. Although the lack of p53 function did not attenuate the initial phases of programmed cell death, analysis of apoptosis in the final stage revealed suppression of its incidence in p53 knock-out cells. Analyses of the apoptotic pathway in the execution phase revealed delayed stimulation of caspase-3 in p53-deficient cells 8 h after PDT, however we found it similar together with PARP cleavage in both cell lines at the same time (24 h after PDT) when differences in nuclear fragmentation were detected. Clonogenic assay revealed differences in ability to repopulate, especially high under hypoxic conditions, when harvested and seeded 8 h after PDT. Stimulation of programmed cell death onset in wt-p53 expressing cells was documented by induction in protein levels of anti-apoptotic Mcl-1 and pro-apoptotic Bax, whereas induction of Mcl-1 in p53-deficient cells was less prominent, and the level of Bax did not respond to PDT treatment. Interestingly, the level of Bcl-2 did not react to HY-PDT at all, in either cell line.

Conclusions

Bringing the evidence together, we demonstrate that despite its insignificant impact on overall toxicity, expression of the p53 protein affects the clonogenic efficiency of HCT-116 cells. Since destruction of tumor tissue and its vascular system as a consequence of PDT tends to lead to hypoxia, superior survival of tumour cells under these conditions might cause recurrence of cancer disease. Unfortunately, there is so far no literature discussing in detail the p53-dependent mechanisms of apoptosis regulation after PDT. Further studies will therefore be required to identify key molecular targets which might in future be treated pharmacologically in order to overcome the risk of disease recurrence.

Acknowledgements

This work was supported by the Slovak Research and Development Agency under the contracts No. VVCE-0001-07 and No. APVV 0321-07, and by the Scientific Grant Agency of the Ministry of Education of the Slovak Republic No. VEGA 1/0240/08. The authors are grateful to Viera Balážová for assistance with technical procedures. Thanks also to Andrew J. Billingham for proofreading the manuscript.

Notes and references

1 P. Agostinis, A. Vantieghem, W. Merlevede and P.A. de Witte, Hypericin in cancer treatment: more light on the way, *Int. J. Biochem. Cell Biol.*, 2002, **34**, 221–241.
2 R.W. Redmond and J.N. Gamlin, A compilation of singlet oxygen yields from biologically relevant molecules, *Photochem. Photobiol.*, 1999, **70**, 391–475.
3 E. Fox, R.F. Murphy, C.L. McCully and P.C. Adamson, Plasma pharmacokinetics and cerebrospinal fluid penetration of hypericin in nonhuman primates, *Cancer Chemother. Pharmacol.*, 2001, **47**, 41–44.
4 J.M. Jacobson, L. Feinman, L. Liebes, N. Ostrow, V. Koslowski, A. Tobia, B.E. Cabana, D. Lee, J. Spritzler and A.M. Prince, Pharmacokinetics, safety, and antiviral effects of hypericin, a derivative of St. John's wort plant, in patients with chronic hepatitis C virus infection, *Antimicrob. Agents Chemother.*, 2001, **45**, 517–524.
5 S. Marchal, A. Fadloun, E. Maugain, M.A. D'Hallewin, F. Guillemin and L. Bezdetnaya, Necrotic and apoptotic features of cell death in response to Foscan photosensitization of HT29 monolayer and multicell spheroids, *Biochem. Pharmacol.*, 2005, **69**, 1167–1176.
6 E. Delaey, A. Vandenbogaerde, W. Merlevede and P. de Witte, Photocytotoxicity of hypericin in normoxic and hypoxic conditions, *J. Photochem. Photobiol., B*, 2000, **56**, 19–24.
7 T. Utsumi, M. Okuma, T. Kanno, Y. Takehara, T. Yoshioka, Y. Fujita, A.A. Horton and K. Utsumi, Effect of the antiretroviral agent hypericin on rat liver mitochondria, *Biochem. Pharmacol.*, 1995, **50**, 655–662.
8 T. Enoch and C. Norbury, Cellular responses to DNA damage: cell-cycle checkpoints, apoptosis and the roles of p53 and ATM, *Trends Biochem. Sci.*, 1995, **20**, 426–430.
9 T. Soussi, p53 alterations in human cancer: more questions than answers, *Oncogene*, 2007, **26**, 2145–2156.
10 S. Bladt and H. Wagner, Inhibition of MAO by fractions and constituents of hypericum extract, *J. Geriatr. Psychiatr. Neurol.*, 1994, **7**, S57–S59.
11 S. Fan, M.L. Smith, D.J. Rivet, D. Duba, Q. Zhan, K.W. Kohn, A.J. Fornace and P.M. O'Connor, Disruption of p53 function sensitizes breast cancer MCF-7 cells to cisplatin and pentoxifylline, *Cancer Res.*, 1995, **55**, 1649–1654.
12 J.K. Hsieh, D. Yap, D.J. O'Connor, V. Fogal, L. Fallis, F. Chan, S. Zhong and X. Lu, Novel function of the cyclin A binding site of E2F in regulating p53-induced apoptosis in response to DNA damage, *Mol. Cell. Biol.*, 2002, **22**, 78–93.
13 S. Hansen, T.R. Hupp and D.P. Lane, Allosteric regulation of the thermostability and DNA binding activity of human p53 by specific interacting proteins. CRC Cell Transformation Group, *J. Biol. Chem.*, 1996, **271**, 3917–3924.
14 B. Vogelstein, D. Lane and A.J. Levine, Surfing the p53 network, *Nature*, 2000, **408**, 307–310.

15 M. Oren, Decision making by p53: life, death and cancer, *Cell Death Differ.*, 2003, **10**, 431–442.
16 K.H. Vousden and D.P. Lane, p53 in health and disease, *Nat. Rev. Mol. Cell Biol.*, 2007, **8**, 275–283.
17 A.M. Fisher, N. Rucker, S. Wong and C.J. Gomer, Differential photosensitivity in wild-type and mutant p53 human colon carcinoma cell lines, *J. Photochem. Photobiol., B*, 1998, **42**, 104–107.
18 W.G. Zhang, X.W. Li, L.P. Ma, S.W. Wang, H.Y. Yang and Z.Y. Zhang, Wild-type p53 protein potentiates phototoxicity of 2-BA-2-DMHA in HT29 cells expressing endogenous mutant p53, *Cancer Lett.*, 1999, **138**, 189–195.
19 A.M. Fisher, A. Ferrario, N. Rucker, S. Zhang and C.J. Gomer, Photodynamic therapy sensitivity is not altered in human tumor cells after abrogation of p53 function, *Cancer Res.*, 1999, **59**, 331–335.
20 V. Heinzelmann-Schwarz, A. Fedier, R. Hornung, H. Walt, U. Haller and D. Fink, Role of p53 and ATM in photodynamic therapy-induced apoptosis, *Lasers Surg. Med.*, 2003, **33**, 182–189.
21 A.A. Eshraghi, D.J. Castro, M.B. Paiva, I.P. Graeber, N. Jongewaard, S. Arshadnia, G. Lamas, J. Soudant and R.E. Saxton, Laser chemotherapy of human carcinoma cells with three new anticancer drugs, *J. Clin. Laser Med. Surg.*, 1997, **15**, 15–21.
22 J. Mikeš, J. Kleban, V. Sačková, V. Horváth, E. Jamborová, A. Vaculová, A. Kozubík, J. Hofmanová and P. Fedoročko, Necrosis predominates in the cell death of human colon adenocarcinoma HT-29 cells treated under variable conditions of photodynamic therapy with hypericin, *Photochem. Photobiol. Sci.*, 2007, **6**, 758–766.
23 F. Bunz, A. Dutriaux, C. Lengauer, T. Waldman, S. Zhou, J.P. Brown, J.M. Sedivy, K.W. Kinzler and B. Vogelstein, Requirement for p53 and p21 to sustain G2 arrest after DNA damage, *Science*, 1998, **282**, 1497–1501.
24 M. Niyazi, I. Niyazi and C. Belka, Counting colonies of clonogenic assays by using densitometric software, *Radiat. Oncol.*, 2007, **2**, 4.
25 B. Vojtešek, J. Bartek, C.A. Midgley and D.P. Lane, An immunochemical analysis of the human nuclear phosphoprotein p53. New monoclonal antibodies and epitope mapping using recombinant p53, *J. Immunol. Methods*, 1992, **151**, 237–244.
26 N. Zacal, M. Espiritu, G. Singh and A.J. Rainbow, Increased BNip3 and decreased mutant p53 in cisplatin-sensitive PDT-resistant HT29 cells, *Biochem. Biophys. Res. Commun.*, 2005, **331**, 648–657.
27 M. Weller, Predicting response to cancer chemotherapy: the role of p53, *Cell Tissue Res.*, 1998, **292**, 435–445.
28 T.J. Dougherty, C.J. Gomer, B.W. Henderson, G. Jori, D. Kessel, M. Korbelik, J. Moan and Q. Peng, Photodynamic therapy, *J. Natl. Cancer Inst.*, 1998, **90**, 889–905.
29 C.M.N. Yow, C.K. Wong, Z. Huang and R.J. Ho, Study of the efficacy and mechanism of ALA-mediated photodynamic therapy on human hepatocellular carcinoma cell, *Liver Int.*, 2007, **27**, 201–208.
30 H.B. Lee, A.S. Ho and S.H. Teo, p53 Status does not affect photodynamic cell killing induced by hypericin, *Cancer Chemother. Pharmacol.*, 2006, **58**, 91–98.
31 Y.A. Lazebnik, S.H. Kaufmann, S. Desnoyers, G.G. Poirier and W.C. Earnshaw, Cleavage of poly(ADP-ribose) polymerase by a proteinase with properties like ICE, *Nature*, 1994, **371**, 346–347.
32 R.U. Janicke, P. Ng, M.L. Sprengart and A.G. Porter, Caspase-3 is required for alpha-fodrin cleavage but dispensable for cleavage of other death substrates in apoptosis, *J. Biol. Chem.*, 1998, **273**, 15540–15545.
33 E.A. Slee, C. Adrain and S.J. Martin, Executioner caspase-3, -6, and -7 perform distinct, non-redundant roles during the demolition phase of apoptosis, *J. Biol. Chem.*, 2001, **276**, 7320–7326.
34 A. Coutant, J. Lebeau, N. Bidon-Wagner, C. Levalois, B. Lectard and S. Chevillard, Cadmium-induced apoptosis in lymphoblastoid cell line: involvement of caspase-dependent and -independent pathways, *Biochimie*, 2006, **88**, 1815–1822.
35 Z.Q. Wu, R. Zhang, C. Chao, J.F. Zhang and Y.Q. Zhang, Histone deacetylase inhibitor trichostatin A induced caspase-independent apoptosis in human gastric cancer cell, *Chin. Med. J.*, 2007, **120**, 2112–2118.
36 V. Sačková, L. Kuliková, J. Mikeš, J. Kleban and P. Fedoročko, Hypericin-mediated photocytotoxic effect on HT-29 adenocarcinoma cells is reduced by light fractionation with longer dark pause between two unequal light doses, *Photochem. Photobiol.*, 2005, **81**, 1411–1416.
37 I.L. Botchkina, R.A. Rowehl, D.E. Rivadeneira, M.S. Karpeh jr., H. Crawford, A. Dufour, J. Ju, Y. Wang, Y. Leyfman and G.I. Botchkina, Phenotypic subpopulations of metastatic colon cancer stem cells: Genomic Analysis, *Cancer Genomics Proteomics*, 2009, **6**, 19–30.
38 N.Y. Frank, A. Margaryan, Y. Huang, T. Schatton, A.M. Waaga-Gasser, M. Gasser, M.H. Sayegh, W. Sadee and M.H. Frank, ABCB5-mediated doxorubicin transport and chemoresistance in human malignant melanoma, *Cancer Res.*, 2005, **65**, 4320–4333.
39 F. Zeppernick, R. Ahmadi, B. Campos, C. Dictus, B.M. Helmke, N. Becker, P. Lichter, A. Unterberg, B. Radlwimmer and C.C. Herold-Mende, Stem cell marker CD133 affects clinical outcome in glioma patients, *Clin. Cancer Res.*, 2008, **14**, 123–129.
40 M.I. Koukourakis, A. Giatromanolaki, J. Skarlatos, L. Corti, S. Blandamura, M. Piazza, K.C. Gatter and A.L. Harris, Hypoxia inducible factor (HIF-1a and HIF-2a) expression in early esophageal cancer and response to photodynamic therapy and radiotherapy, *Cancer Res.*, 2001, **61**, 1830–1832.
41 G. Denecker, H. Dooms, G. Van Loo, D. Vercammen, J. Grooten, W. Fiers, W. Declercq and P. Vandenabeele, Phosphatidyl serine exposure during apoptosis precedes release of cytochrome c and decrease in mitochondrial transmembrane potential, *FEBS Lett.*, 2000, **465**, 47–52.
42 S.R. Stowell, S. Karmakar, C.M. Arthur, T. Ju, L.C. Rodrigues, T.B. Riul, M. Dias-Baruffi, J. Miner, R.P. McEver and R.D. Cummings, Galectin-1 induces reversible phosphatidylserine exposure at the plasma membrane, *Mol. Biol. Cell*, 2009, **20**, 1408–1418.
43 G. Kroemer, L. Galluzzi, P. Vandenabeele, J. Abrams, E.S. Alnemri, E.H. Baehrecke, M.V. Blagosklonny, W.S. El-Deiry, P. Golstein, D.R. Green, M. Hengartner, R.A. Knight, S. Kumar, S.A. Lipton, W. Malorni, G. Nuñez, M.E. Peter, J. Tschopp, J. Yuan, M. Piacentini, B. Zhivotovsky and G. Melino, Classification of cell death: recommendations of the Nomenclature Committee on Cell Death 2009, *Cell Death Differ.*, 2009, **16**, 3–11.
44 P. Agostinis, A. Donella-Deana, J. Cuveele, A. Vandenbogaerde, S. Sarno, W. Merlevede and P. de Witte, A comparative analysis of the photosensitized inhibition of growth-factor regulated protein kinases by hypericin-derivatives, *Biochem. Biophys. Res. Commun.*, 1996, **220**, 613–617.
45 J. Kleban, J. Mikeš, V. Horváth, V. Sačková, J. Hofmanová, A. Kozubík and P. Fedoročko, Mechanisms involved in the cell cycle and apoptosis of HT-29 cells pre-treated with MK-886 prior to photodynamic therapy with hypericin, *J. Photochem. Photobiol., B*, 2008, **93**, 108–118.
46 V. Sačková, P. Fedoročko, B. Szilárdiová, J. Mikeš and J. Kleban, Hypericin-induced photocytotoxicity is connected with G2/M arrest in HT-29 and S-phase arrest in U937 cells, *Photochem. Photobiol.*, 2006, **82**, 1285–1291.
47 S. Maddika, S.R. Ande, S. Panigrahi, T. Paranjothy, K. Weglarczyk, A. Zuse, M. Eshraghi, K.D. Manda, E. Wiechec and M. Los, Cell survival, cell death and cell cycle pathways are interconnected: implications for cancer therapy, *Drug Resist. Updates*, 2007, **10**, 13–29.
48 G. Micali, F. Lanuzza and P. Currò, High-performance liquid chromatographic determination of the biologically active principle hypericin in phytotherapeutic vegetable extracts and alcoholic beverages, *J. Chromatogr., A*, 1996, **731**, 336–339.
49 D. Zhai, C. Jin, Z. Huang, A.C. Satterthwait and J.C. Reed, Differential regulation of Bax and Bak by anti-apoptotic Bcl-2 family proteins Bcl-B and Mcl-1, *J. Biol. Chem.*, 2008, **283**, 9580–9586.